COVARIANCE ESTIMATION AND AUTOCORRELATION OF NORAD TWO-LINE ELEMENT SETS

THESIS

Victor P. Osweiler, Captain, USAF

AFIT/GSS/ENY/06-M09

DEPARTMENT OF THE AIR FORCE
AIR UNIVERSITY

AIR FORCE INSTITUTE OF TECHNOLOGY

Wright-Patterson Air Force Base, Ohio

The views expressed in this thesis are those of the author and do not reflect the official policy or position of the United States Air Force, Department of Defense, or the U.S. Government.

AFIT/GSS/ENY/06-M09

COVARIANCE ESTIMATION AND AUTOCORRELATION OF NORAD TWO-LINE ELEMENT SETS

THESIS

Presented to the Faculty

Department of Aeronautics and Astronautics

Graduate School of Engineering and Management

Air Force Institute of Technology

Air University

Air Education and Training Command

In Partial Fulfillment of the Requirements for the

Degree of Master of Science (Space Systems)

Victor P. Osweiler, BS

Captain, USAF

March 2006

AFIT/GSS/ENY/06-M09

COVARIANCE ESTIMATION AND AUTOCORRELATION OF NORAD TWO-LINE ELEMENT SETS

Victor P. Osweiler, BS
Captain, USAF

Approved:

Lt Col Nathan A. Titus (Chairman)	date
Dr. William E. Wiesel (Member)	date
Lt Col Kerry D. Hicks (Member)	date

AFIT/GSS/ENY/06-M09

Abstract

This thesis investigates NORAD two-line element sets (TLE) containing satellite mean orbital elements for the purpose of estimating a covariance matrix and formulating an autocorrelation relationship. Orbit propagation is performed using Simplified General Perturbations Number 4 (SGP4) analytical model as implemented within Satellite Took Kit. For a given satellite, TLEs from a span of two weeks are used to calculate position and velocity differences of estimated state vectors in order to characterize their variance behavior and compute a covariance matrix for the most recent TLE. Six satellites and eight time spans are investigated, with all state vector differences evaluated in satellite-based coordinate systems. An autocorrelation relationship for each satellite is generated to characterize confidence levels of the orbit predictions. Trends in the deterministic dynamics and errors in the model are observed and discussed. Covariance matrix estimates and associated TLEs are presented.

To My Mother

Acknowledgments

This thesis could not have been accomplished without the support from several incredibly talented and insightful people. First, I would like to express my sincere appreciation to my advisor, Lt Col Nathan Titus, for his support and guidance throughout my entire time at AFIT, especially during the course of this research. Additionally, I would like to extend my gratitude to Dr. William Wiesel for sharing his expertise and recommendations, which shaped this work.

I am also indebted to Mr. David Vallado and Dr. T.S. Kelso, who were instrumental in this endeavor. Both generously dedicated their time, knowledge, and assistance for which I will always be grateful. I would like to give thanks to Dr. Michael Gabor for his counsel in improving this body of work.

On a more personal level, I want to thank my family and friends who enabled me to persevere through this entire process. Their unconditional support inspired me, making the pursuit of this degree possible. I thank you all!

Victor P. Osweiler

Table of Contents

Page

List of Figures

Page

Page

List of Tables

Page

COVARIANCE ESTIMATION AND AUTOCORRELATION OF NORAD TWO-LINE ELEMENT SETS

I. Introduction

Background Information

The North American Aerospace Defense Command (NORAD) mission of space surveillance carries the responsibility of tracking almost 10,000 man-made objects in orbit around the Earth (17). The Space Surveillance Network (SSN), operated by Air Force Space Command and tasked with space surveillance, tracks and collects data on man-made objects that are 10cm and larger (18). NORAD uses the tracking data from the SSN to maintain its space catalog, which includes both operational and "dead" satellites, launch vehicles and rocket bodies, and space debris. Every object in the space catalog has a unique identifier and its mean orbital elements are routinely calculated. These mean orbital elements describe the motion of the satellite and can be used to predict the trajectory of the orbit.

Current and historical satellite orbital elements are available from a few locations on the World Wide Web, such as Space-Track.org or CelesTrak.com. The format in which orbital elements are released is called a two-line element set, or TLE. TLEs are used with the Simplified General Perturbations Number 4 (SGP4) analytical orbital

model to determine an object's position and velocity vectors at a specific time, or epoch. The speed of the analytical theory makes it advantageous for use in quickly determining a computationally-intensive process, such as determining close approaches or conjunctions of the entire catalog (10:2). However, the accuracy of the TLE data is not very good, so numerically derived state vectors—six independent elements which provide the position and velocity vectors in three dimension space—are often used to fine tune the calculations after an initial selection with SGP4 (22). Due to the mathematical formulation, the numerically derived state vectors have a covariance matrix associated with them, indicating the relative uncertainty in the solution. The combination of TLEs and state vectors are necessary for a number of routine space-related operations, such as command and control and collision avoidance analysis.

However, no associated level of accuracy, or uncertainty, is provided with two-line element sets. Such information typically accompanies a solution of deterministic dynamics, i.e., a covariance matrix resulting from the orbit determination process. The covariance matrix contains estimates for the closeness of the fit with the chosen dynamics. When propagated forward in time along with the state vector, the covariance matrix provides a dynamical representation of the accuracy of the predicted state, and can provide clues to indicate trends in the overall accuracy that can be expected for the satellite (19:690).

Problem Statement

Currently, NORAD two-line element sets released for public use contain no associated accuracy information. With error covariance estimates, users of TLE data in several space operations and space-related fields—especially conjunction analysis—could obtain an estimate of the confidence of their space situational awareness calculations, and increase their ability to achieve mission success.

Research Objectives

The primary focus of this thesis is to estimate a covariance matrix of a NORAD two-line element set state vector using only publicly available TLEs. For a given satellite, TLEs from a span of two weeks are propagated to each others epochs using SGP4. Position and velocity differences between the estimated state vectors are computed in order to characterize their variance behavior and compute a covariance matrix for the most recent TLE in the time span. The secondary focus of this research is to determine if the autocorrelation function of the position difference data for the same satellite provides insight into the confidence of the covariance estimate.

The primary objectives of this research are to develop and demonstrate algorithms for computing the covariance and autocorrelation function. Secondary objectives include evaluating the variances and covariances for satellites in different orbits as they change over time. In addition to analyzing the consistency of the covariance estimates, the dependability of propagated TLE state vectors with respect to the length of prediction will be evaluated using the autocorrelation relationship.

II. Literature Review

The purpose of this chapter is to provide the reader with sufficient background of the topics involved in this research effort, as well as a comprehensive summary of related research and studies.

Space Surveillance

As of February 2006, the NORAD database of two-line element sets contains more than 56 million TLEs for nearly 29,000 objects, dating back to 1959. About two-thirds of those objects have decayed, leaving just over 9,600 currently in orbit around Earth (17). As stated above, the SSN observes these objects for NORAD to maintain its catalog, and TLEs are usually updated daily.

The SSN collects data using both passive and active instruments, then forwards the data to the Cheyenne Mountain Operations Center (CMOC) to be cataloged. Comprised primarily of radar sensors for tracking near-earth objects (below approximately 6,000 kilometers altitude) and electro-optical sensors for deep-space objects (above 6,000 kilometers altitude), the SSN is a globally distributed network of sensors (11). Three categories of sensors encompass the SSN: dedicated, collateral, and contributing. Examples of dedicated sensors include three Ground-based Electro-Optical Deep Space Surveillance (GEODSS) sites, phased array radar at Eglin Air Force Base, and Maui Optical Tracking and Identification Facility (MOTIF). Collateral sensors include numerous phased array radars, such as PAVE PAWS and BMEWS, and

contributing sensors include the Haystack X-band radar and Air Force Maui Optical Station (AMOS). See Figure 1 for a map of the SSN sensors.

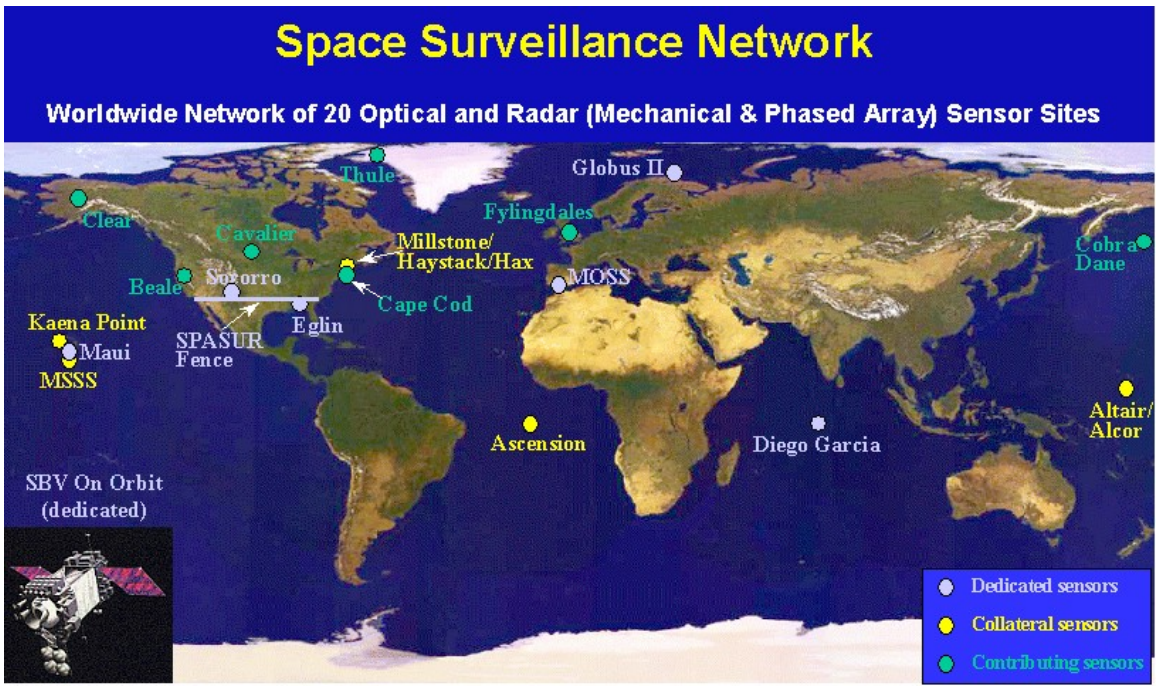

Figure 1. Space Surveillance Network (18)

In the early days of space surveillance, orbital elements for all known satellites were updated as necessary and listed in what was referred to as the space bulletin, the forerunner to today's space catalog. Observing stations used this bulletin for planning purposes, such as to predict times of satellite overpasses (6).

Today, NORAD posts the element sets for nearly all the objects it tracks at www.space-track.org. Approved, registered users can search and download data for a specific satellite or for a group, selecting start and stop dates to match their time period of interest. Also available are daily files of every TLE updated on that day; information on recent satellite decays and decay predictions; and comprehensive satellite situation

reports and recent catalog change reports. Orbital elements are available for approximately 91% of the objects in the space catalog, with the remaining objects being either classified or "lost" meaning they have not been tracked for approximately thirty days (11). Users of TLE data range from current space mission planners and operators to academic researchers.

Another online repository where TLE data can be found is CelesTrak (celestrak.com), a well-known website managed by Dr. Kelso. In addition to the availability of current and historical TLE data, CelesTrak contains exceptional resources for both novices and experienced analysts. Highly respected and easy to access, CelesTrak is where TLEs in this study were gathered. Before detailing the exact format of the TLE, a description of SGP4, the dynamic force analytic model used to calculate the mean orbital elements, is described.

Simplified General Perturbations Model

The generation of TLE data is rooted in a rather confusing period of U.S. space surveillance. Various analytical, numerical, and semi-analytical models for orbit propagation have been developed over the past half century. Extensive work has been accomplished by many experts in an attempt to reproduce/verify the version of SGP4 used by NORAD today (6; 22). Below is a brief history of the development of SGP4 and some unique, yet critical, characteristics of the model.

SGP4 History.

Beginning in the 1950s and continuing into the 1960s, several different analytical theories were developed to solve for the motion of an orbiting satellite. Hoots et al. offer a description of the theoretical foundations as well as their implementation into different operational systems of the U.S space surveillance system (6; 8). In the early 1960s, the Simplified General Perturbations model, termed SGP, was instituted as the U.S. "principle analytical prediction model for centralized processing [and] was implemented at many of the satellite tracking sites around the world." This model accounted for the zonal harmonics (J_2, J_3, J_4, J_5 terms) solution that Brouwer developed in 1959 as well as for atmospheric drag. Implementation of the atmospheric drag was based on the work of Richard Smith, who had previously worked the issue with the Navy Positions and Partials as functions of Time (PPT3) analytical model. In 1964, SGP was implemented as the primary orbital prediction model for the Space Detection and Tracking Systems (SPADATS) Center in Colorado Springs (6:175-176).

An important influence on the implementation of the various models, such as drag and zonal harmonics, during the beginning stages was the capability of available computers. This often resulted in truncating expansions and simplifying models so that the computers of the day could perform the necessary computations. While computers have improved dramatically since then, this influence remains on the operational code today (22).

The Air Force implemented a refined version of the SGP model in 1970, termed SGP4, based primarily on Brouwer's work from 1959. This updated version addressed

the secular effect of drag by using power density functions, encapsulating the ballistic coefficient known as B*. At this time only the main terms that modeled the secular effect of drag were retained by SGP4. Another simplification to SGP4 was that "gravitational modeling was shortened by retaining…only those long- and short-periodic terms in position that do not contain eccentricity as a factor" (6:176). So as Vallado explains, much of the full gravity solution that Brouwer had developed was not included in SGP4 (22).

In 1967, a semi-analytical treatment accounting for lunar and solar gravitational effects on longer period orbits (12-hour) as well as geopotential resonance effects (Earth's tesseral harmonics) was developed by Bowman. By 1977, Hujsak incorporated portions of Bowman's work into SGP4, but in a first-order model, allowing for the perturbations to be extended to geosynchronous satellites (6:176).

Via a compatibility survey in 1980, Hoots discovered that varying versions of both SGP and SGP4 were being used by the world-wide technical and operator community, despite the fact that it was supposed to be "the sole model for satellite catalog maintenance" for the Air Force (6:176). As the first public release of the SGP4 source code in 1980, *Spacetrack Report Number 3* (8), could have standardized and synchronized the user community. But as Vallado explains, subsequent refinements to the model have occurred in a non-standardized manner and with little or no documentation/coordination, leaving the user community in a state of confusion even today (22).

Hoots et al. provide a complete list of the equations for SGP4, including atmospheric drag, third-body forces, deep-space coefficients, and resonance effects, in 2004 (6). Also, Vallado offers "source code, test cases, results, and analysis of a version of SGP4 designed to be similar to the operational AFSPC code" (22).

SGP4 Uniqueness.

As mentioned earlier, SGP4 has some unique characteristics which require attention. Foremost, NORAD element sets must be used with one of the Simplified General Perturbations models. It is imperative to understand that the major perturbation forces acting on a satellite are "incorporated into the mean orbital element values of the TLE in a very specific way" (11). As Kelso and Alfano explain, in order to minimize force modeling error, the SGP4 orbital theory must be used for orbit propagation. Since TLEs are generated from SGP4 using the SSN observations, unnecessary error is introduced when performing orbit propagation with something other than SGP4 (10). A workaround involves converting the TLE into a state vector—position and velocity vectors—for the specific epoch of that TLE, and then converting those vectors into the desired elements. But even this must be done in a specific way, as described by Vallado (19:667-669).

The second area requiring special attention when using SGP4 is a list of parameters which, if not chosen correctly, can lead to erroneous results. The list includes the choice of coordinate system, time system, and discrepancies in the format of TLE data. These and other parameters have caused much confusion over the last 30+ years, but extensive resources exist that could minimize future misunderstanding (6; 8; 22).

With that said, the coordinate system of TEME (true equator, mean equinox) of Date, time system of UTC, and TLE format described at Space Track and CelesTrak are accepted for this study. Kelso points out another critical concept applicable to this study:

> *Only ideal orbits describe true ellipses and have constant orbital elements. Real orbits experience both periodic and secular (trending) effects in their elements. Because of this, orbital element sets with different epochs will have different values (and different associated errors) for the remaining orbital elements.* (11)

Finally, an assumption made throughout this work involves the accuracy of SGP4 propagation within STK7.0. Based on work by Vallado and Kelso, the author assumes the SGP4 propagation routine within STK matches the official AFSPC version well enough for purposes of this study (10:2; 22).

Two-Line Element Sets.

A two-line element set is a representation of a satellite's orbital elements with additional information specific to that satellite. Comprised of two 69-character lines of data, TLEs contain information about the satellite such as the Catalog Number, International Designator, and a SGP4 term for the atmospheric drag of the object. The TLE values for inclination, right ascension of the ascending node, eccentricity, argument of perigee, mean anomaly, and mean motion represent six independent measurements which describe the motion of the satellite. The epoch defines the time to which all of the time-varying fields in the element set are referenced (11). Equation 2.1 lists these six elements in familiar Keplerian classical orbital element (COE) notation (note the overbar signifies mean value)

$$i \qquad \Omega \qquad e \qquad \omega \qquad M \qquad \bar{n} = \sqrt{\frac{\mu}{\bar{a}^3}} \tag{2.1}$$

An additional term included in a two-line element set is the B* atmospheric drag-like term, which is not constant. According to Vallado, it is "always modified" from one TLE to the next and essentially "an arbitrary free parameter in differential correction" (19:115). B* has units of (Earth radii)$^{-1}$ and is found by

$$B^* = \frac{1}{2}\frac{c_D A}{m}\rho_0 R_\oplus \tag{2.2}$$

where

c_D = *coefficient of drag*
A = *satellite cross-sectional area*
ρ_0 = *atmospheric density at perigee*
m = *mass of satellite*
$R_\oplus$ = *radius of Earth*

TLEs contain additional terms that are used by SGP, but not by SGP4. These terms include the first time derivative of mean motion and second time derivative of mean motion. Figure 2 illustrates the format and content of a two-line element set. The top line, referred to as Line 0, is not a standard part of the TLE. It is an optional addition to a TLE which identifies the name of the satellite—NOAA 6 in this example. On Space-Track, users have the option to include this line when requesting TLE data. A more detailed explanation of the format and of each character in a two-line element are provided in Appendix A.

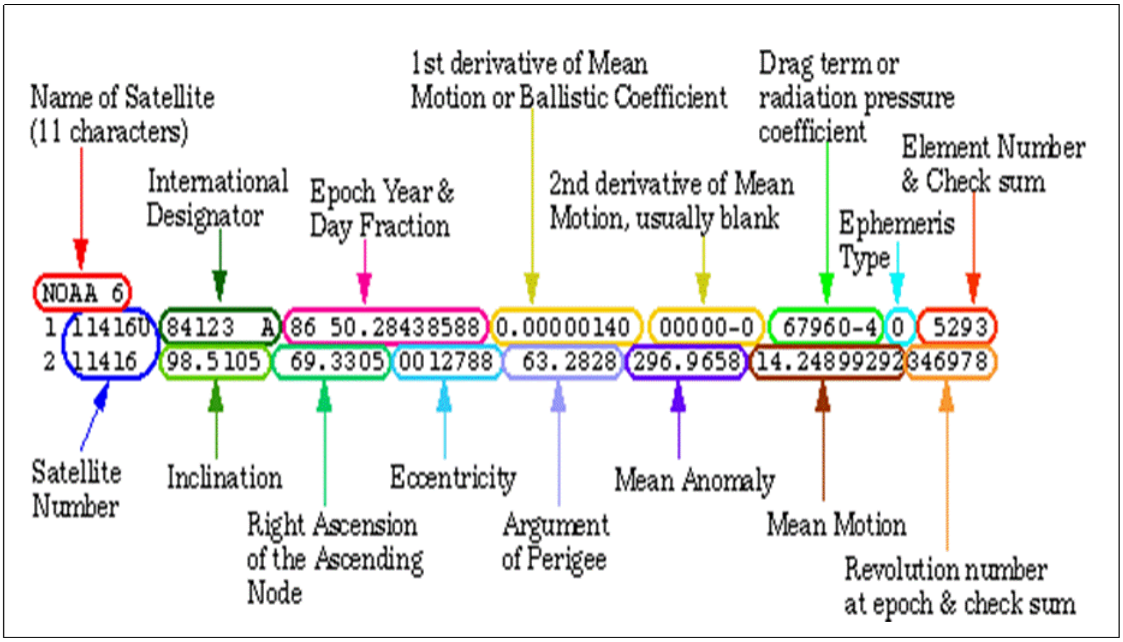

Figure 2. NORAD Two-line Element Set (15)

Estimation Theory

The foundation of estimation theory consists of several fundamental concepts, such as the Central Limit Theorem, multidimensional probability theory, Gaussian distribution functions, the estimation operator, and techniques of linearization for nonlinear dynamical systems. The method of least squares, credited to Karl Gauss, relies on the Principle of Maximum Likelihood, both of which are described below. A weighted average can be utilized to reflect the a priori assumptions of the accuracy of different instruments, or of measurements, when solving for a desired estimate. The following is assembled from Wiesel (25).

Central Limit Theorem.

As the "keystone of estimation theory" the Central Limit Theorem "justifies the assumption that the error statistics of measured data will be Gaussian" (25:8). Consider a measurement x_i comprised of three parts $x_i = x_0 + e_i + b$ where x_o is the true value, e_i is the true random error in the measurement, and b is the bias. Given a large number N of independent errors e_i, the total error sum is given as

$$e = \sum_{i=1}^{N} e_i \tag{2.3}$$

After assigning the unknown probability distribution for each error e_i as $w(e_i)$, and as long as there is no dominate individual error source, the Central Limit Theorem holds true that a large number of measurements will be Gaussian. The probability distribution of the total error is shown to be

$$f(e) = \frac{1}{\sqrt{2\pi}\sigma} \exp\left\{ -\frac{\left(\langle e \rangle - e\right)^2}{2\sigma^2} \right\} \tag{2.4}$$

where $\langle e \rangle$ is the mean error of the measurements and σ is the standard deviation. Unbiased measurements should have a mean error of zero. However, if there is a dominating error source e_d, then $e \approx e_d$ and the probability distribution of the total error is $f(e) \approx w(e_d)$.

When dealing with unbiased measurements with Gaussian error statistics, the estimation operator $E(-)$ is used to show three fundamental concepts. First, defining the estimator operator as

$$E(-) = \int_{-\infty}^{\infty} (-)\, f(x)dx \tag{2.5}$$

where $f(x)$ is the probability density function (assumed to be Gaussian), the three fundamental concepts (25:19) are:

- The expected value of a measurement is the true value, or $E(x) = x_0$. (The true value is not likely to be known, however)
- The average error of the measurements equals zero, meaning $E(e) = 0$
- The average squared error is known as the variance, shown as $E(e^2) = \sigma^2$

If a bias is noticed and can be calculated, it should be removed thereby allowing the measurements to be treated as unbiased.

Principle of Maximum Likelihood.

Starting with *N* independent measurements, x_i, of a desired true value, *x*, and the standard deviation of that data, σ_i, then the joint probability of achieving this set of data is the product of the individual Gaussian distributions

$$P(x_1, x_2, ..., x_n) = (2\pi)^{-\frac{N}{2}} \left[\prod_{i=1}^{N} \sigma_i^{-1} \right] \times \exp\left(-\sum_{i=1}^{N} \frac{(x_i - x_o)^2}{2\sigma_i^2} \right) \tag{2.6}$$

Yet the true value is unobtainable, so replacing x_0 with an estimate, $\bar{x}$, yields

$$P(x_1, x_2, ..., x_n) = (2\pi)^{-\frac{N}{2}} \left[\prod_{i=1}^{N} \sigma_i^{-1} \right] \times \exp\left(-\sum_{i=1}^{N} \frac{(x_i - \bar{x})^2}{2\sigma_i^2} \right) \tag{2.7}$$

To obtain the maximum probability of Equation (2.7) with respect to $\bar{x}$, the exponential term, being negative, should be minimized. Taking the derivative of the argument and setting it equal to zero leads to the following steps

$$\sum_{i=1}^{N} \frac{(x_i - \bar{x})}{\sigma_i^2} = 0 \tag{2.8}$$

and solving for the desired value of the estimate

$$\bar{x} = \frac{\sum_{i=1}^{n} \frac{x_i}{\sigma_i^2}}{\sum_{i=1}^{n} \frac{1}{\sigma_i^2}} \tag{2.9}$$

This method is commonly known as the method of least squares.

Covariance Matrix.

This section covers how a covariance matrix is formulated, what information it contains, how it propagates with a dynamic system, and how transformations of the covariance matrix are performed.

The covariance matrix, *P*, of an object can be used to compute the probability that it will be in a certain region of space. As an indication of the statistical correlation between random variables, the covariance is the expectation of the product of deviations of those variables from their means (4:31). For any vector, *v*, the covariance can be expressed as

$$P_v = E\left[(v - m)(v - m)^T \right] \tag{2.10}$$

where *m* is the mean of the vector, or $m = E[v]$. The expected value of a vector is the vector containing expected values of the respective elements (4:34).

Conversely, allow a system state vector, X, to be assembled from the position and velocity vectors of a satellite at a given epoch. Wiesel shows the state vector can be specified with respect to time by writing the equations of motion (25:31).

$$\frac{dX}{dt} = g(X,t) \tag{2.11}$$

or if the explicit solution is known in terms of an initial state vector and time

$$X(t) = h(X(t_0),t) \tag{2.12}$$

Either of these equations specify how the true state vector, X_0, the estimated state, $\bar{X}$, and any nearby trajectories change with time.

If we collect N independent measurements, or predictions, of the state vector X_i then the true errors of the measurements could be calculated. However, according to Wiesel, we never can really know the true state vector and thus cannot calculate the true errors (25:21). Substituting the true state with a chosen best estimate, $\bar{X}$, and the true errors with the residuals, we can write

$$\delta X_i = X_i - \bar{X} \tag{2.13}$$

where δX_i are the residuals in the state vector estimates. The covariance matrix of the state vector under these assumptions is found to be

$$P_X = E\left[\left(\delta X_i - m\right)\left(\delta X_i - m\right)^T\right] \tag{2.14}$$

where *m* is a vector comprised of the mean elements of the respective elements of the residual state vectors.

For a state vector of length *n*, the covariance matrix is an $n \times n$ symmetric matrix with diagonal entries, known as variances, equal to the mean squared errors of the state variables. Off-diagonal terms are indicators of cross-correlation between elements of the state. Positive values indicate a direct dependence and negative values an inverse one.

As long as the error in the state remains small, it can be propagated by means of the state transition matrix Φ in the following relationship

$$\delta X(t) = \Phi(t, t_0)\, \delta X(t_0) \tag{2.15}$$

Since we are dealing with deterministic dynamics, the covariance at time t_0 can be found, also using the state transition matrix

$$P_X(t) = \Phi(t, t_0)\, P_X(t_0)\, \Phi^T(t, t_0) \tag{2.16}$$

State vector error covariance growth is usually dominated by the initial position and velocity covariance. But a second contributor to the growth is the force model used for propagation. Incorrect, or insufficient, modeling of the present forces will contribute to the uncertainty.

It is common for the covariance matrix to undergo a transformation of variables or coordinate systems. Vallado provides several useful satellite flight dynamics covariance transformations in detailed form (21). For a simple example, assume that the variables *x* and *y* are related to one another by the rotation matrix *R* as

$$\delta x = R\, \delta y \tag{2.17}$$

Now let P_x be the covariance in terms of the *x* variables. The covariance in terms of the *y* variables can be found by two rotations

$$P_y = R^T P_x R \tag{2.18}$$

Autocorrelation

Suppose we have an ensemble of functions of time (measurements) resulting from a random process, with $\{x(t)\}$ denoting the ensemble and $x(t)$ representing any observed member. The first moments of the probability distribution function are commonly measured and referred to as the autocorrelation and cross-correlation functions (4:36). Specifically, the autocorrelation function is defined as

$$\varphi_{xx}(t_1,t_2) = E\left[x(t_1)\,x(t_2)\right] = \int_{-\infty}^{\infty} dx_1 \int_{-\infty}^{\infty} dx_2\; x_1\, x_2\; f_2\left(x_1,t_1;x_2,t_2\right) \tag{2.19}$$

where the joint probability density function is

$$f_2\left(x_1,t_1;x_2,t_2\right) = \frac{\partial^2 F_2\left(x_1,t_1;x_2,t_2\right)}{\partial x_1\,\partial x_2} \tag{2.20}$$

When $E\left[x(t_1)\right]$ and $E\left[x(t_2)\right]$ are both zero, the autocorrelation function equals the covariance of the random variable, P_x (4:36).

Given a string of data, z_i for $i=1,2\ldots,N$ taken at constant time intervals, Δt, Gelb offers the sample mean and sample autocorrelation function (4:86) as

$$m = \frac{1}{N}\sum_{i=1}^{N} z_i \tag{2.21}$$

$$\hat{\varphi}_{zz}(\ell \Delta t) = \frac{1}{N-\ell} \sum_{i=1}^{N-\ell} (z_i - m)(z_{i+\ell} - m)^T \quad , \text{ for } \ell = 0,1,...,N-1 \tag{2.22}$$

where $\ell \Delta t$ represents the shift parameter, or lag. This function is also referred to as the auto-covariance, and is regarded as "unbiased" because it corrects for the number of overlapping elements when it divides by the $(N-\ell)$ term. A useful next step is to divide Equation (2.22) by the variance of the data to get a normalized autocorrelation function, which results with a value of 1.0 for zero lag shift (5). The final calculation is

$$R_z = \frac{\hat{\varphi}_{zz}(\ell \Delta t)}{\sigma_z{}^2} \tag{2.23}$$

Relevant Research

A literature search revealed a handful of previous studies which involved estimating or evaluating a covariance matrix for NORAD TLEs. Many of these studies seemed to be driven by improving conjunction analysis. Most had access to higher accuracy (than TLEs) orbital elements from commercially-controlled satellites or the actual SSN observations from which to compare TLEs. The studies covered most all orbit types (i.e. LEO, GEO). However, actual covariance or variance values were not commonly included in these reports.

COVGEN Study. (16)

In 1999, Aerospace Corporation started a program called Covariance Generation (COVGEN) with the purpose of generating general error information based solely on public TLEs. COVGEN was intended for improving collision avoidance analysis. Peterson et al. reported that COVGEN "produced reasonable estimates of the error for

approximately 58% of all of the objects in the space catalog" for the 18-month study period. Additionally, 99% of COVGEN error ellipsoids for certain GEO satellites—meaning a TLE state vector plus its own unique COVGEN covariance—included the "true" state vectors obtained from high precision commercial sources (16:201-207).

Their method started with a pair-wise differencing of a set of TLEs for a 14-day time span, then computed residuals (observed – calculated measurements) in a satellite-based coordinate system, performed a quadratic least squares fit, calculated a standard deviation from those, and removed outliers (TLEs beyond 3-sigma). They then calculated a second best fit of the remaining residuals, and used that as the time-varying error estimation.

Peterson and his co-authors used a separate method for determining the error at epoch because of the noisiness of the raw differences. The error at epoch for LEO satellites were determined by calculating the root-sum-square (RSS) of the observations in each component over the first 1.5 days (16:203). For higher altitude objects, they directly compared each SGP4 TLE to a high-precision state vector available from a commercial source.

The subsequent covariance estimate was comprised of the initial error at epoch plus the time-dependent error growth. This included both linear and quadratic terms, and represented the best fit through the observations using a least squares estimate. Wanting to establish a covariance that including the actual RTN—the satellite-based coordinate system chosen—differences, they scaled the final covariance estimate based upon how

many of the RTN residuals were within the estimated ellipsoid, referencing them to a standard normal distribution and choosing 3-sigma as the goal.

Peterson et al. found that LEO satellites had a worse average percentage of estimation accuracy than other orbit classes, which is understandable given they are subject to larger forces of drag. Lastly, the COVGEN error ellipsoids were a lower precision covariance, (termed "SGP4 quality") compared to a high-precision covariance.

One aspect of the COVGEN study that was not completely clear was the exact manner in which the TLEs were propagated to each other with SGP4 and how the RTN differences for a 14-day time interval were computed. Stating "a time series of [TLEs] over an arbitrary time span for a given object is reduced to a set of RTN differences over a 14-day time span" does not convey the methodology used (16:202).

This thesis, in many ways, is an extension of the COVGEN work. Whereas Peterson's team omitted outlying TLEs and calculated an initial error at the epoch separately, they did not remove observed biases from each component. Also, the fit span used in their calculation of the covariance was an 18-month window over which Aerospace had collected NORAD TLEs. This thesis uses only the 14-day time window from which TLEs are gathered to calculate the covariance matrix and accounts for (subtracts) the biases in each component. This methodology is explained in more detail in Chapter III.

Space Warfare Center Assessment. (9)

Kaya and Snow developed a program that could evaluate element set prediction accuracy for the entire space catalog. Their method assigned a rating to individual

satellites based on the accuracy of its element sets when compared to SSN observations. Using SGP4, they performed 10-day predictions for orbits with a period under 225 minutes, and 30-day predictions for longer period satellites. A few aspects of their research are implemented in this thesis, including binning the residual data and using a quadratic least squares fit. However, they did not remove biases from the computed residuals, meaning they assumed zero mean and a normal distribution (9:1941). Further, covariance matrices, if calculated, were not reported in this study.

INTELSAT Comparisons. (2)

Chan and Navarro conducted a study of time history differences between TLE and INTELSAT orbital elements. Their study covered 1 year of data, focusing on INTELSAT satellites in GEO. Starting with TLE orbital elements and using a tested version of the TLE propagator SDP8 for GEO, they compared with INTELSAT-proprietary orbital elements derived from their dual station ranging system. Their force model including the geopotential harmonic coefficients as well as complete solar and lunar perturbations. They observed "systemic biases in the orbit differences over different ocean regions…from time history plots" and suggested "one reason for the biases could be attributed to the differences in the modeling of the terrestrial geopotential harmonics between TLE model and INTELSAT model" (2:776).

Their results showed the largest difference between the TLE and INTELSET orbit propagations (given in the orbital reference frame) was in the transverse (along-track) direction, 2 orders of magnitude larger than the radial and normal directions differences.

Chan and Navarro further studied the effects of a satellite station-keeping maneuvers to investigate if TLE orbital elements would degrade (even for a single TLE) as a result of the maneuver. They found that "there is no significant degradation in the TLE accuracy due to station-keeping maneuvers within a TLE update cycle" as well as "no apparent correlation between the errors at TLE updates and the proximity of maneuvers prior to the update" (2:777). Lastly, Chan and Navarro investigated the short-term perturbations for semi-major axis. Using their truth data values and truth data mean for semi-major axis, they found a simple method for adding back in the short-term perturbations from the sun and moon that are not accounted for in the TLEs. This method reduced the residual errors between their truth and the TLEs.

IRIDIUM Comparison. (1)

This study focused on 9 Iridium satellites in pure drifting orbits (non-maneuvering and non-station kept), for varying time periods. The satellites were in near-circular (frozen) orbits at altitudes ranging from 672 km to 710 km.

Starting with a "truth reference" database of orbit estimates for these Iridium satellites, Boyce III evaluated a large set (~2600) of corresponding NORAD TLEs for their accuracy and "to assess the efficacy of using [them] for collision avoidance." By calculating the differences of the in-track and radial positions between the truth and TLE orbits at corresponding epochs, Boyce's goal was to "quantify these differences, which are ascribed to TLE error, in terms of the known standard deviations of the Iridium measurements" (1:2133).

Boyce determines a least squares best fit between the true IRIDIUM data and corresponding TLEs, then computes standard deviations which collectively serve as his "probability cloud." Boyce compares the fit and probability cloud thus derived with the orbit state represented by the TLE itself in order to determine the TLE accuracy. This final comparison is made at the epoch of the TLE. Expectations are that the "true" position of the satellite should be within 3 standard deviations in each dimension.

The author restricts his analysis to a two-dimensional, in-plane view of the problem, ignoring the cross-track motion as it is "negligible…since the primary perturbations over small time scales are drag and radiation pressure" (1:2134).

Quoting a standard deviation of 2-4 meters for his truth model, Boyce states it's "not unusual for the NORAD semi-major axis (SMA) to be in error by several tens of meters at epoch." After plotting the differences between the TLE-derived mean SMAs and the true mean SMA derived from the "true" Iridium orbit determination, Boyce notices a draping effect in parts of the graphs. There appears to be some structure in the plots; a monthly oscillatory pattern is noticeable in a few different areas of Boyce's graphs.

The graphs show the largest concentration of differences in the +/- 50 meter region for SMA. In one figure, there is a secondary concentration of differences in SMA values, between +100 to +150 meters. This bifurcation effect becomes less apparent, meaning the data points appear more random, during other time spans. He goes on to investigate these areas related to the large-scale trend of atmospheric drag experienced by the Iridium satellites as a group. Noting times of increased a-dot due to drag coinciding

with the more random time spans, Boyce overlays a plot of negative drag a-dot values over his ΔSMA plots. The overlay appears to match well, indicating times of maximum drag are responsible for the disappearance of the bifurcation (1:2137).

Finally, Boyce shows an oscillatory pattern in the in-track error, equal to approximately 1 month. Stating this pattern is "inherent in the NORAD data", Boyce suggests the pattern may be due to the monthly solar cycle, but recommends more research (1:2138).

III. Methodology

This chapter covers the methodology by which the covariance and autocorrelation relationships are estimated. Prior to tackling the primary objectives, preliminary work is required, including selecting the satellites and time windows of interest, gathering TLE data, and choosing a "truth" reference orbit from which to evaluate propagation estimates. Next, coordinate system choices and transformations are defined. The method by which the TLEs are propagated and compared to each other follows, accompanied with an explanation of data binning. Finally, the actual formulations of the covariance matrix at the primary epoch of each time window and the autocorrelation function for each satellite are discussed.

Satellite Selection

The selection of satellites for analysis was based on a number of factors. The first consideration was selecting satellites for which post-processed, highly accurate, reference orbits existed in the event they could be treated as "truth" orbits. Precise Orbit Ephemeris (POE) data exists for most Global Positioning System (GPS) satellites and several geodetic satellites, which typically have on-board laser reflectors used for precise range measurements. With Earth-based satellite laser ranging (SLR) capabilities of ~1cm range accuracy, post-processed POE data is often used as truth data (19:243). These truth orbits enable very accurate comparisons of the TLE propagation estimates as well as evaluations of the accuracy of any derived covariance matrix. The second consideration was selecting TLE sets from satellites in different orbit altitudes in order to investigate

different perturbation forces, such as atmospheric drag in LEO and solar radiation pressure. Lastly, time windows for TLE propagation were selected based on anticipated availability of POE data and the possibility of witnessing trends due to varying solar activity. Given these criteria, the selected satellites and some of their orbital elements (approximated) are summarized in Table 1.

Table 1. Summary of Satellites

Study #	Satellite Name	Catalog Number	Orbit Altitude	Eccentricity	Inclination	B*
1	LAGEOS-1	# 08820	5,850 km	0.004	109.8	0.0001
2	TOPEX	# 22076	1,340 km	0.0008	66	0.0001
3	GPS IIR-03	# 25933	20,140 km	0.0015-0.0036	52	0
4	GRACE-1	# 27391	480 km	0.0014 – 0.0022	89	Varies
5	ICESAT	# 27642	600 km	0.0002 - 0.0011	94	Varies
6	FAST	# 24285	350 km perigee to 4,150 km apogee	0.2	82.9	Varies

Satellite6, the FAST satellite, is included to have at least one non-circular orbit. FAST is not a geodetic satellite; therefore it is not assumed that POE data exists for it. However, as a LEO satellite with an eccentricity of ~0.2, it is expected that FAST experiences a number of perturbative forces which are of interest for analysis purposes, such as atmospheric drag, solar radiation pressure, and third-body effects.

The selected time windows are summarized in Table 2. Dates are provided in three formats: by TLE epoch date format for year and date (YYDDD), calendar date, and Julian date. Each time window covers fifteen full days. For example, in the first time

window, all TLEs between 0000 hours on 1 March 2003 and 2400 hours on 15 March 2003 will be pulled from the raw TLE data files and propagated per the method described below. As stated before, all TLEs used in this study were obtained from CelesTrak.com, primarily for consistency purposes.

Table 2. Summary of Time Windows

	TLE format (YYDDD)		Calendar Date		Julian Date	
Time Window	Start Date	End Date	Start Date	End Date	Start Date	End Date
1	03060	03075	1-Mar-03	16-Mar-03	731641	731656
2	03079	03093	20-Mar-03	3-Apr-03	731660	731674
3	03270	03285	27-Sep-03	12-Oct-03	731851	731866
4	03290	03305	17-Oct-03	1-Nov-03	731871	731886
5	04045	04060	14-Feb-04	29-Feb-04	731991	732006
6	04065	04080	5-Mar-04	20-Mar-04	732011	732026
7	04150	04165	29-May-04	13-Jun-04	732096	732111
8	04280	04295	6-Oct-04	21-Oct-04	732226	732241

Satellite-based Coordinate Systems

Coordinate systems which are based in the orbital plane of the satellite—with the origin moving in sync with the satellite as it orbits the Earth—have many advantages over Earth-based systems such as describing relative motion or investigating effects of drag. Two satellite-based coordinate systems of particular interest for this study are described below. Both have two axes in the orbital plane with the third axis normal to that plane. For

RTC Coordinate System. (21)

The RTC system (for radial, transverse, and cross-track) is one satellite-based coordinate system utilized in this study. It is also known as RSW or RTN. The R axis always points from the Earth's center along the radius vector (position vector) toward the satellite, as it moves through its orbit. Dividing by its magnitude provides the R unit vector. The C axis is found by crossing the radius vector into the velocity vector, and normalizing it gives the C unit vector. Finally, the direction of the T axis and the T unit vector are found by crossing the C and R unit vectors. The T axis is in the orbital plane, perpendicular to the radius vector.

Given a state consisting of a position $\vec{r}$ and velocity $\vec{v}$ which are in Earth Centered Inertial (ECI) coordinates, the unit vectors and transformation matrix for the RTC coordinate system are given in Equation (3.1). (See Vallado (19:157-158) for a definition of the ECI coordinate system).

$$\hat{R} = \frac{\vec{r}}{|\vec{r}|} \quad , \quad \hat{C} = \frac{\vec{r} \times \vec{v}}{|\vec{r} \times \vec{v}|} \quad , \quad \hat{T} = \hat{C} \times \hat{R}$$

$$R_{ECI \to RTC} = \left[\hat{R} \vdots \hat{T} \vdots \hat{C} \right]^T \tag{3.1}$$

$$\vec{r}_{RTC} = R_{ECI \to RTC} \, \vec{r}_{IJK} \quad , \quad \vec{v}_{RTC} = R_{ECI \to RTC} \, \vec{v}_{IJK}$$

The transverse axis (T) points in the direction of, but not necessarily parallel to, the velocity vector. It is exactly collinear to the velocity vector for circular orbits or at apogee and perigee for elliptical orbits. Also, differences measured in the transverse

direction are commonly known as along-track displacements, or errors, and differences measured in the C axis direction are known as cross-track errors.

The RTC coordinate system is "often used to describe orbital errors, relative positions, and displacements of satellite orbits" (21:8).

VNC Coordinate System. (21)

The second satellite-based coordinate system of interest is the VNC (for velocity, normal, and cross-track). This system is also known as the NTW system. The V axis is tangential to the orbit and always points to the velocity vector. The C axis is found the same way as for the RTC system above—by crossing the position vector into the velocity vector. The N axis lies in the orbital plane, normal to the velocity vector, and is found by crossing the V unit vector into the C unit vector. The VNC coordinate system and transformation matrix from a state vector of position, $\vec{r}$, and velocity, $\vec{v}$, which are given in Earth Centered Inertial (ECI) coordinates are found by

$$\hat{V} = \frac{\vec{v}}{|\vec{v}|} \quad , \quad \hat{C} = \frac{\vec{r} \times \vec{v}}{|\vec{r} \times \vec{v}|} \quad , \quad \hat{N} = \hat{V} \times \hat{C}$$

$$R_{ECI \to VNC} = \left[\hat{V} \vdots \hat{C} \vdots \hat{N} \right]^T \tag{3.2}$$

$$\vec{r}_{VNC} = R_{ECI \to VNC} \, \vec{r}_{IJK} \quad , \quad \vec{v}_{VNC} = R_{ECI \to VNC} \, \vec{v}_{IJK}$$

Displacements along the velocity vector are known as in-track errors, which are not the same as along-track variations in the RTC system. The distinction is that in-track errors are in the direction of the V axis, parallel to the velocity vector. Along-track

variations are in the direction of the T axis, which is along the velocity vector (21). If the satellite is in a circular orbit, these two coordinate systems (RTC and VNC) align.

The VNC coordinate system is helpful when analyzing effects due to drag since drag always acts along the relative velocity vector. Depending on the satellite altitude, this system is also useful for solar radiation pressure (SRP) analyses (21:9).

Orbit Propagation

The focus of this study involves estimating the covariance matrix and the autocorrelation function for a set of TLE data. To achieve this, comparison differences between the TLEs are needed. The method employed to generate the comparison data involves propagating all of the TLEs in a given time window to specific times, then calculating the difference between the estimated state vectors. The specific times are chosen to be the exact epochs of the respective TLEs. The state vector differences are known as residuals. All of the residuals are then combined to compute the two desired quantities.

For this study, orbit propagation is achieved using SGP4 within STK7.0. Utilizing the STK/MATLAB Interface, an algorithm written in MATLAB calls the SGP4 orbit propagation routine via MATLAB Aerospace Toolbox (ATB) commands. MATLAB reads in TLEs from locally saved source data files downloaded from CelesTrak. The methodology for accomplishing the orbit propagation is discussed next, followed by an explanation of binning the residual data.

For a given time window, the last (most recent) TLE epoch is considered the prime epoch, t_0. All TLEs are propagated forward in time to the epochs of each and every TLE that is more recent than it. See Figure 3 for an illustration of this technique.

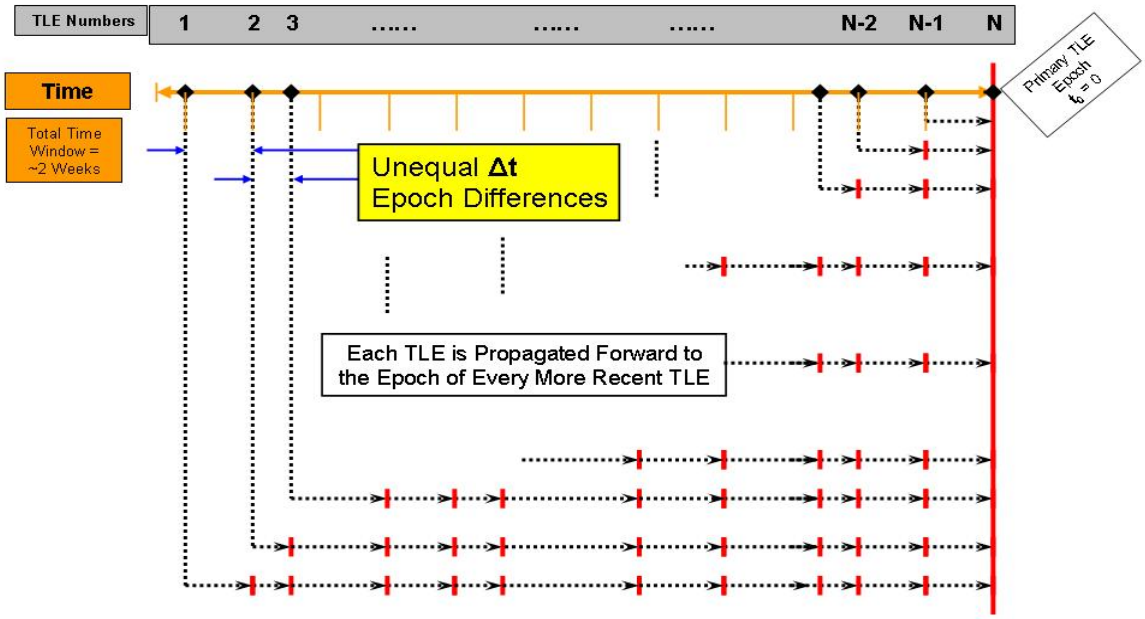

Figure 3. Pair-wise Differencing Propagation Method

TLE Pair-Wise Differencing.

The TLE pair-wise differencing employed in this study necessitates explanation. To avoid confusion, the N^{th} TLE for a given time window is always considered the "prime" TLE of interest. During the propagation algorithm, the term "primary TLE" applies to the TLE whose turn it is for the others to be propagated to it. This identification transfers sequentially from one TLE to the next.

Starting with the N^{th} TLE as the first "primary", the position $\vec{r}$ and velocity $\vec{v}$ vectors are computed at its own exact epoch. These vectors are now considered the "calculated" measurements as well as the best estimate of the state vector at this epoch. Initially computed in the Earth Centered Fixed (ECF) coordinate system, they are converted to Earth Centered Inertial (ECI). These two steps are done using MATLAB ATB commands. The ECI vectors are transformed to the satellite-based coordinate systems explained above, RTC and VNC, and their respective transformation matrices are saved for future calculations.

Next, the $(N-1)^{th}$ TLE (termed "secondary TLE") is propagated forward to the exact epoch of the primary TLE, and its position and velocity vectors are determined. Again, these secondary vectors are determined in the ECI coordinate system. These vectors are considered the "observed" measurements. The relative position and velocity vectors are then determined in the ECI frame following the traditional order (25) of (observed – calculated = residual) by Equation (3.3):

$$\begin{aligned} \delta\vec{r}_{ECI} &= \vec{r}_{observed} - \vec{r}_{calculated} \\ \delta\vec{v}_{ECI} &= \vec{v}_{observed} - \vec{v}_{calculated} \end{aligned} \tag{3.3}$$

Next, the ECI residual vectors are transformed to both satellite-based coordinate systems using their respective transformation matrix from the primary TLE transformation above. The importance lies in that the residuals are now based in the satellite coordinate system established by the primary TLE. In other words, the primary TLE establishes the origin for its satellite-based coordinate system and all secondary

TLEs propagated to it are referenced from that origin. Transforming the residual vectors (the VNC coordinate frame residuals are found in the same exact manner) by

$$\delta\vec{r}_{RTC} = R_{ECI\rightarrow RTC}\,\delta\vec{r}_{ECI}$$
$$\delta\vec{v}_{RTC} = R_{ECI\rightarrow RTC}\,\delta\vec{v}_{ECI} \tag{3.4}$$

The N^{th} TLE remains the primary until every TLE in the time window has been propagated to its epoch. The steps above are repeated for each secondary TLE and their results are stored. The first batch of residuals, when the primary TLE is the prime TLE of the time window, is of particular interest because the covariance matrix is computed from them. The next section discusses this in more detail.

Following the computation of the residuals related to the N^{th} TLE, the $(N-1)^{th}$ TLE becomes the new primary and the entire propagation loop repeats. For this second iteration, one less comparison will be made as there is one less TLE to "reach back to" and propagate to the primary epoch. Eventually, the 2^{nd} TLE in the time window becomes the final primary TLE, and only the 1^{st} TLE is propagated to its epoch, giving us one last set of residual vectors. All of the above steps are performed for both the RTC and VNC frames.

Throughout the pair-wise differencing the epoch time difference, Δt, of every comparison between a primary and secondary TLE is stored. These epoch differences will determine where the residual data will be binned in the subsequent section of the methodology. An important aspect of this study is the manner in which the binned data is handled for different computations.

Data Binning.

In Chapter II, the discussion on autocorrelation made an assumption of observations taken at equal time intervals. Unfortunately, TLE "observations" are provided at unequal time intervals. Therefore the Δt values resulting from the pair-wise comparison can be any value. The set of position residuals, $\delta\vec{r}_m$, and velocity residuals, $\delta\vec{v}_m$, where m = 1 to the number of differenced TLE pairs, are binned according to the corresponding epoch time difference, Δt_m. Table 3 shows the breakdown of the bins. Choosing appropriate bin sizes is a trade between the error that will be introduced by translating observations in time and the number of observations available in each bin. Bin intervals of one day are chosen to keep the overall computational time reasonable for this initial study.

Table 3. Delta Epoch Bin Ranges for 15 Bins

	TLE Epoch Difference (in days)	
Bin #	**Minimum**	**Maximum**
1	**>0**	**<0.5**
2	**≥0.5**	**<1.5**
3	**1.5**	**2.5**
4	**2.5**	**3.5**
5	**3.5**	**4.5**
6	**4.5**	**5.5**
7	**5.5**	**6.5**
8	**6.5**	**7.5**
9	**7.5**	**8.5**
10	**8.5**	**9.5**
11	**9.5**	**10.5**
12	**10.5**	**11.5**
13	**11.5**	**12.5**
14	**12.5**	**13.5**
15	**13.5**	**14.5**

Statistics Formulations

There are three major areas of computation which use the results of the pair-wise propagation comparisons. The first is a statistical analysis of all the position residuals, $\delta\vec{r}_m$, by bin number. Again, m = 1 to the number of differenced pairs. The second is a generation of the covariance matrix for the state vector of the prime TLE. This covariance uses only the position and velocity residuals which are computed at the epoch of the prime TLE. Finally, the autocorrelation function is formulated for each satellite, combining position residuals from all eight time windows into a larger set of data, $\{\delta\vec{r}_m\}$.

Position Residuals.

Statistics on the entire set of position residuals are computed, enabling the accuracy and variability of the TLEs to be investigated in reference to the amount of time they were propagated. The mean, variance, and standard deviation of each bin are computed. All three depend on the number of samples in the bin, N_b for $b = 1,2,...,15$. The three statistics are found in each component of the position residual data (VNC and RTC) for each bin. The mean, variance, and standard deviation by bin number are

$$\vec{m}_b = \frac{\sum_{i=1}^{N_b}\left(\delta\vec{r}_i\right)}{N_b} \tag{3.5}$$

$$\vec{\sigma}_b{}^2 = \frac{\sum_{i=1}^{N_b}\left(\left(\delta\vec{r}_i\right)^2\right) - \left(N_b\ \vec{m}_b{}^2\right)}{\left(N_b - 1\right)} = \frac{\sum_{i=1}^{N_b}\left(\left(\delta\vec{r}_i\right)^2\right) - \frac{\left(\sum_{i=1}^{N_b}\left(\delta\vec{r}_i\right)\right)^2}{N_b}}{\left(N_b - 1\right)} \tag{3.6}$$

$$\bar{\sigma}_b = \sqrt{\bar{\sigma}_b^{\,2}} \tag{3.7}$$

Although these quantities are computed for sample sizes $N \geq 2$, in many instances the bins have small sample sizes. Therefore, conclusions from this study should be viewed as preliminary only. In the event a bin has less than two sample points, these values are not computed and that bin will not be evaluated.

Covariance Matrix Generation.

A primary objective of this thesis is estimating the covariance of a dynamical system. Treating each TLE propagated to the epoch of the Nth TLE as independent estimates of the state vector, the deviation of those measurements about the true state vector, X_o, is the true error, e_i. As the true state is unknown, the best estimate of the state vector is substituted. In this study the computed Nth TLE state vector, $\bar{X}_{epoch}$, is considered the best estimate of the state. Since the true state is unknown, the true error cannot be known either and must be substituted with the residuals at the epoch, δX_{epoch}, which are found from the propagated estimates. The residuals and their mean can now be used to compute the covariance matrix of the state vector. From Equation (2.14), formulating the covariance matrix, *P*, of the state vector, $\bar{X}_{epoch}$, begins with

$$P_{epoch} = E\left[\left(\delta X_{epoch} - m\right)\left(\delta X_{epoch} - m\right)^T\right] \tag{3.8}$$

leading to

$$P_{epoch} = \frac{\sum_{i=1}^{N-1} \left(\delta X_{epoch} - m \right)_i \left(\delta X_{epoch} - m \right)_i^T}{N-1} \tag{3.9}$$

where N-1 is the number of residuals calculated at the prime epoch. The mean vector of the state vector residuals at the epoch is found by

$$m = \frac{\sum_{i=1}^{N-1} \left(\delta X_{epoch} \right)_i}{N-1} \tag{3.10}$$

When computing the covariance matrix, the binned data is not used and the epoch differences, Δt, are not implemented as any sort of factor or weight. The covariance matrix, originally found in the satellite-based coordinate system, can be transformed back to ECI and even Keplerian classical orbital elements if desired. Equation (2.18) leads to

$$P_{ECI} = R^T \; P_{RTN} \; R \tag{3.11}$$

where R is the rotation from the ECI system to the respective satellite-based coordinate system from Equation (3.3) or (3.4).

Autocorrelation Function.

The autocorrelation function reveals relationships within the data according to a shift parameter, known as lag, which in this study is the difference of the TLE epochs (in days). Actually, the shift parameter is bins, which are based on the TLE epoch differences. Correlation has no units.

Autocorrelation Considerations.

There are two prefatory considerations to note before generating the autocorrelation function. They involve the time interval between data points and the length of data (number of data points). First, the autocorrelation function assumes that the string of data is taken at constant time intervals. The second consideration is that sufficient data is required to prevent statistical limitations. Gelb explains it this way: "finite data length implies an inability to determine the form of an autocorrelation function at large shifts, whereas finite data spacing implies an inability to determine the form at small shifts" (4:89).

The technique of binning the residuals lends itself to the formulation of the autocorrelation function. By binning the residual data, the first concern is eliminated because the data is now spaced at "equal" time intervals. Addressing the second consideration is more challenging, but the following method is implemented in this study to achieve an appropriate length of data.

The pair-wise differencing technique from before resulted in only 15 bins. Recognizing that 15 data points does not constitute a large sample size, an alteration to the bins used for computing the statistics above is made for the bins used for the autocorrelation function. This alteration involves shortening the time span of each bin in order to increase the length of data. An example follows: by "thinning" the bins from 1 day to 0.5 day, the data length can be doubled from 15 to 30. One implication of smaller bins is that at least one data point will still be needed in each bin in order to formulate the autocorrelation function.

Preliminary analysis showed that 0.5 day was a suitable bin width for all scenarios. Narrowing the bins to less than one half day resulted in inconsistent results; an "aliasing"-type effect, in which large fluctuations from one value to the next, was observed. Thus, 0.5 day was chosen as the bin width for all satellites' autocorrelation function.

Propagation Time Window Extension.

Having established the need for binning the position residuals with their associated Δt and selecting the minimum bin width for this study, initial autocorrelation functions were generated. However, using the 15 days of TLE propagation from before proved to be still not a large enough sample size to generate an adequate autocorrelation function. As Glover explains, a "general rule of thumb" for auto-covariance and autocorrelation calculations "is to not let 'n' get any bigger than about one-fifth of 'N' ", where *n* is the largest lag of interest and *N* is the total number of samples (5). The *n* value can also be thought of as the lag which makes the most sense given the physical nature of the data.

Using the suggested bin breakdown of $\Delta t = 0.5$ day for 15 days, then N=30 and n=6, resulting in "legitimate" autocorrelation values for approximately 3 days. This appeared to be an insufficient length of time to evaluate the autocorrelation function. Choosing 7 days as a more suitable length of time to have valid autocorrelation values required 35 days of propagation. Keeping bin widths set to 0.5 day, 35 days of propagation leads to N=70 and n=14, where n=14 equates to 7 days of legitimate results. For a complete table of the bins for this autocorrelation formulation, refer to Appendix B.

Expansion of the propagation window to 35 days was performed only for the autocorrelation portion of this research. The TLE pair-wise differencing technique is repeated exactly as before, meaning the Δt and $\delta \vec{r}$ computations are made in the same manner, but according to the extended time window intervals listed in Table 4.

Table 4. Expanded Time Windows for Autocorrelation

	TLE format (YYDDD)		Julian Date	
Time Window	**Start Date**	**End Date**	**Start Date**	**End Date**
1E	**03040**	**03095**	**731621**	**731676**
2E	**03059**	**03113**	**731640**	**731694**
3E	**03250**	**03325**	**731831**	**731886**
4E	**03270**	**03325**	**731851**	**731906**
5E	**04025**	**04080**	**731971**	**732026**
6E	**04045**	**04100**	**731991**	**732046**
7E	**04130**	**04185**	**732076**	**732131**
8E	**04260**	**04315**	**732206**	**732261**

Extending the time windows may have associated consequences in the results. One such consequence may be that short-term periodic perturbation effects (i.e. solar activity) may be lost. Note the intervals from Table 4 are actually 55 days. The reason for the extra amount of propagation is to obtain a larger sampling of data points that will be binned and eventually averaged, with the intent of achieving a better statistical representation for the measurements. The next section extends this concept by explaining exactly which data are used in the autocorrelation formulation.

Autocorrelation Data Assignment.

Only one value at each time step is required for the autocorrelation function. Therefore, the critical step when using binned data is the mean values of each bin are substituted as the time series measurements. In order to assign a statistically accurate value for each autocorrelation measurement, the number of data samples in each bin is increased by combining all 8 time windows for each satellite. The entire set of position residuals, $\delta\bar{r}_m$, from each extended propagation time window (55 days), are combined. Since each time window is propagated in the same manner, it is assumed the position residuals, $\delta\bar{r}_m$, can be combined from multiple time windows.

Similar to before, the residuals are parsed into bins based on their epoch difference, Δt, which now can range from zero to 55 days. Only residuals with $\Delta t < 35$ days are binned; all others are discarded. The sample points in each bin, N_{bin} affect its mean, therefore must be summed while binning. Similar to a least squares method, the residuals are squared before assigning the autocorrelation measurements, z_i according to

$$z_i = \frac{1}{N_{bin}} \sum_{i=1}^{N_{bin}} \left(\delta r_i\right)^2 \tag{3.12}$$

Now at equal time intervals apart, the binned data represents the 70 data points (35 days at 0.5 days apart) from which the autocorrelation function is generated. Equations (2.22) and (2.23) are implemented with $\Delta t = 0.5\ days$ and $N = 70$ by

$$\hat{\varphi}_{zz}(\ell \Delta t) = \frac{1}{N-\ell} \sum_{i=1}^{N-\ell} (z_i - m)(z_{i+\ell} - m)^T \quad , \text{ for } \ell = 0,1,...,N-1 \tag{2.21}$$

$$R_z = \frac{\hat{\varphi}_{zz}(\ell \Delta t)}{\sigma_z^{\,2}} \tag{2.22}$$

The algorithms implemented in this research are coded and performed in MATLAB. The complete code is provided in Appendix C.

IV. Results and Analysis

With the methodology developed, the TLE pair-wise propagation comparisons can be accomplished and the results analyzed. Examination of the position residuals from the propagation runs provides insight into the dynamics of the satellite as well as the quality of the TLE data. Trends in the resultant plots and covariance matrices represent tools for this analysis. The covariance matrices are presented and evaluated. Finally, the autocorrelation results characterize how the residual data relates to a time-shifted version of itself, thus providing insight into confidence levels of the TLE propagation.

Position Vector Residuals

Plots are produced in both VNC and RTC coordinate systems, but five of the six satellites in this study are in circular orbits, thus their two frames are nearly identical in orientation. The two frames are not identical for Satellite 6, FAST, which has an eccentric (e = ~0.2) LEO orbit. Since drag acts along a satellite's velocity vector, all plots in this chapter will be in the VNC—velocity (in-track), normal (along-radial), cross-track—coordinate system. (The position residual plots for the RTC coordinate frame are practically identical to the VNC plots, adding little insight into this portion of analysis, even for FAST).

To reiterate, residuals are computed by sequentially propagating a secondary TLE to a primary TLE, always in a time-forward propagating direction. The result of this method is a varying reference orbit, or "truth", that is equal to the computed state vector of the primary TLE at its own epoch.

Results from the pair-wise propagation comparisons for the 48 scenarios (6 satellites for 8 time windows) vary dramatically. Given the range of satellite orbits and varying perturbation effects this is expected, but makes analyzing and generalizing the results difficult. For each scenario scatter plots are generated of the position residuals versus the corresponding delta epochs. Two primary characteristics of each scatter plot are analyzed. The first involves the overall curve of the residuals as TLEs are propagated further in time. Specifically, the trend of the errors in each of the different coordinate components as Δt increases. This behavior relates to the dynamics of the satellite and the perturbation effects it experiences. The second characteristic is the width, or deviation, of the residual data as the error trend (first characteristic) moves. This appears to be more indicative of errors in the TLE data itself.

Utilizing bins to show behavior at equal increments of time, error bars are added to each scatter plot. Centered on the mean of the bin and extended in both directions by the standard deviation, sigma (σ), the error bars reflect the accuracy and variability of the residuals bin by bin. Finally a second-order, least squares, best fit curve to all of the residuals in the time window is added. All of these steps are performed separately for each coordinate component.

Figure 4 illustrates both of the characteristics described above. First, all three components have an overall trend in their error from the reference orbit, characterized by scatter points and the best fit curves (dotted lines). The normal and cross-track errors are relatively small in magnitude and have near-constant growth rates. As time advances, the range of errors in the cross-track and normal directions is bounded by approximately 0.25

km. The velocity errors, however, are much larger and grow more rapidly. The velocity component has a maximum error one order of magnitude larger: 2 km after ten days.

Next, observe the spread of the residuals throughout the entire scatter plot. The error bars show the amount of dispersion of the data in each bin. After only one day the velocity component has a substantial variance; the amount of deviation for each bin remains large up to eleven days, reaching a maximum in bin 10. Data past ten days is scarce; typically at these delta epochs, the bin variances decrease while the position residuals maximize. Notice the two velocity component groupings, one between -0.4 and -1.1 km and the other in the bottom right corner of the scatter plot. These groupings indicate inaccuracies of the TLE data itself rather than physical effects of the dynamics or perturbations.

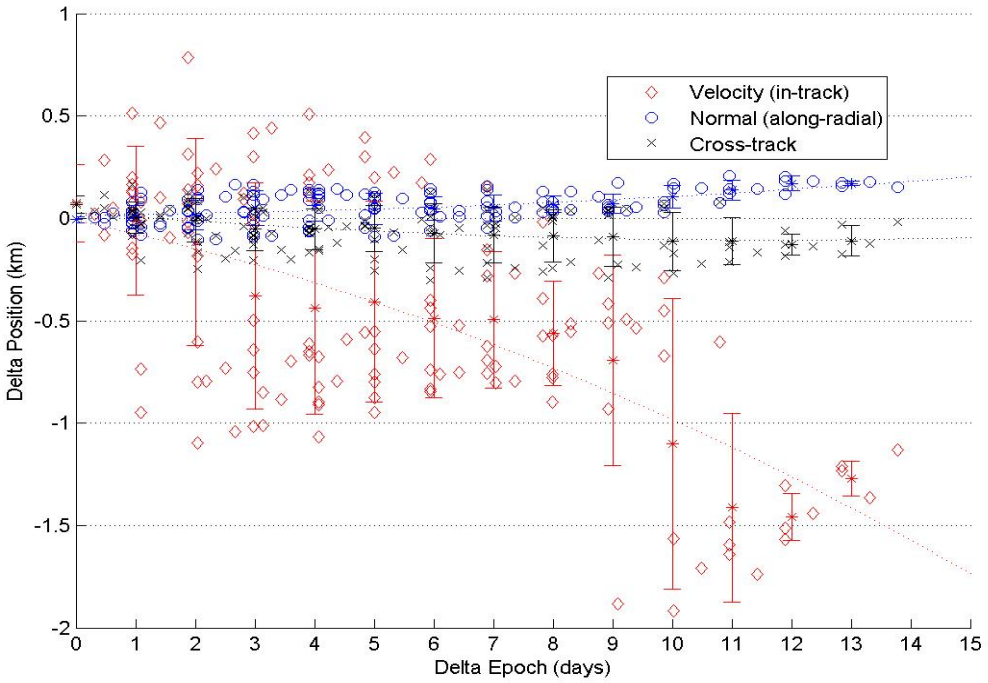

Figure 4. Scenario 11 – LAGEOS – VNC Position Differences

Scenario 11 refers to a naming convention used throughout this chapter: the first digit of the scenario number corresponds to the satellite number, the second to the time window. Refer to Tables 1 and 2 for the satellites and time windows. Scenario 11 is displayed again in Figure 5 using subplots so the behavior of each component can be discerned separately.

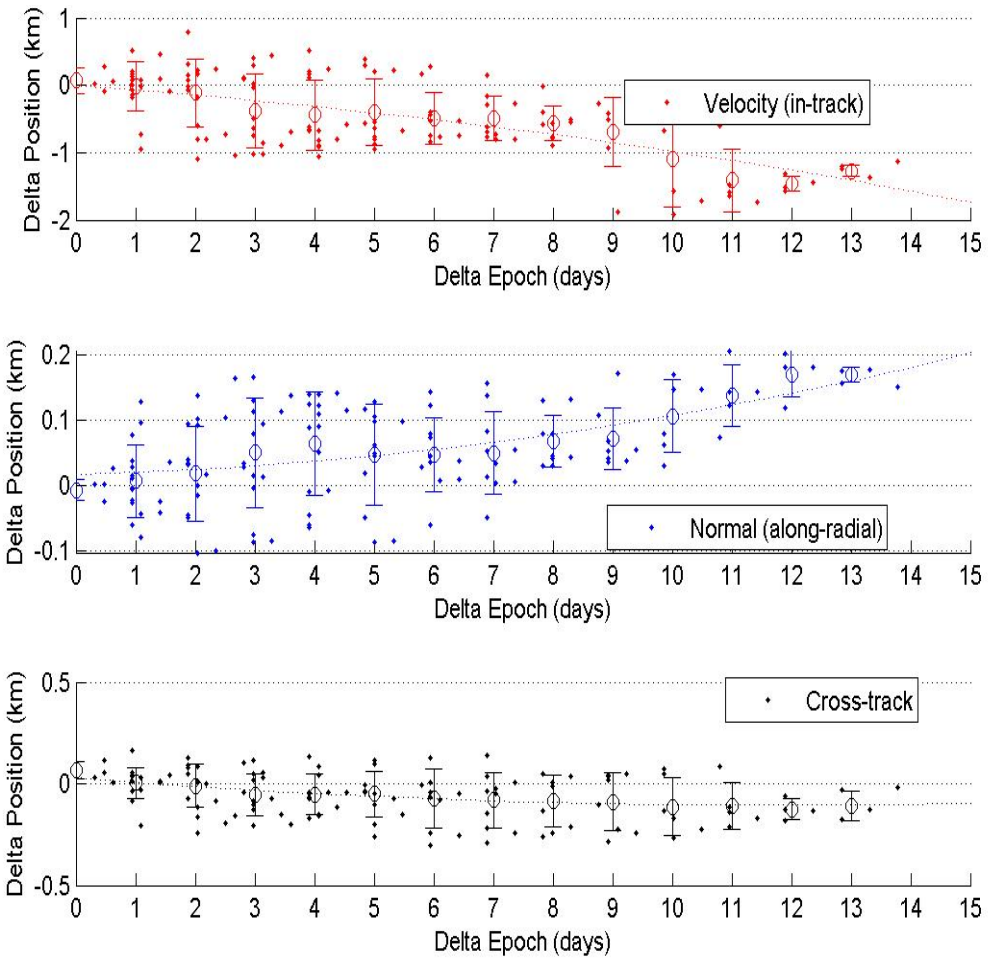

Figure 5. Scenario 11 – LAGEOS – VNC Position Differences (Subplots)

Figure 5 allows for the individual components to be investigated with more clarity as the cross-track and normal errors often overlap and/or bunch together. However, the

velocity component data is often two orders of magnitude greater than the other two components, preventing close examination of its behavior in a subplot. Subplots will be displayed in place of full plots when prudent, but as explained below the velocity component residuals are the primary interest and usually necessitate full plots.

LAGEOS is above the effects of drag and large gravity disturbances of Earth, while below (in altitude) the major third-body disturbances, meaning it has no significant perturbations acting on it (19:663). Therefore, its maximum position differences, especially for the velocity component, represent our best expectations throughout this study. Scenarios for each of the other satellites are presented in Figures 6-10.

TOPEX, at 1340 km, is also above the effects of drag, but subject to greater gravity disturbances. The position residuals in Figure 6 are fairly well-behaved—the mean of each bin is nearly zero with small variances out to 6 days of propagation. As expected, the velocity residuals for TOPEX are an order of magnitude larger than the baseline calibration satellite, LAGEOS, but considerably less than the LEO satellites represented in Figures 8-10.

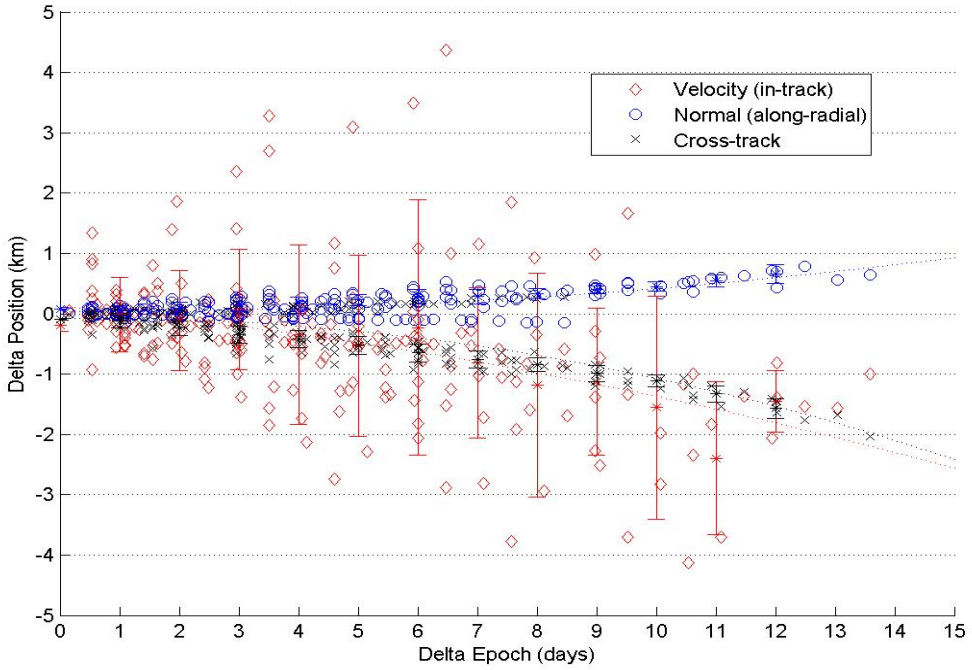

Figure 6. Scenario 26 – TOPEX – VNC Position Differences

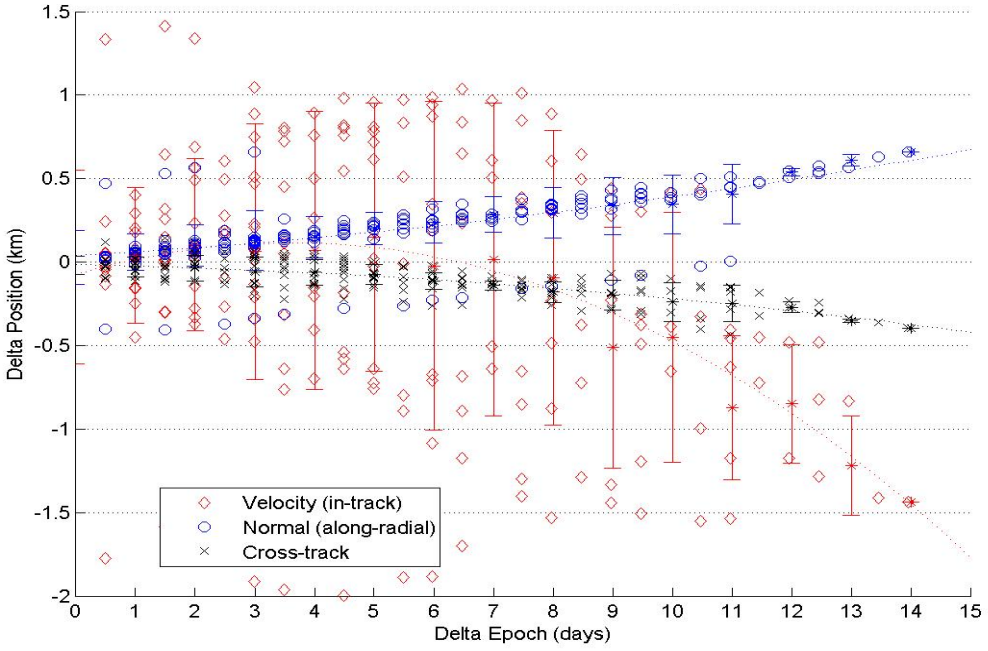

Figure 7. Scenario 32 – GPS – VNC Position Differences

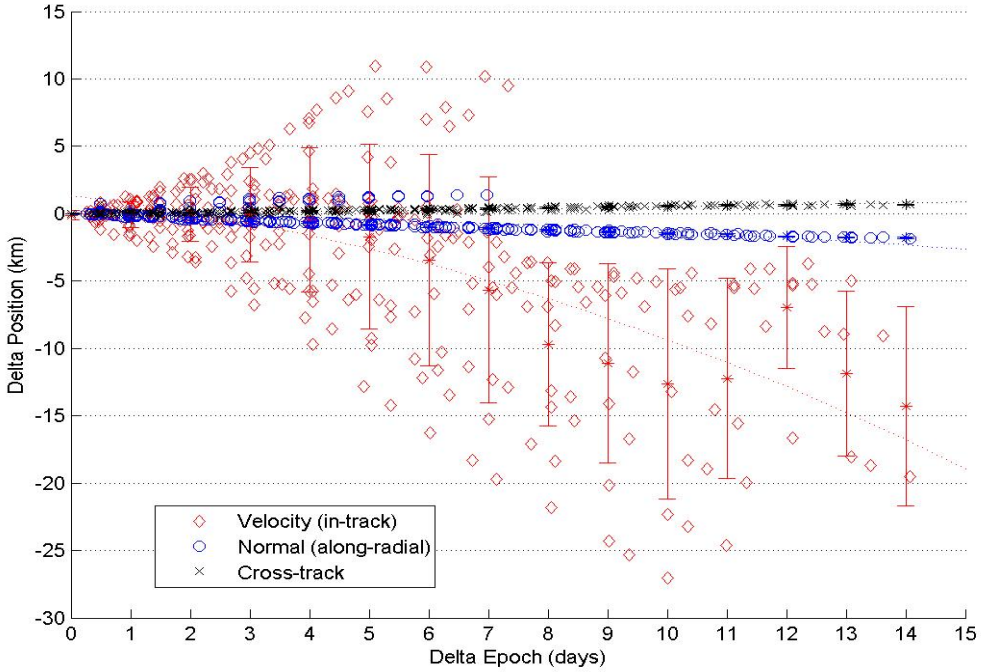

Figure 8. Scenario 43 – GRACE – VNC Position Differences

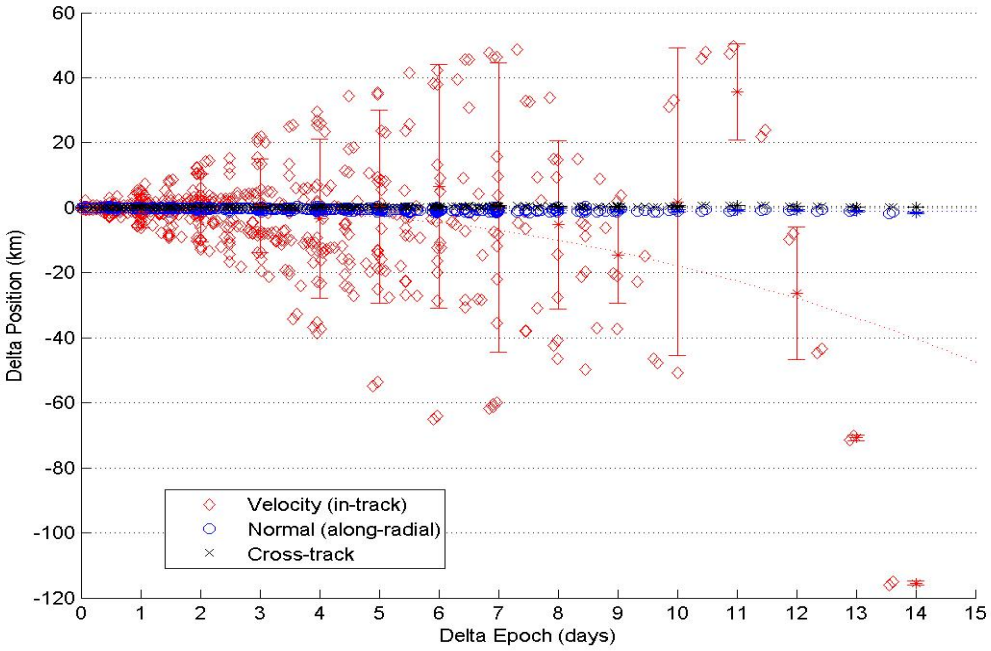

Figure 9. Scenario 52 – ICESAT – VNC Position Differences

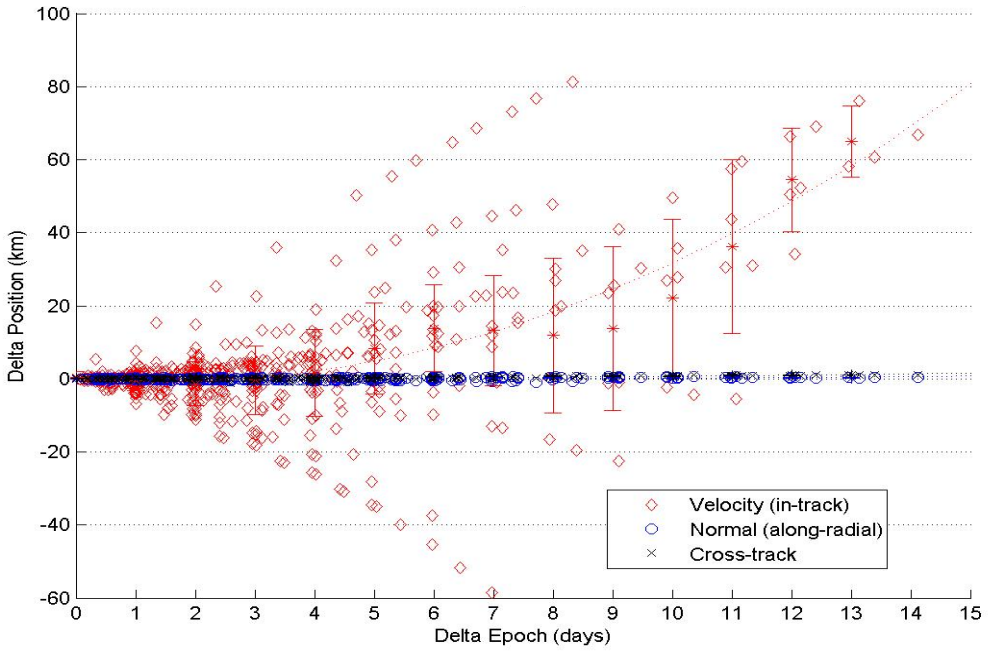

Figure 10. Scenario 67 – FAST – VNC Position Differences

Figures 7-10 represent the "best-case" scenarios for those respective satellites, in regards to the minimum range of position errors for that time window. The velocity component residuals in these four plots, overall, are rather evenly distributed with near-zero means for bins up to 5 or more days. Biases are observed in nearly all 48 scenarios, generally more pronounced in velocity and normal component residuals. Note the growing biases of the normal residuals in Figure 7 and 8, equating to increasing TLE prediction error in the radial component, or range estimate. Of all the satellites in this study, the GPS satellite has the highest relative errors in cross-track and normal components as compared to the velocity component. Figure 7 is an example of this finding. A possible explanation is that in a circular MEO orbit, the GPS satellite experiences disturbances in the three components in a distributed fashion, i.e. there is not a dominate force acting on any single component of the GPS satellite.

Figures 8-10 represent LEO satellites; hence, the significant increase of velocity component residuals due to atmospheric drag. For many reasons, errors in this component will be the principal focus of analysis from here on. Foremost is an interest to evaluate the effects of drag on these three LEO satellites. Also, except for the GPS satellite as described above, the normal and cross-track errors are negligible when compared to the velocity errors. Next, residuals in the velocity component correspond to errors in the mean anomaly and semi-major axis. Perturbation forces acting on the mean anomaly have both secular and periodic effects, and the secular effects are of particular interest for this study. Finally, drag acts along the velocity vector and is the largest perturbation for satellites with an orbital altitude less than 800 km. For these reasons, the remaining analysis of the pair-wise comparisons will focus on the velocity component errors.

Using the variance of the different bins and the overall trend of the velocity residuals as criteria, Figures 11-16 present a second set of scenarios, one for each satellite. All of these figures contain scatterings of anomalous residuals. Notice in Figure 11 a string of velocity errors underneath the majority of data points, 2- to 3-sigma away from the bin norms. Figures 12 and 13 also have strings, or groupings, of these aberrant TLE predictions, most noticeably above the majority of data points for days 1-5. Figures 15 and 16 illustrate this behavior both above and below 2-sigma deviation of most bin means.

Analysis of this behavior points to specific TLEs that, when propagated, repeatedly result in bad predictions of the state vector. This adversely affects the

residuals in two manners. First, when this TLE is propagated forward to other TLE epochs, the computed residuals are likely to be greater. Similarly, when this TLE is the primary, secondary TLEs propagated to it will be compared to a worse reference state vector. Although not implemented in this study, it may be beneficial to establish a detection technique and associated tolerance level in order to remove these aberrant TLEs, then repeat the pair-wise propagation in order to investigate possible improvements to the computed covariance and autocorrelation function.

Another artifact exhibited in each of the scenarios displayed in Figures 11-16 are fast-growing error biases in the velocity component residuals. These secular errors may be due to one or multiple perturbation effects, appearing to be linear for the higher satellites (LAGEOS, GPS) and quadratic for the LEO satellites.

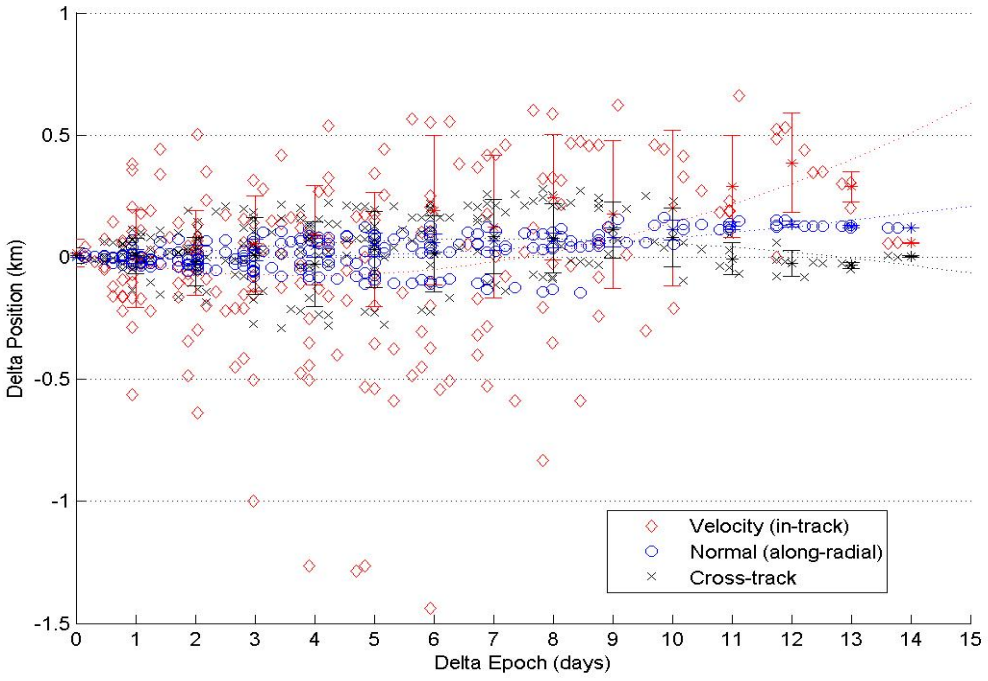

Figure 11. Scenario 18 – LAGEOS – VNC Position Differences

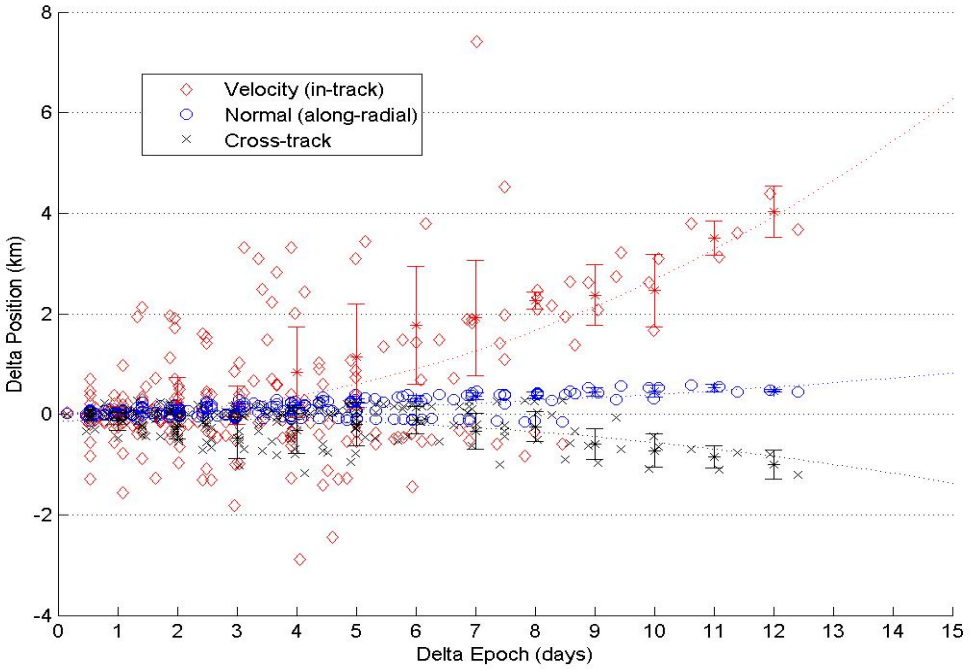

Figure 12. Scenario 24 – TOPEX – VNC Position Differences

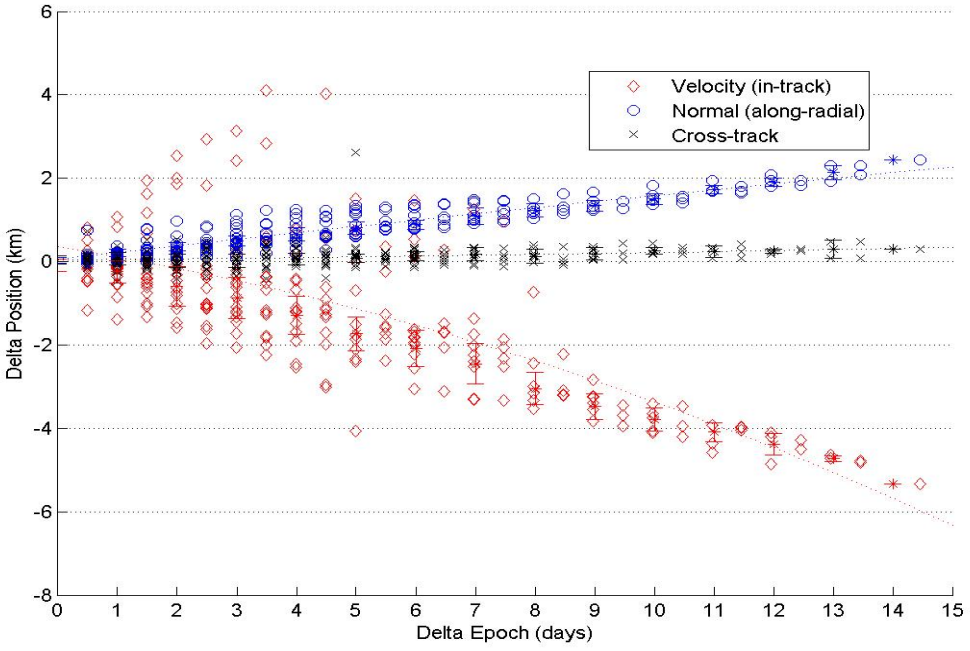

Figure 13. Scenario 38 – GPS – VNC Position Differences

Figure 14 illustrates the secular error growth in all three components for scenario 45. Notice the magnitude and trend of the velocity component errors. The always-positive, increasing slope signifies that secondary TLEs are continuously over-estimating the velocity of the satellite at the primary state vector epoch. The primary cause of this is most likely due to mis-modeling of the atmospheric drag, which actually increases the relative velocity of the satellite. As Vallado explains, the drag paradox is tied to the conservation of energy of the satellite (potential vs. kinetic) so decreasing the size of the orbit (what atmospheric drag effectively does) increases the average motion of the satellite (19:632-634).

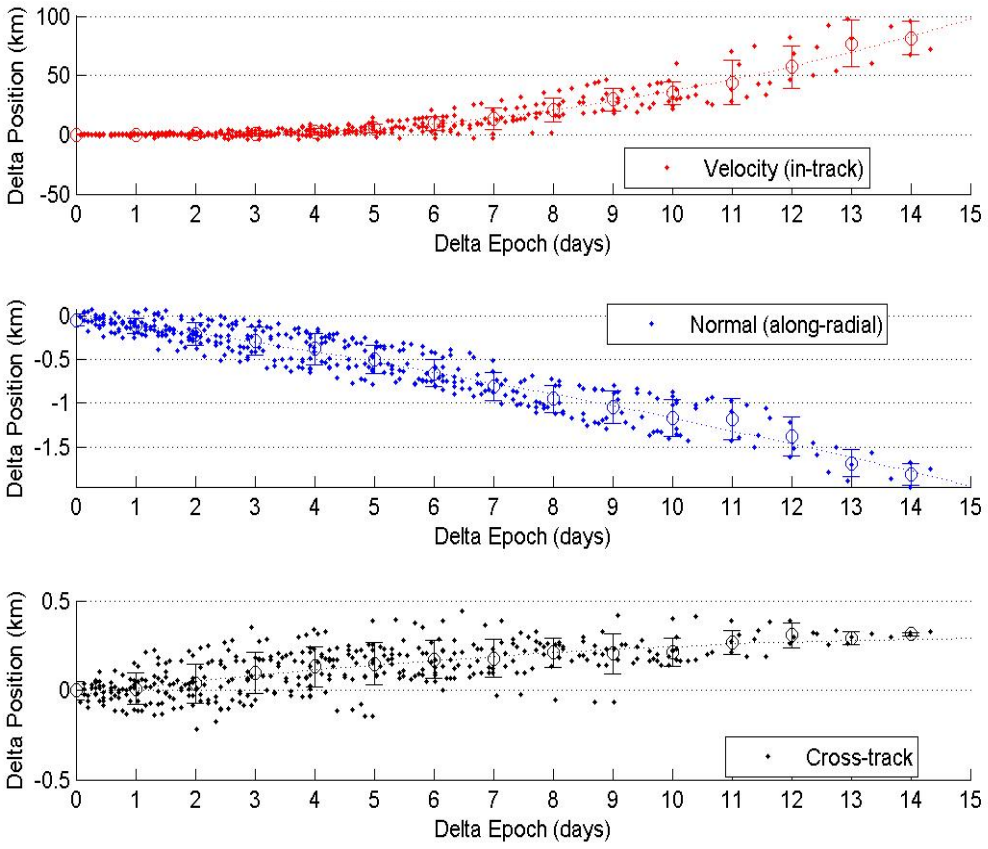

Figure 14. Scenario 45 – GRACE – VNC Position Differences

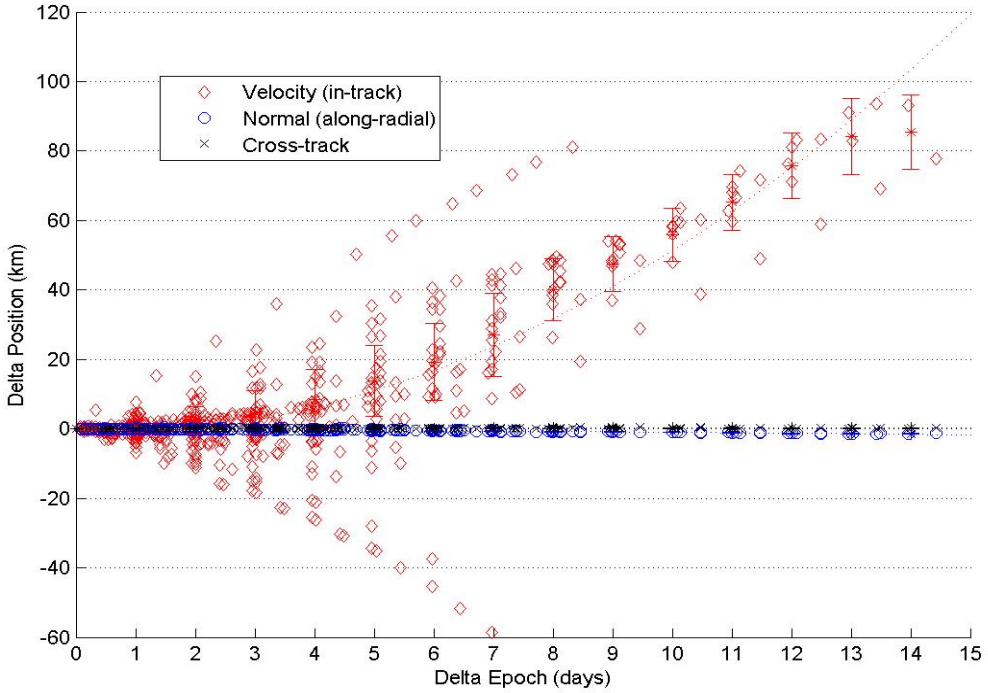

Figure 15. Scenario 58 – ICESAT – VNC Position Differences

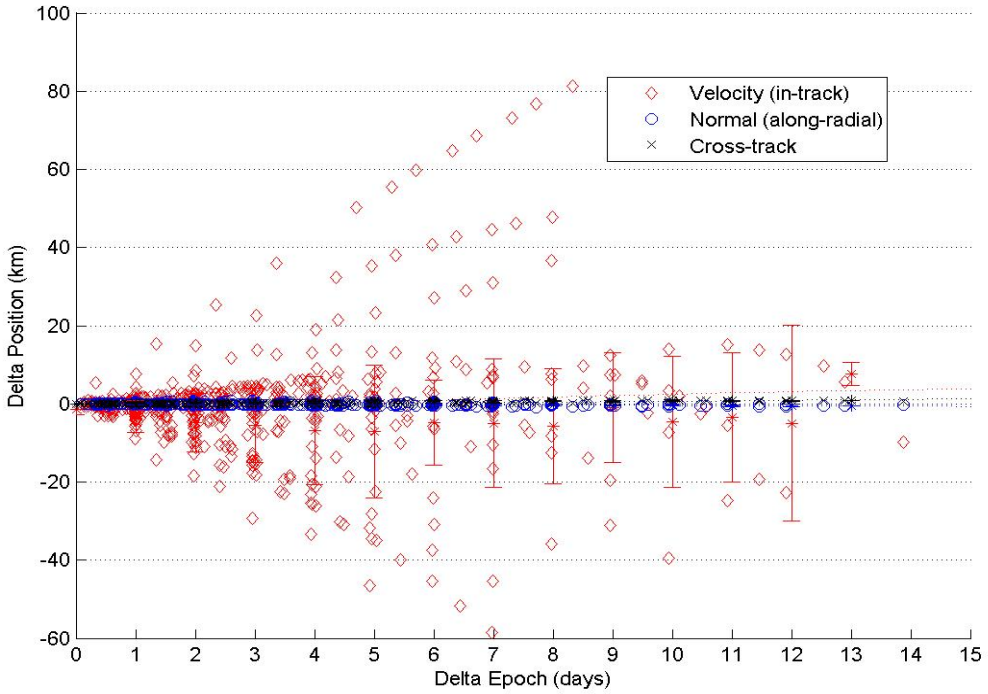

Figure 16. Scenario 64 – FAST – VNC Position Differences

Covariance Matrix Results

Using the method described in Chapter 3, full 6x6 covariance matrices are generated at the epoch of the N^{th} TLE for each of the 48 scenarios. As expected, the variances and covariances vary in accordance with the different satellite orbits and characteristics. LAGEOS again serves as the ideal baseline with the lowest covariance values—indicating the best certainty of the state vector computation from the TLE.

Table 5 is an example of a LAGEOS covariance matrix. Values along the diagonal of the matrix represent the variances, indicating the accuracy fits for the six state elements correlating to themselves. Off-diagonal terms are indicators of cross-correlation between elements of the state. Positive values indicate a direct dependence and negative values an inverse one. The notation R_v means the position vector in the velocity component, R_n is position vector in the normal component, and so on. Units of the individual cells are equal to the product of the corresponding row and column units.

The largest value in Table 5 corresponds to the residual data with the highest variance at the epoch. As anticipated from the scatter plots above, analysis of all study scenarios shows that the velocity component of the position vector is the largest value of the covariance matrix every time. This indicates the worst certainty associated with the state vector estimate is in this element.

Table 5. Covariance Matrix – Scenario 11 – LAGEOS

TIME1	R_v (km)	R_n (km)	R_c (km)	V_v (km/sec)	V_n (km/sec)	V_c (km/sec)
R_v (km)	0.378619709	-0.034359821	0.027715274	1.55115E-05	-0.000171498	-1.90966E-05
R_n (km)	-0.034359821	0.004002483	-0.002717183	-1.81855E-06	1.5463E-05	1.89775E-06
R_c (km)	0.027715274	-0.002717183	0.008430228	1.22177E-06	-1.21872E-05	-5.33055E-06
V_v (km/sec)	1.55115E-05	-1.81855E-06	1.22177E-06	8.26397E-10	-6.9792E-09	-8.54481E-10
V_n (km/sec)	-0.000171498	1.5463E-05	-1.21872E-05	-6.9792E-09	7.79043E-08	8.3125E-09
V_c (km/sec)	-1.90966E-05	1.89775E-06	-5.33055E-06	-8.54481E-10	8.3125E-09	3.77679E-09

From Table 5, a maximum position variance/covariance value of only 0.38 km^2 is extremely small, given that the LAGEOS satellite is at an altitude of 5850 km. Due to its very stable orbit, LAGEOS often serve as a "calibration" satellite for many applications and research efforts. The values from Table 5 and from the other LAGEOS scenarios substantiate choosing it as the baseline satellite for this study.

At the opposite end of the spectrum in regards to certainty levels from the covariance estimate, Table 6 shows the *P* matrix for FAST in scenario 66. The velocity component of the position certainty is near 1150 km^2, which equates to a standard deviation of 34 km. Further, the normal and cross-track components have approximate standard deviations of 0.4 km and 0.5 km, respectively.

Table 6. Covariance Matrix – Scenario 66 – FAST

TIME6	R_v (km)	R_n (km)	R_c (km)	V_v (km/sec)	V_n (km/sec)	V_c (km/sec)
R_v (km)	1147.728674	8.074180665	14.01528528	-0.0422397	-0.802354779	-0.000988356
R_n (km)	8.074180665	0.173306919	0.187077627	-0.000383117	-0.005688293	6.51534E-05
R_c (km)	14.01528528	0.187077627	0.288314835	-0.000582194	-0.009833417	1.46676E-05
V_v (km/sec)	-0.0422397	-0.000383117	-0.000582194	1.62582E-06	2.95652E-05	-3.60249E-08
V_n (km/sec)	-0.802354779	-0.005688293	-0.009833417	2.95652E-05	0.000560934	6.51418E-07
V_c (km/sec)	-0.000988356	6.51534E-05	1.46676E-05	-3.60249E-08	6.51418E-07	1.54189E-07

The velocity component (in-track) variances from the covariance estimates for LAGEOS, TOPEX and GPS are displayed together in Figure 17. The x-axis corresponds to the time window. All three satellites have consistent values throughout the time windows, and compare in magnitude relatively close (1-2 orders of magnutide).

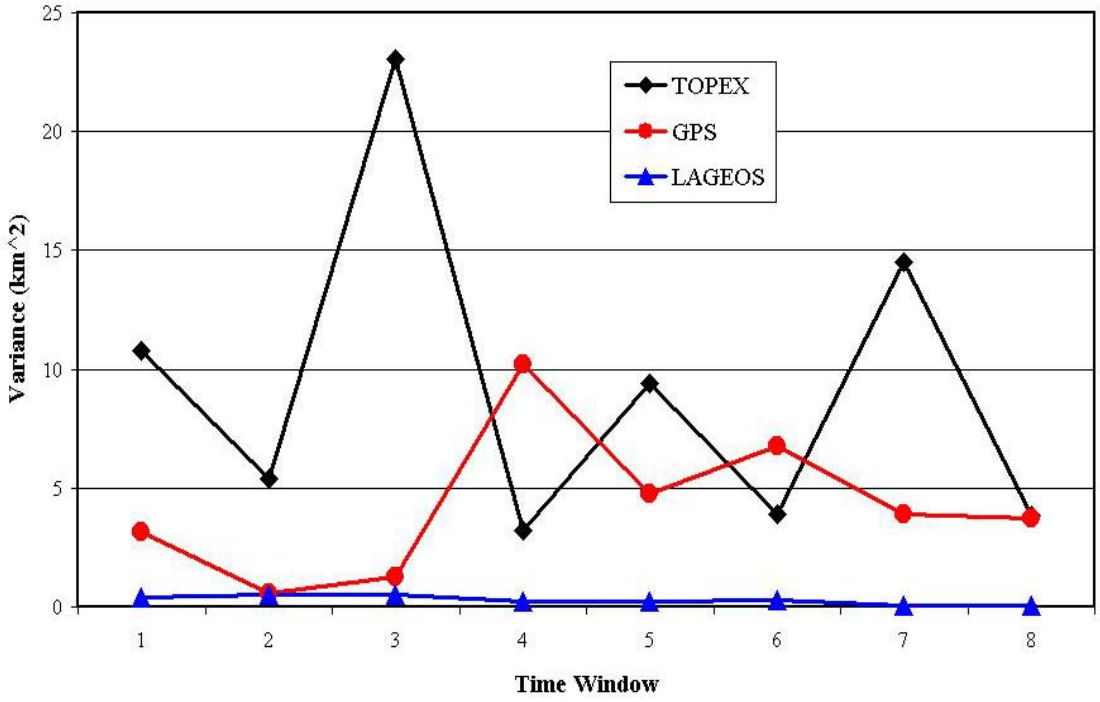

Figure 17. In-track Position Variances – Satellites Above Drag Effects

Conversely, covariances for the LEO satellites exposed to atmospheric drag are much larger than, have little to no consistency, and complicate analysis for those scenarios. Figure 18 shows the in-track component position variances from the covariance matrices for the eight time windows for GRACE, ICESAT, and FAST. Note: the ICESAT variance for time window 3 has been replaced in the plot with a value of

zero due to the magnitude of the computed value (326,400 km^2) dominating the scale of the plot.

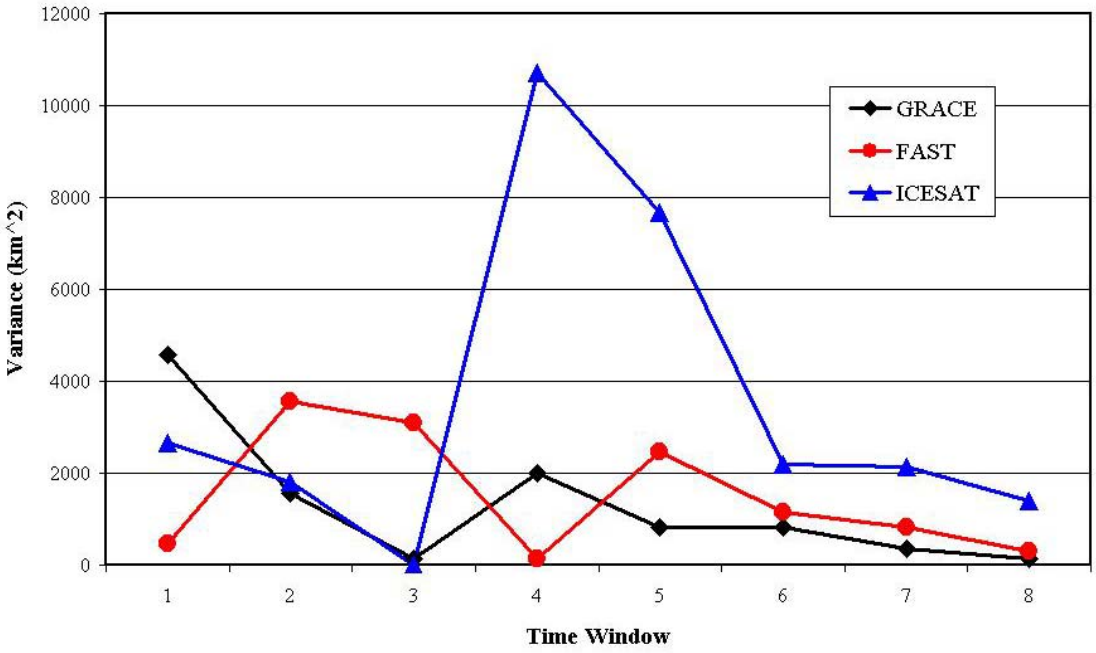

Figure 18. In-track Position Variances – LEO Satellites Subject to Drag

For the LEO satellites experiencing atmospheric drag, the discrepancies between the best and worst covariance estimates is dramatic. As an example, the respective minimum and maximum variances for GRACE are 130 km^2 and 4600 km^2.

Average covariance matrices are not offered in this report due to the low number of time windows evaluated. A higher number of covariance estimates, and subsequent analysis of those results evaluated for statistical confidence, could warrant estimating an average covariance.

Covariance matrices for every scenario, in both VNC elements and classical orbital elements (COE), are listed in Appendix D. Each covariance matrix is initially computed in the satellite-based coordinate systems (VNC and RTC). Next, the

covariance matrix is transformed from VNC to ECI coordinates using the transformation matrix generated during the pair-wise propagation routine from before. Refer to Equation 2.18. Finally, using an existing coded algorithm found at CelesTrak, the ECI coordinate system covariance is transformed to a classical orbital elements covariance. The prime TLEs, or N^{th} TLE, for each time window corresponding to the covariance matrices in Appendix D are provided in Appendix E.

Autocorrelation Function Results

An obvious question when working with a historical set of TLE data is, "To what extent does a given TLE depend on its predecessors?" Autocorrelation is a normalized representation of how similar data is to a time-shifted version of itself. Normalization is achieved by dividing the auto-covariance of the data by the variances, so the range of values for autocorrelation is between [−1, +1]. An autocorrelation value of +1 indicates perfect positive correlation at the corresponding time shift amount, or lag. A value of 0 signifies no direct correlation within the data at that corresponding lag. Finally, a negative value indicates an opposite correlation relationship.

For the same reasons given above for the covariance matrix results, all of the autocorrelation plots presented are calculated in the VNC coordinate system. They are created using Equations (2.22) and (2.23) according to the data bins in Appendix B. As explained before, n=14 and N=70 represent the targeted lag and overall number of sample points. With n=14, it is expected that the autocorrelation function has legitimate results for the first 7 days of propagation. With this caveat, the entire autocorrelation

function out to 35 days of propagation is provided. Figure 19 shows the autocorrelation for LAGEOS. Note the x-axis scale is in days, and each day is an increment of two in the lag variable (i.e. day = 1,2,3,… → n = 2,4,6,…).

Notice that the largest correlation for all three components in the autocorrelation figures occurs at zero lag. A zero lag shift implies that the level of confidence in the prediction at any time is equal to the variance of the data for that time. As lag increases to the right, correlation decreases—indicating a period of "decorrelation." In Figure 19, the three components closely follow one another through this decorrelation period, then pass the legitimate data span limit of 7 days, and eventually reach a value of zero correlation near 12 to 13 days. Beyond that, the correlation function becomes negative, reaching a minimum value around 25 days, where it then begins to increase in value for the first time.

When the correlation is near 1.0, a high correlation indicates that whatever the position residuals are at this time lag, they are a good predictor of residuals at nearby lags. Near a lag of 7 days, the correlation values for all components are between 0.3 and 0.4, suggesting a reduced but still positive correlation exists between the TLE predictions. The zero crossing between lags of 12 and 13 days signifies when no correlation is present. This first "zero" is known as the decorrelation time, interpreted as the amount of lag (time) when we no longer have any knowledge of the quality of the residual as a predictor. This lag is beyond the legitimate data span limit of 7 days, but a value of zero correlation is expected eventually. Due to changing forces in the physical world and the use of simplified models, we cannot expect to have positive correlation of

our error forever. The trend of the autocorrelation from day 7 to the zero crossing appears stable and well-behaved, but still must be taken with some caution. Negative values of the correlation function indicate that lags for those amounts of time have an opposite relationship to lags with positive correlation. For instance, whereas the position residual at a lag of two days is a good predictor of one at a lag of one day, the position residual from 25 days lag is a poor predictor of one at one day.

LAGEOS correlation values show a small amount of the aliasing effect—mentioned in Chapter 3—in the normal component, but overall the three components are practically identical for the entire propagation time span. Once again, this supports the contention that LAGEOS is a baseline satellite and orbit for this study. The autocorrelation functions for the remaining satellites are provided in Figures 20-24.

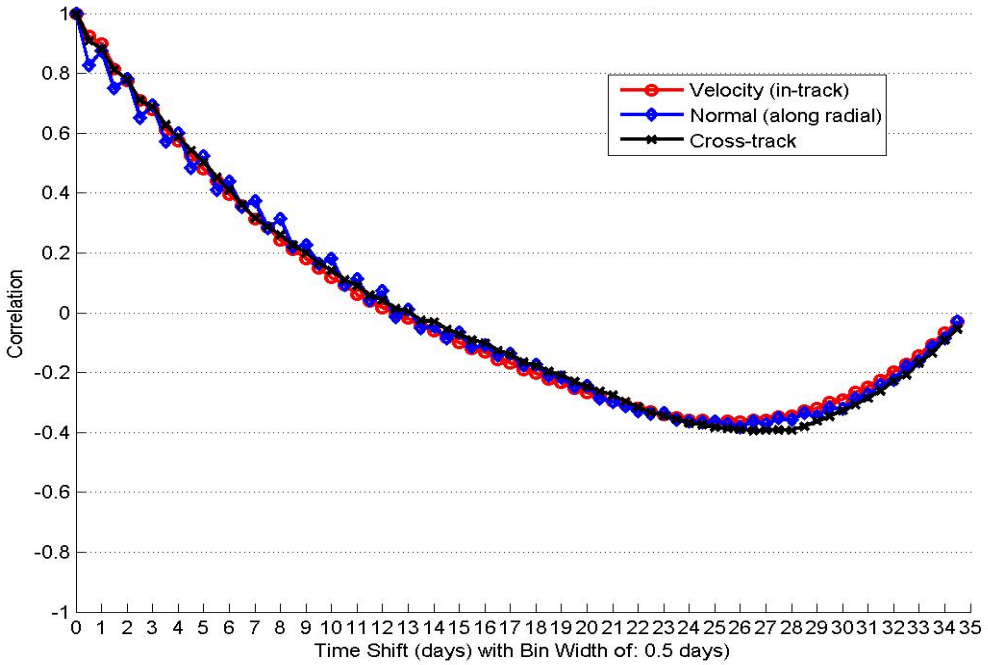

Figure 19. LAGEOS – Normalized Autocorrelation

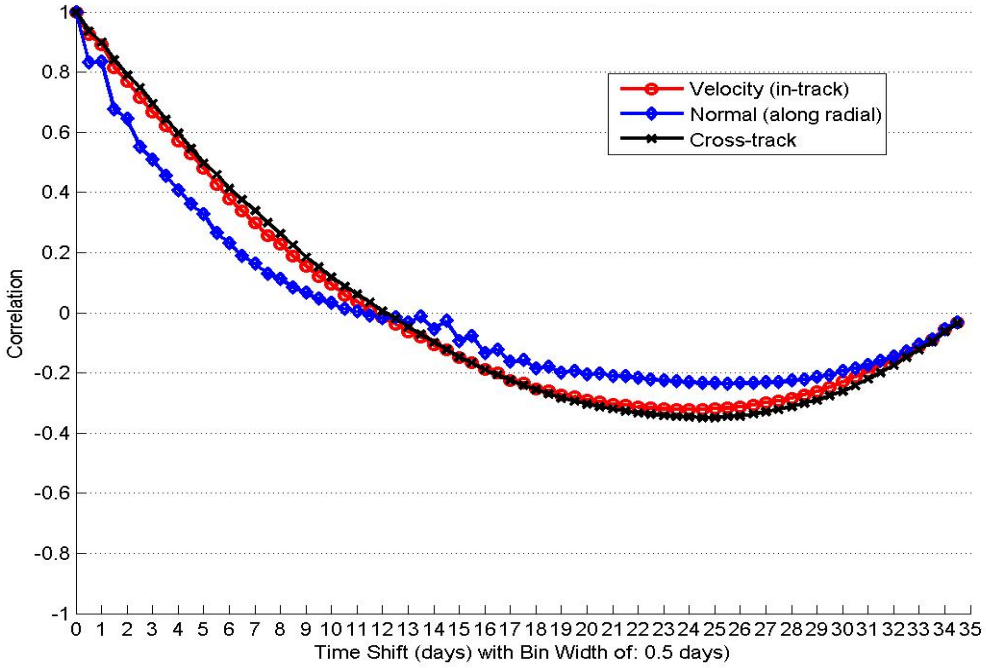

Figure 20. GRACE – Normalized Autocorrelation

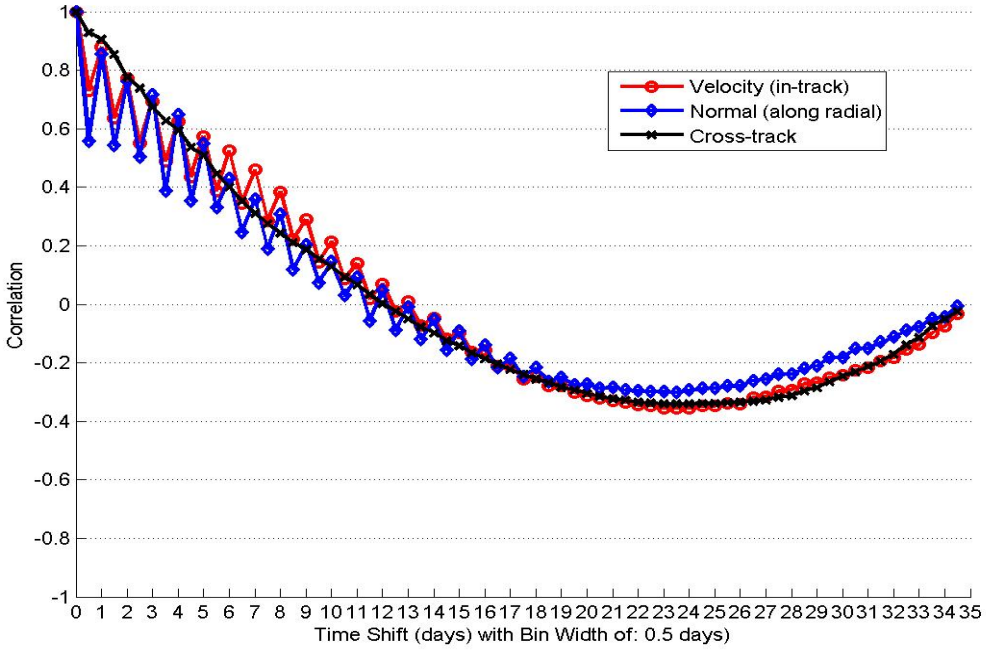

Figure 21. ICESAT – Normalized Autocorrelation

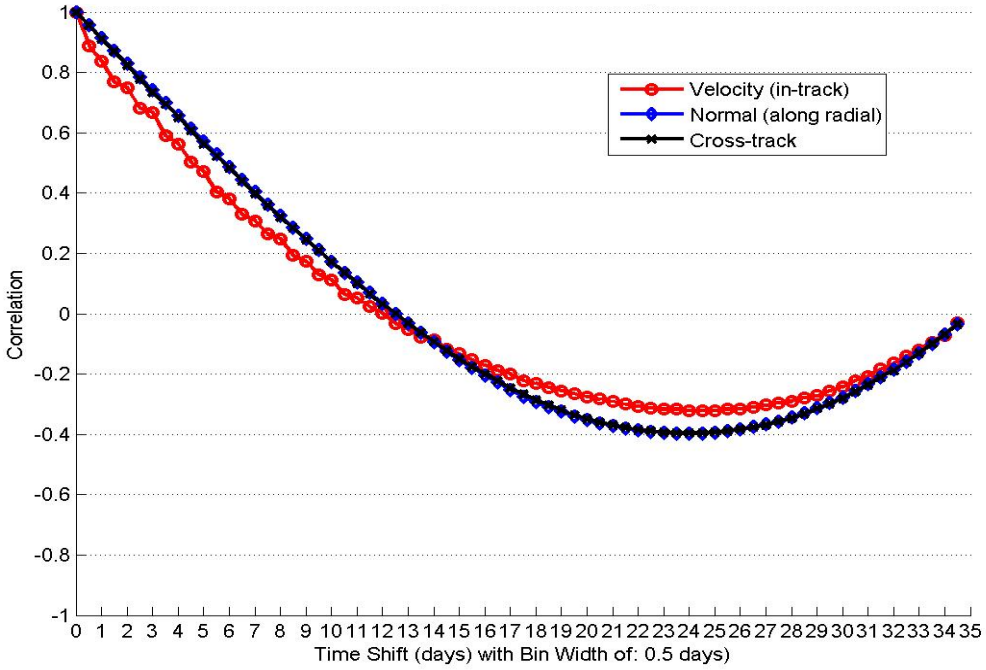

Figure 22. TOPEX – Normalized Autocorrelation

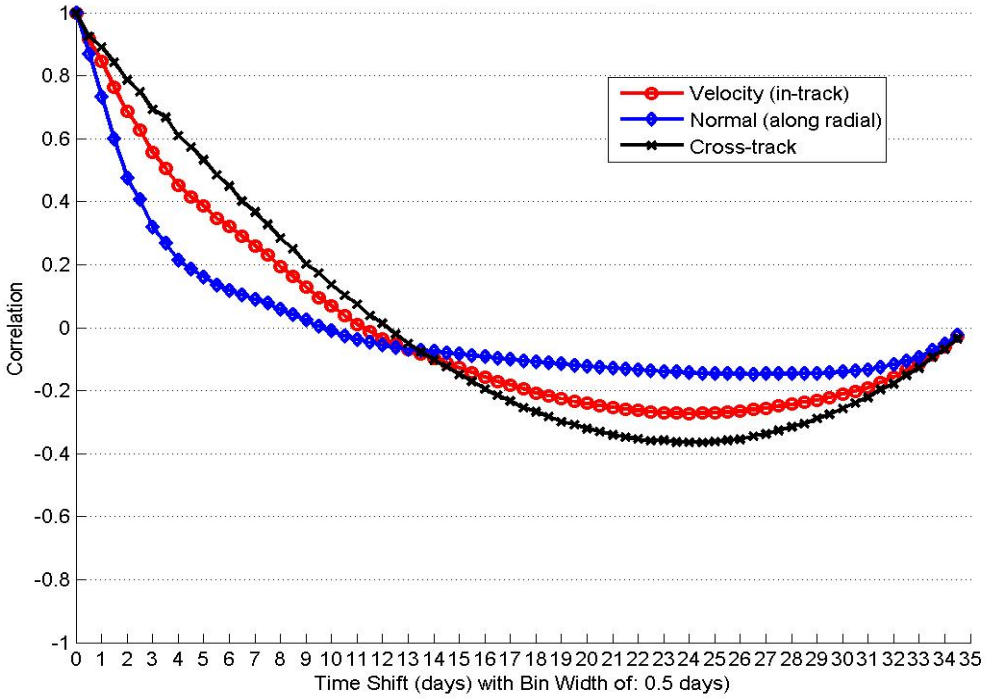

Figure 23. FAST – Normalized Autocorrelation

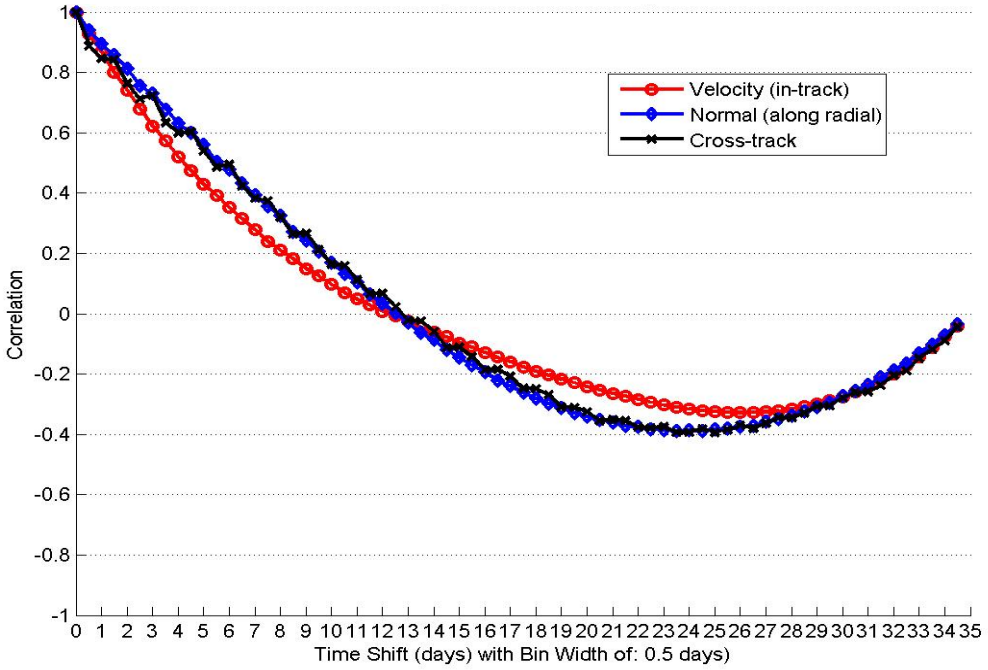

Figure 24. GPS – Normalized Autocorrelation

Notice that the cross-track component in each figure almost always has the highest positive correlation when compared to the other components. This is not unexpected as the cross-track component generally had the minimum amount of error and smallest variances from the position residual data. For instances when this autocorrelation trend is not true, the cause appears to be the aliasing effect. The autocorrelation function for ICESAT, shown in Figure 21, has the most pronounced aliasing effect of the six satellites. Analysis showed this is attributed to the number of sample points parsed into conjoining bins during the autocorrelation formulation. Given the bounds of this study, the aliasing effect was not investigated further.

In Figures 20, 21, and 23 observe how the normal component of the position residuals for the three satellites which experience drag shows a faster decline in the amount of correlation than the velocity and cross-track components. Further, the normal

component correlation function appears to flatten towards a value of zero for GRACE and FAST, in Figures 20 and 23 respectively, more than the remaining satellites. The explanation for these observations is most likely related to atmospheric drag and mis-modeling of its effects on LEO satellites. Further research is needed to investigate this behavior more thoroughly.

V. Conclusions and Recommendations

Conclusions

Using only NORAD two-line element sets, this work demonstrates the ability to estimate the orbital covariance matrix for a given TLE. For six different satellites, residual vectors are computed from a pair-wise propagation technique using SGP4 and eight different sets of historical TLEs. Those residual vectors are analyzed for overall behavior related to the dynamics of the satellite and perturbation effects. Covariance matrices approximating the relative uncertainty in the solution of a TLE state vector are calculated. Finally, an autocorrelation function for each satellite is formulated, indicating the relationship between the position residual data of the TLE predictions and a time-shifted version of itself.

Results from the position residuals scatter plots and covariance matrices show that SGP4 propagation performs considerably better for orbits above the effects of drag. The LEO satellites in this study which experience drag had very inconsistent covariance results, especially in the velocity component (in-track error) of the satellite position vector in the satellite-based coordinate system. Further, as demonstrated by the scatter plots of the position residuals, TLE predictions using SGP4 worsened as the amount of propagation time increased. Quadratic secular error growth due to atmospheric drag was observed in the position's velocity component for all satellites affected by drag. Conversely, satellites above the effects of drag showed a smaller magnitude and more distributed amount—between components of the coordinate system—of propagation error.

The autocorrelation function was studied to estimate an amount of time that TLEs for a specific satellite, or perhaps class of satellites in similar orbits, could be propagated and still have a relative accuracy warranting their use in estimating the covariance of a state vector. Although this preliminary study combined the extended propagation time windows in order to obtain a sufficient amount of data points, the results imply that state vector errors from TLEs older than approximately ten days have no positive correlation to errors in state vectors from reference TLEs. Extending this to efforts of obtaining a highly accurate covariance matrix for a state vector from a given TLE using only public TLEs, say for conjunction analysis, the results suggest using only TLEs that are not older than a few days.

Autocorrelation results were surprisingly similar for all satellites in this study, in particular the amount of time before a correlation of zero was reached in the position residual data. The fact that all three components had a zero crossing at nearly the same amount of time for every satellite is cause for suspicion. For example, correlation in the cross-track direction might be expected to stay positive for a longer length of time than in the velocity direction given it showed more stable error results. Further, based on the scatter plots and covariance calculations, positive correlation of the more stable orbits in this study (satellites above atmospheric drag) was expected to have a longer length of time than for the orbits with larger magnitude perturbations.

Recommendations for Future Research

Initial intentions for generating the covariance matrix involved evaluating its accuracy by using higher accuracy truth data, i.e. POE data. By combining the

covariance matrix with the state vector estimate from the primary TLE, a confidence in the methodology for generating the covariance could be obtained. If the true state vector position is located within the TLE state estimate plus an error ellipsoid created from its covariance matrix, the method for generating the covariance could be investigated for accuracy and consistency.

Without truth data, whether POE data or SSN observations, an internal method for discriminating bad data should have been utilized, such as removing TLEs with errors greater than 3-sigma. By removing aberrant TLEs discovered from the pair-wise comparisons, then re-running the propagation routine, the covariance results and autocorrelation functions might be improved. The bounds of this study did not incorporate this possible improvement.

Alternate methods for estimating the covariance matrix could be implemented using the pair-wise differencing technique in this thesis. One possibility is using the binned data mean values and mean of the overall time window in a manner similar to the one used in this study. A logical addition to such a study would be to compare each of the different methods to each other. Further, it is expected that obtaining POE data and using it as the truth orbit would allow for a more accurate evaluation of the TLE residuals and covariance matrix estimate.

Taking the different covariance estimates and propagating them with the state vector, while continuing to compare them to POE data, could validate if any one method performs best. This would require a propagator other than SGP4, however.

No additional parameters were included in the generation and analysis of the covariance matrix. Adding a drag-related parameter, like the B* term from the set of TLEs, may provide insight into whether the covariance estimates are too conservative (optimistic).

Appendix A. TLE Format Full Description

The following information is from CelesTrak.com (12)
TLE Data for each satellite can consist of two or three lines of data. The following example is without the Line 0 which contains the character satellite name.

1 NNNNNU NNNNNAAA NNNNN.NNNNNNNN +.NNNNNNNN +NNNNN-N +NNNNN-N N NNNNN
2 NNNNN NNN.NNNN NNN.NNNN NNNNNNN NNN.NNNN NNN.NNNN NN.NNNNNNNNNNNNN

Lines 1 and 2 are the standard Two-Line Orbital Element Set Format identical to that used by NORAD and NASA. The format description is as follows:

Line 1	
Column	**Description**
01	Line Number of Element Data
03-07	Satellite Number
08	Classification (U=Unclassified)
10-11	International Designator (Last two digits of launch year)
12-14	International Designator (Launch number of the year)
15-17	International Designator (Piece of the launch)
19-20	Epoch Year (Last two digits of year)
21-32	Epoch (Day of the year and fractional portion of the day)
34-43	First Time Derivative of the Mean Motion
45-52	Second Time Derivative of Mean Motion (decimal point assumed)
54-61	BSTAR drag term (decimal point assumed)

63	Ephemeris type
65-68	Element number
69	Checksum (Modulo 10) (Letters, blanks, periods, plus signs = 0; minus signs = 1)

Line 2	
Column	**Description**
01	Line Number of Element Data
03-07	Satellite Number
09-16	Inclination [Degrees]
18-25	Right Ascension of the Ascending Node [Degrees]
27-33	Eccentricity (decimal point assumed)
35-42	Argument of Perigee [Degrees]
44-51	Mean Anomaly [Degrees]
53-63	Mean Motion [Revs per day]
64-68	Revolution number at epoch [Revs]
69	Checksum (Modulo 10)

All other columns are blank or fixed.

Appendix B: Bins for Expanded Autocorrelation Time Window

The following table is the bin breakdown for the autocorrelation function. The parameters for this work are: 35 days of propagation, bin width = 0.5 day, N=70. NOTE: Grayed cells represent "legitimate" data span for the desired length of 7 days, n=14. Bin #1 is only 0.25 days in width as a result of the coding algorithm implemented.

	TLE Epoch Difference (in days)	
Bin #	Minimum	Maximum
1	0	0.25
2	0.25	0.75
3	0.75	1.25
4	1.25	1.75
5	1.75	2.25
6	2.25	2.75
7	2.75	3.25
8	3.25	3.75
9	3.75	4.25
10	4.25	4.75
11	4.75	5.25
12	5.25	5.75
13	5.75	6.25
14	6.25	6.75
15	6.75	7.25
16	7.25	7.75
17	7.75	8.25
18	8.25	8.75
19	8.75	9.25
20	9.25	9.75
21	9.75	10.25
22	10.25	10.75
23	10.75	11.25
24	11.25	11.75
25	11.75	12.25
26	12.25	12.75
27	12.75	13.25
28	13.25	13.75
29	13.75	14.25
30	14.25	14.75
31	14.75	15.25
32	15.25	15.75
33	15.75	16.25

34	16.25	16.75
35	16.75	17.25
36	17.25	17.75
37	17.75	18.25
38	18.25	18.75
39	18.75	19.25
40	19.25	19.75
41	19.75	20.25
42	20.25	20.75
43	20.75	21.25
44	21.25	21.75
45	21.75	22.25
46	22.25	22.75
47	22.75	23.25
48	23.25	23.75
49	23.75	24.25
50	24.25	24.75
51	24.75	25.25
52	25.25	25.75
53	25.75	26.25
54	26.25	26.75
55	26.75	27.25
56	27.25	27.75
57	27.75	28.25
58	28.25	28.75
59	28.75	29.25
60	29.25	29.75
61	29.75	30.25
62	30.25	30.75
63	30.75	31.25
64	31.25	31.75
65	31.75	32.25
66	32.25	32.75
67	32.75	33.25
68	33.25	33.75
69	33.75	34.25
70	34.25	34.75

Appendix C. MATLAB Code

The following code was written and run in MATLAB. This code performs the TLE propagation algorithms and statistical computations. The main code is provided first, with supporting sub-functions second.

```
%{
This code performs pair-wise comparisons of Two-line Element sets (TLEs)
by propagating the TLEs using SGP4 within Satellite ToolKit.
Running this code requires MATLAB Aerospace Toolbox and STK 7.0.  See
help files for "atb" functions used in this code.
This code is set up for evaluating 6 different satellites during 8 separate
time windows.

Three primary functions are performed by this code:
1) Position residuals resulting from the pair-wise comparisons are plotted.
2) Covariance matrices for the state vector that is computed for the most recent TLE of each time window.
3) An autocorrelation function is formulated by extending the time windows
of propagation and then combining all of them together.
Reference thesis document mentioned below for more information.

 author    :    Capt Victor Osweiler      23 March 2006

In support of Masters Degree from Air Force Institute of Technology (AFIT).
Thesis Designator:  AFIT/GSS/ENY/06-M09.
Thesis Title:
"COVARIANCE ESTIMATION AND AUTOCORRELATION OF NORAD TWO-LINE ELEMENT
SETS"

 inputs    :
This script opens, reads in, and uses TLEs in their standard defined
format.  TLEs are saved in one file for each satellite, in a specific
location on the available network (or hard drive).
The script can be modified to read TLEs from an alternate location.

outputs    :
   Plots             -
   Excel Files       -
   Covariance Matrix  - 6x6 satellite-based coordinate system covariance
   Covariance Matrix  - 6x6 classical orbital elements covariance matrix
   Autocorrelation Function  -

 Sub-functions called in the code :
      Epoch2Date      from Vallado
      TwoDigit        from Vallado
      rv2vnc
      rv2rtc
      mag             from Vallado
      COVCT2CL        from Vallado

%}
```

```
% ------------------------------------------------------------------

clear all;
clc;
warning off MATLAB:xlswrite:AddSheet;
agiInit;

% ---------------------------------------------------------
% Options in script:  choose whether to plot, write excel
% files, do autocorrelation function and plot, as well as the
% satellite numbers to evaluate and the number of time windows to use
% NOTE:  see below for time period windows
toplotornottoplot = true;
logfit = false;
writeexcel = true;
autocorrelate = false;
% ---------------------------------------------------------

% satellite # to work with (from 1 to 6)
% NOTE:  see below for satellite catalog numbers
for satnr = 1:6

% time window # to work with (from 1 to 8)
% NOTE:  see below for TLE epoch dates for the 8 windows
for timeloop = 1:8

% set STK internal clock to default value
atbSetEpoch(1972, 1, 1, 0, 0, 0, 'Z', 0);

t = timeloop;

dout = ['I:\My Documents\Thesis\Output\output_',...
   num2str(satnr),num2str(t),'.txt'];
diary(dout)
satnr, t
temp1 = num2str(satnr);
temp2 = num2str(timeloop);
temp3 = [temp1,temp2];
temp4 = str2num(temp3);
fignr = temp4;

format long g;
TLEsize = 142;
buffer = 30;

% The following dates are the start and end dates in YYDDD.00000000 format
% that I will use for my time windows of propagation
startdates = ['03060.00000000';'03079.00000000';'03270.00000000';
   '03290.00000000';'04045.00000000';'04065.00000000';
   '04150.00000000';'04280.00000000']
enddates = ['03075.00000000';'03093.00000000';'03285.00000000';
   '03305.00000000';'04060.00000000';'04080.00000000';
   '04165.00000000';'04295.00000000']
```

```
%%%% This are the extended time windows which had to be implemented for
%%%% the autocorrelation function.
% startdates = ['03040.00000000';'03059.00000000';'03250.00000000';
%     '03270.00000000';'04025.00000000';'04045.00000000';
%     '04130.00000000';'04260.00000000']
% enddates = ['03095.00000000';'03113.00000000';'03305.00000000';
%     '03325.00000000';'04080.00000000';'04100.00000000';
%     '04185.00000000';'04315.00000000']

for i = 1:8
   stimewindow(i) = Epoch2Date(startdates(i,:));
   etimewindow(i) = Epoch2Date(enddates(i,:));
end;
timewindow = [stimewindow' etimewindow']
startdate = timewindow(t,1)
enddate = timewindow(t,2)
satids = ['08820';'22076';'25933';'27391';'27642';'24285'];
catnr = satids(satnr,:)
fname = ['sat',catnr,'.2le']

fi = fopen(['I:\My Documents\Thesis\TLEs\',fname],'rt')
% fi = fopen(fname,'rt');
% fi = fopen('I:\My Documents\Thesis\Main MATLAB Code\sat27642.txt','rt');
% fi = fopen('sat27642.2le','rt')
% if (fi = -1) % file does not exist, do what?

if (fi ~= -1) % file exists
   fseek(fi,0,'eof');
   totalcount = ftell(fi)/TLEsize;
   fseek(fi,0,'bof');
   line = textscan(fi,'%s%s','delimiter','\n');
   anydata = false;
   for (n = 1:totalcount)
      line1 = char(line{1}(n,1));
      edate = Epoch2Date(line1(19:32));
      if (edate > startdate)
         anydata = true;
         break;
      end; % if
   end; % for n
   n;
   if (anydata) % if there is a TLE after the start date
      count = 0;
      n;
      for i = n:totalcount
         line1 = char(line{1}(i,1));
         line1 = [line1(1:1),' ',line1(3:69)];
         line2 = char(line{2}(i,1));
         line2 = [line2(1:1),' ',line2(3:69)];
         edate = Epoch2Date(line1(19:32));
         if (edate > enddate)
            break;
         end; %if past enddate
         count = count + 1;
```

```
        name = ['TLE',TwoDigit(count)];
        atbTLESetInfo(name,line1,line2)
    end; % for i
    m = 0;
    count
%%% clear delta PosDiffVNC VelDiffVNC PosDiffRTC PosDiffRTC data;
    points = zeros(15,1);
    sumVNC = zeros(15,3);
    sumVNC2 = zeros(15,3);
    sumRTC = zeros(15,3);
    sumRTC2 = zeros(15,3);
    data = zeros(20,3,count,count);

%%%%%% Begin double loop of propagating each TLE in the time window to
%%%%%% every other TLE which follows it (is more recent in time).
%%%%%% Outer loop: Start with the last TLE in the time window, go backward.
    for j = count:-1:1
        jName = ['TLE',TwoDigit(j)];
        jEpochSec = atbTLEEpoch(jName);
        jDate = atbEpochSecToDate(jEpochSec);
        atbSetEpoch(jDate);
[priTimes,priPosECF,priVelECF] = atbTLEProp(jName,0.0,0.0,1.0);
[priPosECI, priVelECI] = atbCbfToCbi('Earth',priTimes,priPosECF,priVelECF);
[priPosVNC,priVelVNC,transVNC] = rv2vnc(priPosECI(:,1),priVelECI(:,1));
[priPosRTC,priVelRTC,transRTC] = rv2rtc(priPosECI(:,1),priVelECI(:,1));

        if j == count   % when primary TLE is Nth TLE of time window
            j
            truthPosECI = priPosECI/1000
            truthVelECI = priVelECI/1000
            truthPosVNC = priPosVNC/1000
            truthVelVNC = priVelVNC/1000
            truthPosRTC = priPosRTC/1000
            truthVelRTC = priVelRTC/1000
            truthtransVNC = transVNC
            truthtransRTC = transRTC
        end;

%%%%%% Inner loop: Start with the last TLE in the time window, go backward.
        for k = count:-1:1
            if (j ~= k)   % Don't compare the same TLE to itself
                kName = ['TLE',TwoDigit(k)];
                kEpochSec = atbTLEEpoch(kName);
                if (kEpochSec < -0.001)   % Only compare TLE if more
                                          % than 0.001 seconds away
    m = m + 1;  % continuos counter for every j,k pair

% Calculate the number of days that kEpoch is away from jEpoch.  This is
% the epoch time difference between the "K-th" TLE from the "J-th" TLE
    delta(m) = -kEpochSec/86400;

% Notice below for the propagation of the "K-th" TLE, atbTLEProp has both
% a TimeStart and a TimeStop of 0.0 sec, meaning that the TLE will be
% propagated to the epoch tim, which was assigned above to the "J-th" TLE
```

```
        [secTimes, secPosECF, secVelECF] = atbTLEProp(kName,0.0,0.0,1.0);
        [secPosECI, secVelECI] = ...
           atbCbfToCbi('Earth',secTimes,secPosECF,secVelECF);

% Calculate the relative position and velocity of the "K-th" TLE with
% respect to the "J-th" TLE, in the ECI coordinate frame
        relPosECI = secPosECI(:,1) - priPosECI(:,1);
        relVelECI = secVelECI(:,1) - priVelECI(:,1);
        %old name: PosVNC(:,m) = transVNC*relPosECI/1000;

% Then convert these relative position & velocity vectors to the
% satellite-based coordinate system of the "J-th" TLE by using the
% transformation matrix from above (i.e. see the "rv2rtc" function).
% (Because vectors from atbTLEProp are in meters and
% meters/sec, divide the vectors below by 1000 to put in  km  and  km/sec)
        PosDiffVNC(:,m) = transVNC*relPosECI/1000;
        VelDiffVNC(:,m) = transVNC*relVelECI/1000;
        PosDiffRTC(:,m) = transRTC*relPosECI/1000;
        VelDiffRTC(:,m) = transRTC*relVelECI/1000;

% Build data matrix of TLE numbers, TLE epochs, time differences,
% Positions and Velocities in RTC coordinate system for j and k TLES,
% Positions and Velocities in VNC coordinate system  for j and k TLES,
% as well as their differences
        data(1,1,j,k) = j;
        data(1,2,j,k) = k;
        data(1,3,j,k) = delta(m);
        data(2,1,j,k) = jEpochSec;
        data(2,2,j,k) = jEpochSec + kEpochSec;
        data(2,3,j,k) = kEpochSec;

        % RTC data
        data((3:5),1,j,k) = priPosRTC(:,1)/1000;
        data((3:5),2,j,k) = (priPosRTC(:,1)/1000) + PosDiffRTC(:,m);
        data((3:5),3,j,k) = PosDiffRTC(:,m);
        data((6:8),1,j,k) = priVelRTC(:,1)/1000;
        data((6:8),2,j,k) = (priVelRTC(:,1)/1000) + VelDiffRTC(:,m);
        data((6:8),3,j,k) = VelDiffRTC(:,m);
        data((9:11),(1:3),j,k) = transRTC(:,:);

        % VNC data
        data((12:14),1,j,k) = priPosVNC(:,1)/1000;
        data((12:14),2,j,k) = (priPosVNC(:,1)/1000) + PosDiffVNC(:,m);
        data((12:14),3,j,k) = PosDiffVNC(:,m);
        data((15:17),1,j,k) = priVelVNC(:,1)/1000;
        data((15:17),2,j,k) = (priVelVNC(:,1)/1000) + VelDiffVNC(:,m);
        data((15:17),3,j,k) = VelDiffVNC(:,m);
        data((18:20),(1:3),j,k) = transVNC(:,:);

% Separate the Position Difference data into bins depending on the epoch
% time difference (in days).  Separate the data into bins as follows:
%   Bin 1:   0.0 - 0.49 days
%   Bin 2:   0.5 - 1.49 days
%     ...       ...
```

```
%   Bin 15:  13.5 - 14.49 days
      bin = floor(delta(m) + 1.5);
      if (bin < 16)
         points(bin) = points(bin) + 1;

         sumRTC(bin,1) = sumRTC(bin,1) + PosDiffRTC(1,m);
         sumRTC(bin,2) = sumRTC(bin,2) + PosDiffRTC(2,m);
         sumRTC(bin,3) = sumRTC(bin,3) + PosDiffRTC(3,m);
         sumRTC2(bin,1) = sumRTC2(bin,1) + (PosDiffRTC(1,m))^2;
         sumRTC2(bin,2) = sumRTC2(bin,2) + (PosDiffRTC(2,m))^2;
         sumRTC2(bin,3) = sumRTC2(bin,3) + (PosDiffRTC(3,m))^2;

         sumVNC(bin,1) = sumVNC(bin,1) + PosDiffVNC(1,m);
         sumVNC(bin,2) = sumVNC(bin,2) + PosDiffVNC(2,m);
         sumVNC(bin,3) = sumVNC(bin,3) + PosDiffVNC(3,m);
         sumVNC2(bin,1) = sumVNC2(bin,1) + (PosDiffVNC(1,m))^2;
         sumVNC2(bin,2) = sumVNC2(bin,2) + (PosDiffVNC(2,m))^2;
         sumVNC2(bin,3) = sumVNC2(bin,3) + (PosDiffVNC(3,m))^2;
      end; % if bin < 16

               end; % if delta between J and K is negative
            end; % if j <> k
         end; %k
      end; % for j
   end; % if there is TLE data after the start date
end; % if file exists

fclose(fi);
% --------------------------------------------------------------------

sat_alt_at_epoch = mag(truthPosECI)-6378;
% [p,a,ecc,incl,omega,argp,nu,m,arglat,truelon,lonper ] =...
%     RV2COE(truthPosECI(:,1),truthVelECI(:,1))
% [p,a,ecc,incl,omega,argp,nu,m,arglat,truelon,lonper ] =...
%     RV2COE(priPosECI(:,1)/1000,priVelECI(:,1)/1000)
sat_alt_at_epoch
min_delta_epoch = min(delta)
max_delta_epoch = max(delta)

% --------------------------------------------------------------------
% This section calculates the variance of only the POSITION data
% differences in both the RTC and VNC coordinate frames FOR THE ENTIRE 2
% WEEK TIME WINDOW, USING THE BINS TO CALCULATE MEAN, VARIANCE, AND ST.DEV

RTCmean = zeros(15,3);   % Initialize the 6 matrices
RTCvar = zeros(15,3);
RTCstdev = zeros(15,3);
VNCmean = zeros(15,3);
VNCvar = zeros(15,3);
VNCstdev = zeros(15,3);

for i = 1:15
   if (points(i) > 1)
      RTCmean(i,:) = sumRTC(i,:)/points(i);
```

```
  RTCvar(i,1) = (sumRTC2(i,1) - points(i)*RTCmean(i,1)^2)/(points(i) - 1);
  RTCvar(i,2) = (sumRTC2(i,2) - points(i)*RTCmean(i,2)^2)/(points(i) - 1);
  RTCvar(i,3) = (sumRTC2(i,3) - points(i)*RTCmean(i,3)^2)/(points(i) - 1);
      RTCstdev(i,1) = sqrt(RTCvar(i,1));
      RTCstdev(i,2) = sqrt(RTCvar(i,2));
      RTCstdev(i,3) = sqrt(RTCvar(i,3));

      VNCmean(i,:) = sumVNC(i,:)/points(i);
  VNCvar(i,1) = (sumVNC2(i,1) - points(i)*VNCmean(i,1)^2)/(points(i) - 1);
  VNCvar(i,2) = (sumVNC2(i,2) - points(i)*VNCmean(i,2)^2)/(points(i) - 1);
  VNCvar(i,3) = (sumVNC2(i,3) - points(i)*VNCmean(i,3)^2)/(points(i) - 1);
      VNCstdev(i,1) = sqrt(VNCvar(i,1));
      VNCstdev(i,2) = sqrt(VNCvar(i,2));
      VNCstdev(i,3) = sqrt(VNCvar(i,3));
   else
      RTCmean(i,:) = NaN;
      RTCvar(i,:) = NaN;
      RTCstdev(i,:) = NaN;
      VNCmean(i,:) = NaN;
      VNCvar(i,:) = NaN;
      VNCstdev(i,:) = NaN;
   end; % if points(i) > 1
end; % for i

stats = [points, RTCmean, RTCvar,RTCstdev, VNCmean, VNCvar, VNCstdev];
augment = [delta;PosDiffRTC;VelDiffRTC;PosDiffVNC;VelDiffVNC];
data_at_epoch = data(:,:,count,:);

TLEsTimeInts = squeeze(data_at_epoch(1,3,1,:))
points, RTCmean, RTCvar, RTCstdev, VNCmean, VNCvar, VNCstdev,

% ------------------------------------------------------------------
% This section calculates the covariance matrix from the position AND
% VELOCITY differences in the RTC and VNC coordinate frames.
% ** BUT ONLY AT THE EPOCH OF THE LAST TLE (most current).
% So only position differences from each TLE propagated to the last TLE,
% using that TLE as "truth" value.

RTCtemp = squeeze(data_at_epoch((3:8),3,1,(1:count-1)));
RTCmean_at_epoch = mean(RTCtemp')';
VNCtemp = squeeze(data_at_epoch((12:17),3,1,(1:count-1)));
VNCmean_at_epoch = mean(VNCtemp')';
RTCcov_at_epoch = zeros(6,6);
VNCcov_at_epoch = zeros(6,6);

for q = 1:(count-1)
      RTCcov_at_epoch(:,:) = RTCcov_at_epoch(:,:) + ...
         [(RTCtemp(:,q)-RTCmean_at_epoch(:))*...
          (RTCtemp(:,q)-RTCmean_at_epoch(:))'];
       VNCcov_at_epoch(:,:) = VNCcov_at_epoch(:,:) + ...
         [(VNCtemp(:,q)-VNCmean_at_epoch(:))*...
          (VNCtemp(:,q)-VNCmean_at_epoch(:))'];
end;
```

```
%  (6 x 6) Covariance Matrices at epoch of more recent TLE using all the
%  other TLEs propageted only to this epoch.  In RTC and VNC coord. frames
RTCcov_at_epoch = (1/(count-1)) * RTCcov_at_epoch
VNCcov_at_epoch = (1/(count-1)) * VNCcov_at_epoch

% (6 x 1) column vector of the variances for the components of the
% RTC and VNC coordinate frames
RTCvariances_at_epoch = diag(RTCcov_at_epoch)
VNCvariances_at_epoch = diag(VNCcov_at_epoch)

% (6 x 1) column vector of standard deviations for the components of the
% RTC and VNC coordinate frames
RTCstdev_at_epoch = sqrt(RTCvariances_at_epoch)
VNCstdev_at_epoch = sqrt(VNCvariances_at_epoch)

% Calculate the correlation coefficients for this covariance matrix
for i = 1:6
   for j = 1:6
      if (i ~= j)
         RTCcovar_corr_coeff(i,j) = RTCcov_at_epoch(i,j)...
          /((sqrt(RTCcov_at_epoch(i,i)))*(sqrt(RTCcov_at_epoch(j,j))));
         VNCcovar_corr_coeff(i,j) = VNCcov_at_epoch(i,j)...
          /((sqrt(VNCcov_at_epoch(i,i)))*(sqrt(VNCcov_at_epoch(j,j))));
      end;
      if (i == j)
         RTCcovar_corr_coeff(i,j) = 1;
         VNCcovar_corr_coeff(i,j) = 1;
      end;
   end;
end;

RTCcovar_corr_coeff
VNCcovar_corr_coeff
% ------------------------------------------------------------------------
% Take the covariance_matrix_at_epoch in the satellite-based coordinate
% system, first rotate if back to cartesian coordinates (ECI), then
% transform it to a classical orbital elements covariance
% using Vallado's script, "COVCT2CL".

% ** This must use the "truthtrans" transformation matrix since it
% corresponds to the Nth TLE coordinate system.

cartstate = [truthPosECI;truthVelECI];
cartstate = cartstate*1000; % need to be passed in meters and meters/second

% from RTC
ECIcov1 = [truthtransRTC'*RTCcov_at_epoch((1:3),(1:3))*truthtransRTC,...
   truthtransRTC'*RTCcov_at_epoch((1:3),(4:6))*truthtransRTC;...
   truthtransRTC'*RTCcov_at_epoch((4:6),(1:3))*truthtransRTC,...
   truthtransRTC'*RTCcov_at_epoch((4:6),(4:6))*truthtransRTC];

cartcov1 = ECIcov1*1000;   % need to be passed in meters and meters/second

% from VNC
```

```
ECIcov2 = [truthtransVNC'*VNCcov_at_epoch((1:3),(1:3))*truthtransVNC,...
   truthtransVNC'*VNCcov_at_epoch((1:3),(4:6))*truthtransVNC;...
   truthtransVNC'*VNCcov_at_epoch((4:6),(1:3))*truthtransVNC,...
   truthtransVNC'*VNCcov_at_epoch((4:6),(4:6))*truthtransVNC];

cartcov2 = ECIcov2*1000;   % need to be passed in meters and meters/second

[COEcov1mean,tm1mean] = COVCT2CL(cartcov1,cartstate,'mean');
[COEcov1true,tm1true] = COVCT2CL(cartcov1,cartstate,'true');
[COEcov2mean,tm2mean] = COVCT2CL(cartcov2,cartstate,'mean');
[COEcov2true,tm2true] = COVCT2CL(cartcov2,cartstate,'true');

COE_variances_fromRTC_meananomaly = diag(COEcov1mean)
COE_variances_fromRTC_trueanomaly = diag(COEcov1true)
COE_variances_fromVNC_meananomaly = diag(COEcov2mean)
COE_variances_fromVNC_trueanomaly = diag(COEcov2true)

COEcheck1 = COEcov1mean - COEcov2mean
COEcheck2 = COEcov1true - COEcov2true

% ---------------------------------------
% Build giant matrix of covariance matrices and variances for all the
% respective coordinate systems
Epoch_Cov_All =[RTCcov_at_epoch RTCvariances_at_epoch RTCstdev_at_epoch;...
   VNCcov_at_epoch VNCvariances_at_epoch VNCstdev_at_epoch;...
   RTCcovar_corr_coeff zeros(6,2);...
   VNCcovar_corr_coeff zeros(6,2);...
   COEcov1mean COE_variances_fromRTC_meananomaly zeros(6,1);...
   COEcov1true COE_variances_fromRTC_trueanomaly zeros(6,1);...
   COEcov2mean COE_variances_fromVNC_meananomaly zeros(6,1);...
   COEcov2true COE_variances_fromVNC_trueanomaly zeros(6,1)];

% ---------------------------------------------------------------------
% ---------------------------------------------------------------------
% Write data to Excel file
if (writeexcel)
AugCol = {'Delta-t TLE Epochs (days)';'Position Difference Radial (km)';...
   'Position Difference Transverse (km)';
'Position Difference Cross-track (km)';...
'Velocity Difference Radial (km/sec)';...
'Velocity Difference Transverse (km/sec)';...
'Velocity Difference Cross-track (km/sec)';...
'Position Difference Velocity (km)';...
'Position Difference Normal (km)';...
'Position Difference Cross-track (km)';...
'Velocity Difference Velocity (km/sec)';...
'Velocity Difference Normal (km/sec)';...
'Velocity Difference Cross-track (km/sec)'};

StatRow1={'Statistics by Bin Number for only Position Differences (km)',...
   'Mean values','in RTC frame','by component',...
   'Variance values','in RTC frame','by component',...
   'StDev values','in RTC frame','by component',...
   'Mean values','in VNC frame','by component',...
```

```
    'Variance values','in VNC frame','by component',...
    'StDev values','in VNC frame','by component'};

StatRow2 = {'Sample Points in Bin',...
    'Radial','Transverse','Cross Track',...
    'Radial','Transverse','Cross Track',...
    'Radial','Transverse','Cross Track',...
    'Velocity','Normal','Cross Track',...
    'Velocity','Normal','Cross Track',...
    'Velocity','Normal','Cross Track'};

SheetDescrip = {'Jth TLE Number','Kth TLE Number',...
    'Delta Time between epochs (days)';...
    'Jth TLE epoch (sec)','Kth TLE epoch (sec)',...
    'Delta Time between epochs (sec)';...
    'Jth Radial Position (km)','Kth Radial Position (km)',...
    'Difference Radial Position (km)';...
    'Jth Transverse Position (km)','Kth Transverse Position (km)',...
    'Difference Transverse Position (km)';...
    'Jth Crosstrack Position (km)','Kth Crosstrack Position (km)',...
    'Difference Crosstrack Position (km)';...
    'Jth Radial Velocity (km/sec)','Kth Radial Velocity (km/sec)',...
    'Difference Radial Velocity (km/sec)';...
  'Jth Transverse Velocity (km/sec)','Kth Transverse Velocity (km/sec)',...
    'Difference Transverse Velocity (km/sec)';...
  'Jth Crosstrack Velocity (km/sec)','Kth Crosstrack Velocity (km/sec)',...
    'Difference Crosstrack Velocity (km/sec)';...
    'RTC transformation matrix - R1','R2','R3';'T1','T2','T3';...
    'C1','C2','C3';...
    'Jth Velocity Position (km)','Kth Velocity Position (km)',...
    'Difference Velocity Position (km)';...
    'Jth Normal Position (km)','Kth Normal Position (km)',...
    'Difference Normal Position (km)';...
    'Jth Crosstrack Position (km)','Kth Crosstrack Position (km)',...
    'Difference Crosstrack Position (km)';...
    'Jth Velocity Velocity (km/sec)','Kth Velocity Velocity (km/sec)',...
    'Difference Velocity Velocity (km/sec)';...
    'Jth Normal Velocity (km/sec)','Kth Normal Velocity (km/sec)',...
    'Difference Normal Velocity (km/sec)';...
  'Jth Crosstrack Velocity (km/sec)','Kth Crosstrack Velocity (km/sec)',...
    'Difference Crosstrack Velocity (km/sec)';...
    'VNC transformation matrix - V1','V2','V3';'N1','N2','N3';...
    'C1','C2','C3'};

CovDes1 = {'POSITIONradial_POSITIONradial',...
    'Pr_Pt','Pr_Pc','Pr_Vr','Pr_Vt','Pr_Vc';...
    'Pt_Pr','Ptransverse_Ptransverse','Pt_Pc','Pt_Vr','Pt_Vt','Pt_Vc';...
    'Pc_Pr','Pc_Pt','Pcrosstrack_Pcrosstrack','Pc_Vr','Pc_Vt','Pc_Vc';...
    'Vr_Pr','Vr_Pt','Vr_Pc','Vradial_Vradial','Vr_Vt','Vr_Vc';...
    'Vt_Pr','Vt_Pt','Vt_Pc','Vt_Vr','Vtransverse_Vtransverse','Vt_Vc';...
    'Vc_Pr','Vc_Pt','Vc_Pc','Vc_Vr','Vc_Vt',...
    'VELOCITYcrosstrack_VELOCITYcrosstrack';...
    'POSITIONvelocity_POSITIONvelocity',...
    'Pv_Pn','Pv_Pc','Pv_Vv','Pv_Vn','Pv_Vc';...
```

```
    'Pn_Pv','Pnormal_Pnormal','Pn_Pc','Pn_Vv','Pn_Vn','Pn_Vc';...
    'Pc_Pv','Pc_Pn','Pcrosstrack_Pcrosstrack','Pc_Vv','Pc_Vn','Pc_Vc';...
    'Vv_Pv','Vv_Pn','Vv_Pc','Vvelocity_Vvelocity','Vv_Vn','Vv_Vc';...
    'Vn_Pv','Vn_Pn','Vn_Pc','Vn_Vv','Vnormal_Vnormal','Vn_Vc';...
    'Vc_Pv','Vc_Pn','Vc_Pc','Vc_Vv','Vc_Vn',...
    'VELOCITYcrosstrack_VELOCITYcrosstrack'};

CovDes2 = {'6x6','RTC','Covariance','Correlation','Coefficients','Matrix'};
CovDes3 = {'6x6','VNC','Covariance','Correlation','Coefficients','Matrix'};
CovDes4 = {'R';'T';'C';'Variances';'at';'epoch';...
    'V';'N';'C';'Variances';'at';'epoch'};
CovDes5 = {'R';'T';'C';'StDev';'at';'epoch';...
    'V';'N';'C';'StDev';'at';'epoch'};
CovDes6 = {'6x6','COE','Covariance','Matrix','from RTC transform',...
    'using Mean Anomaly','Variances Column Here','Zero fill column'};
CovDes7 = {'6x6','COE','Covariance','Matrix','from RTC transform',...
    'using True Anomaly','Variances Column Here','Zero fill column'};
CovDes8 = {'6x6','COE','Covariance','Matrix','from VNC transform',...
    'using Mean Anomaly','Variances Column Here','Zero fill column'};
CovDes9 = {'6x6','COE','Covariance','Matrix','from VNC transform',...
    'using True Anomaly','Variances Column Here','Zero fill column'};

xfile = ['I:\My Documents\Thesis\Output\data_sat',...
    catnr,'_t',num2str(t),'.xls'];

for ex = 1:count
    xlswrite(xfile, data_at_epoch(:,:,1,ex),ex);
end;

xlswrite(xfile, SheetDescrip, 'SheetXX Description');
% xlswrite(xfile, TLEsTimeInts, 'times');
xlswrite(xfile, StatRow1, 'Statistics','A1');
xlswrite(xfile, StatRow2, 'Statistics','A2');
xlswrite(xfile, stats, 'Statistics','A3');
xlswrite(xfile, AugCol', 'AugmentMatrix','A1:M1');
xlswrite(xfile, augment', 'AugmentMatrix','A2');
xlswrite(xfile, Epoch_Cov_All, 'Epoch Covariance Data');
xlswrite(xfile, CovDes1, 'Epoch_Cov_All Sheet','A1');
xlswrite(xfile, CovDes2, 'Epoch_Cov_All Sheet','A13');
xlswrite(xfile, CovDes3, 'Epoch_Cov_All Sheet','A19');
xlswrite(xfile, CovDes4, 'Epoch_Cov_All Sheet','G1');
xlswrite(xfile, CovDes5, 'Epoch_Cov_All Sheet','H1');
xlswrite(xfile, CovDes6, 'Epoch_Cov_All Sheet','A25');
xlswrite(xfile, CovDes7, 'Epoch_Cov_All Sheet','A31');
xlswrite(xfile, CovDes8, 'Epoch_Cov_All Sheet','A37');
xlswrite(xfile, CovDes9, 'Epoch_Cov_All Sheet','A43');
end;  % if writeexcel files

% ----------------------------------------------------------------
% ----------------------------------------------------------------
% PLOTTING
if(toplotornottoplot)   % PLOT RUN #1

x = 0.0:0.5:15.0;
```

```
b = 0:1:14;

if (logfit)
   pV = polyfit(delta,log10(abs(PosDiffVNC(1,:))),2);
   pN = polyfit(delta,log10(abs(PosDiffVNC(2,:))),2);
   pC = polyfit(delta,log10(abs(PosDiffVNC(3,:))),2);
else
   pV = polyfit(delta,(PosDiffVNC(1,:)),2);
   pN = polyfit(delta,(PosDiffVNC(2,:)),2);
   pC = polyfit(delta,(PosDiffVNC(3,:)),2);
end; % if logfit

if (logfit)
   fitV = 10.^polyval(pV,x);
   fitN = 10.^polyval(pN,x);
   fitC = 10.^polyval(pC,x);
else
   fitV = polyval(pV,x);
   fitN = polyval(pN,x);
   fitC = polyval(pC,x);
end; % if logfit

figure(fignr*10+1)
clf; figurenr = gcf;
subplot(3,1,1)
hold on;
title({'Positional Differences in NTW (VNC) Coordinate Frame';...
   ['NORAD Catalog Number ',catnr];...
   ['Time Window: ',datestr(startdate),' to ',datestr(enddate)]});
plot(delta,PosDiffVNC(1,:),'r.');
plot(x,fitV,'r:');
errorbar(b,VNCmean(:,1),VNCstdev(:,1),'ro','MarkerSize',6);
legend('Velocity (in-track)','Location','Best');
% axis tight;
xlim([0 15]);
set(gca,'XTick',0:1:15); set(gca,'YGrid','on');
xlabel('Delta Epoch (days)'); ylabel('Delta Position (km)');
hold off;

subplot(3,1,2)
hold on;
plot(delta,PosDiffVNC(2,:),'b.');
plot(x,fitN,'b:');
errorbar(b,VNCmean(:,2),VNCstdev(:,2),'bo','MarkerSize',6);
legend('Normal (along-radial) ','Location','Best');
axis tight; xlim([0 15]);
set(gca,'XTick',0:1:15); set(gca,'YGrid','on');
xlabel('Delta Epoch (days)'); ylabel('Delta Position (km)');
hold off;

subplot(3,1,3)
hold on;
plot(delta,PosDiffVNC(3,:),'k.');
plot(x,fitC,'k:');
```

```
errorbar(b,VNCmean(:,3),VNCstdev(:,3),'ko','MarkerSize',6);
legend('Cross-track','Location','Best');
% axis tight;
xlim([0 15]);
set(gca,'XTick',0:1:15); set(gca,'YGrid','on');
xlabel('Delta Epoch (days)'); ylabel('Delta Position (km)');
hold off;

saveas(figurenr,['I:\My Documents\Thesis\Output\figure_sat',...
   catnr,'_t',num2str(t),'_PosDiffVNC_subplots.jpg']);

% ------------------------------------------------------------

clear pC fitC;
if (logfit)
   pR = polyfit(delta,log10(abs(PosDiffRTC(1,:))),2);
   pT = polyfit(delta,log10(abs(PosDiffRTC(2,:))),2);
   pC = polyfit(delta,log10(abs(PosDiffRTC(3,:))),2);
else
   pR = polyfit(delta,(PosDiffRTC(1,:)),2);
   pT = polyfit(delta,(PosDiffRTC(2,:)),2);
   pC = polyfit(delta,(PosDiffRTC(3,:)),2);
end; % if logfit

if (logfit)
   fitR = 10.^polyval(pR,x);
   fitT = 10.^polyval(pT,x);
   fitC = 10.^polyval(pC,x);
else
   fitR = polyval(pR,x);
   fitT = polyval(pT,x);
   fitC = polyval(pC,x);
end; % if logfit


figure(fignr*10+2)
clf; figurenr = gcf;
subplot(3,1,1)
hold on;
title({'Positional Differences in RSW Coordinate Frame';...
   ['NORAD Catalog Number ',catnr];...
   ['Time Window: ',datestr(startdate),' to ',datestr(enddate)]},...
   'Fontsize',12);
plot(delta,PosDiffRTC(2,:),'b.');
plot(x,fitT,'b:');
errorbar(b,RTCmean(:,2),RTCstdev(:,2),'bo','MarkerSize',6);
legend('Transverse (along-track)','Location','Best');
% axis tight;
xlim([0 15]);
set(gca,'XTick',0:1:15); set(gca,'YGrid','on');
xlabel('Delta Epoch (days)'); ylabel('Delta Position (km)');
hold off;

subplot(3,1,2)
```

```
hold on;
plot(delta,PosDiffRTC(1,:),'r.');
plot(x,fitR,'r:');
errorbar(b,RTCmean(:,1),RTCstdev(:,1),'ro','MarkerSize',6);
legend('Radial','Location','Best');
% axis tight;
xlim([0 15]);
set(gca,'XTick',0:1:15); set(gca,'YGrid','on');
xlabel('Delta Epoch (days)'); ylabel('Delta Position (km)');
hold off;

subplot(3,1,3)
hold on;
plot(delta,PosDiffRTC(3,:),'k.');
plot(x,fitC,'k:');
errorbar(b,RTCmean(:,3),RTCstdev(:,3),'ko','MarkerSize',6);
legend('Cross-track','Location','Best');
% axis tight;
xlim([0 15]);
set(gca,'XTick',0:1:15); set(gca,'YGrid','on');
xlabel('Delta Epoch (days)'); ylabel('Delta Position (km)');
hold off;

saveas(figurenr,['I:\My Documents\Thesis\Output\figure_sat',...
   catnr,'_t',num2str(t),'_PosDiffRTC_subplots.jpg']);

% ------------------------------------------------------

clear pC fitC;
if (logfit)
   pV = polyfit(delta,log10(abs(PosDiffVNC(1,:))),2);
   pN = polyfit(delta,log10(abs(PosDiffVNC(2,:))),2);
   pC = polyfit(delta,log10(abs(PosDiffVNC(3,:))),2);
else
   pV = polyfit(delta,(PosDiffVNC(1,:)),2);
   pN = polyfit(delta,(PosDiffVNC(2,:)),2);
   pC = polyfit(delta,(PosDiffVNC(3,:)),2);
end; % if logfit

figure(fignr*10+3)
clf; figurenr = gcf; hold on;
% plot(delta,(PosDiffVNC),'.');
plot(delta,PosDiffVNC(1,:),'rd');
plot(delta,PosDiffVNC(2,:),'bo');
plot(delta,PosDiffVNC(3,:),'kx');

if (logfit)
   fitV = 10.^polyval(pV,x);
   fitN = 10.^polyval(pN,x);
   fitC = 10.^polyval(pC,x);
else
   fitV = polyval(pV,x);
   fitN = polyval(pN,x);
   fitC = polyval(pC,x);
```

```
end; % if logfit

plot(x,fitV,'r:',x,fitN,'b:',x,fitC,'k:');
errorbar(b,VNCmean(:,1),VNCstdev(:,1),'r*','MarkerSize',6);
errorbar(b,VNCmean(:,2),VNCstdev(:,2),'b*','MarkerSize',6);
errorbar(b,VNCmean(:,3),VNCstdev(:,3),'k*','MarkerSize',6);

title({'Positional Differences in NTW (VNC) Coordinate Frame';...
   ['NORAD Catalog Number ',catnr];...
   ['Time Window: ',datestr(startdate),' to ',datestr(enddate)]},...
   'Fontsize',12);
legend('Velocity (in-track)','Normal (along-radial)','Cross-track',...
   'Location','Best');
% axis tight;
xlim([0 15]);
%ylim([-1 1]);
set(gca,'XTick',0:1:15); set(gca,'YGrid','on');
xlabel('Delta Epoch (days)'); ylabel('Delta Position (km)');
hold off;

saveas(figurenr,['I:\My Documents\Thesis\Output\figure_sat',...
   catnr,'_t',num2str(t),'_PosDiffVNC.jpg']);

% ------------------------------------------------------

clear pC fitC;
if (logfit)
   pR = polyfit(delta,log10(abs(PosDiffRTC(1,:))),2);
   pT = polyfit(delta,log10(abs(PosDiffRTC(2,:))),2);
   pC = polyfit(delta,log10(abs(PosDiffRTC(3,:))),2);
else
   pR = polyfit(delta,(PosDiffRTC(1,:)),2);
   pT = polyfit(delta,(PosDiffRTC(2,:)),2);
   pC = polyfit(delta,(PosDiffRTC(3,:)),2);
end; % if logfit

figure(fignr*10+4)
clf; figurenr = gcf; hold on;
% plot(delta,(PosDiffRTC),'.');
plot(delta,PosDiffRTC(1,:),'rd');
plot(delta,PosDiffRTC(2,:),'bo');
plot(delta,PosDiffRTC(3,:),'kx');

if (logfit)
   fitR = 10.^polyval(pR,x);
   fitT = 10.^polyval(pT,x);
   fitC = 10.^polyval(pC,x);
else
   fitR = polyval(pR,x);
   fitT = polyval(pT,x);
   fitC = polyval(pC,x);
end; % if logfit

plot(x,fitR,'b:',x,fitT,'r:',x,fitC,'k:');
```

```
errorbar(b,RTCmean(:,1),RTCstdev(:,1),'r*','MarkerSize',6);
errorbar(b,RTCmean(:,2),RTCstdev(:,2),'b*','MarkerSize',6);
errorbar(b,RTCmean(:,3),RTCstdev(:,3),'k*','MarkerSize',6);

title({'Positional Differences in RSW Coordinate Frame';...
   ['NORAD Catalog Number ',catnr];...
   ['Time Window: ',datestr(startdate),' to ',datestr(enddate)]},...
   'Fontsize',12);
legend('Radial','Transverse (along-track)','Cross-track',...
   'Location','Best');
% axis tight;
xlim([0 15]);
%ylim([-1 1]);
set(gca,'XTick',0:1:15); set(gca,'YGrid','on');
xlabel('Delta Epoch (days)'); ylabel('Delta Position (km)');
hold off;

saveas(figurenr,['I:\My Documents\Thesis\Output\figure_sat',...
   catnr,'_t',num2str(t),'_PosDiffRTC.jpg']);

% ------------------------------------------------------------

figure(fignr*10+5)
clf;
figurenr = gcf;
subplot(2,1,1)
hold on;

plot(RTCvar(:,1),'ro-','LineWidth',1);
plot(RTCvar(:,3),'gd:','LineWidth',1);
plot(VNCvar(:,2),'bx--','LineWidth',1);
plot(VNCvar(:,3),'k*-.','LineWidth',1);

% text(0,0,['Number of sample points per bin = ',num2str(points(:)')],...
%    'HorizontalAlignment','left','VerticalAlignment','top',...
%    'BackgroundColor',[.7 .9 .7],'FontSize',16);
title({'Variance in Positional Differences';...
   ['for Entire Time Window: ',datestr(startdate),' to ',...
   datestr(enddate)];...
   ['NORAD Catalog Number ',catnr]},'Fontsize',12);
legend('Radial','Cross-track','Normal (along-radial)',...
   'Cross-track','Location','NorthWest');
% axis tight;
xlabel('Bin Number'); ylabel('Variance (km^2)');
set(gca,'XTick',0:1:15);
set(gca,'YGrid','on');
hold off;

subplot(2,1,2)
hold on;
title({'Number of sample points per bin = ';num2str(points(:)')},...
   'FontSize',12);
plot(RTCvar(:,2),'bo-','LineWidth',1);
plot(VNCvar(:,1),'rx-','LineWidth',1);
```

```
legend('Transverse (along-track)','Velocity (in-track)','Location',...
   'NorthWest');
% axis tight;
xlabel('Bin Number'); ylabel('Variance (km^2)');
set(gca,'XTick',0:1:15);
set(gca,'YGrid','on');
hold off;

saveas(figurenr,['I:\My Documents\Thesis\Output\figure_sat',...
   catnr,'_t',num2str(t),'_Variances.jpg']);

end;  % if toplotornottoplot #1 run
%  END PLOTTING SECTION #1
% ------------------------------------------------------------------

% Save the Variance Values from the differenct covariance matrices
% computed above, all at the primary TLE epoch.
% Save for each timeloop.
RTC_Cov_Total(:,:,timeloop) = RTCcov_at_epoch;
VNC_Cov_Total(:,:,timeloop) = VNCcov_at_epoch;
RTC_Var_Total(:,timeloop) = RTCvariances_at_epoch;
VNC_Var_Total(:,timeloop) = VNCvariances_at_epoch;
COE_Var_total(:,timeloop) = COE_variances_fromVNC_meananomaly;

% ------------------------------------------------------
% Create Autocorrelation matrices for each timeloop
% They will be used after timeloop finishes

%%%%  for RTC
% TLEperTimeWindow(timeloop) = count
% tempo1(timeloop) = size(PosDiffRTC,2)
% padamount = 7000 - tempo1(timeloop);
% tempAC1 = [delta' PosDiffRTC'];
% tempAC2 = padarray(tempAC1,[padamount 0],'post');
% AutoCorr(:,:,timeloop) = tempAC2;

%%%%  for VNC
TLEperTimeWindow(timeloop) = count
tempo1(timeloop) = size(PosDiffVNC,2)
padamount = 7000 - tempo1(timeloop);
tempAC1 = [delta' PosDiffVNC'];
tempAC2 = padarray(tempAC1,[padamount 0],'post');
AutoCorr(:,:,timeloop) = tempAC2;
% ------------------------------------------------------

% close all;   %close all figures --> they should be saving to hard drive
diary off;
end;  % for timeloop 1 through 8
%%%%%%%%%%%%%%%%%%%%%%%%%%%%%%%%%%%%%%%%%%%%%%%%%%%%%%%%%%%%%%%%

clc;
if(toplotornottoplot)  % PLOT RUN #2

figure(fignr*10+6)
```

```
clf; figurenr = gcf;
subplot(3,1,1)
hold on;
title({'Variances at Primary TLE Epoch for all 8 Time Windows';...
   ['NORAD Catalog Number ',catnr]});
plot(RTC_Var_Total(2,:),'bo-','LineWidth',2);
legend('Transverse (along-track) Position','Location','BestOutside');
xlim([1 8]); set(gca,'XTick',0:1:8);
set(gca,'YGrid','on'); ylabel('Variance (km^2)');
hold off;

subplot(3,1,2)
hold on;
plot(RTC_Var_Total(1,:),'rd-','LineWidth',2);
plot(RTC_Var_Total(3,:),'kx-','LineWidth',2);
legend('Radial Postion','Cross-track Position','Location','BestOutside');
xlim([1 8]); set(gca,'XTick',0:1:8);
set(gca,'YGrid','on'); ylabel('Variance (km^2)');
hold off;

subplot(3,1,3)
hold on;
plot(RTC_Var_Total(4,:),'rd-','LineWidth',2);
plot(RTC_Var_Total(5,:),'bo-','LineWidth',2);
plot(RTC_Var_Total(6,:),'kx-','LineWidth',2);
legend('Radial Velocity','Transverse Velocity','Cross-track Velocity',...
   'Location','BestOutside');
xlim([1 8]); set(gca,'XTick',0:1:8); set(gca,'YGrid','on');
xlabel('Time Window #'); ylabel('Variance (km^2/sec^2)');
hold off;

saveas(figurenr,['I:\My Documents\Thesis\Output\figure_sat',...
   catnr,'_EpochVariances_subplots.jpg']);

end;  % if toplotornottoplot #2 run

% ------------------------------------------------------------------**
% **********************************************************************
%                    AUTOCORRELATION FUNCTION
% **********************************************************************
% ------------------------------------------------------------------**
if(autocorrelate)
dout2 = ['I:\My Documents\Thesis\Output\AC_output_sat_',...
   num2str(satnr),'.txt'];
diary(dout2)

ACin1 = AutoCorr((1:tempo1(1)),:,1);
ACin2 = AutoCorr((1:tempo1(2)),:,2);
ACin3 = AutoCorr((1:tempo1(3)),:,3);
ACin4 = AutoCorr((1:tempo1(4)),:,4);
ACin5 = AutoCorr((1:tempo1(5)),:,5);
ACin6 = AutoCorr((1:tempo1(6)),:,6);
ACin7 = AutoCorr((1:tempo1(7)),:,7);
ACin8 = AutoCorr((1:tempo1(8)),:,8);
```

```
% Combine all of the position residuals from every time window
% into one giant matrix
giantAC = [ACin1' ACin2' ACin3' ACin4' ACin5' ACin6' ACin7' ACin8'];
AC_overall_mean = mean(giantAC')';

% FOLLOWING 2 OPTIONS TO CHOOSE FOR AUTOCORRELATION FUNCTION
% Binwidth and # of days
binwidth = 0.5;        % Width of each bin set to half day
ndays = 35;            % number of days to pull residuals from

nob = ndays/binwidth;   % total number of bins
ACsamples = zeros(nob,1);
ACsum = zeros(nob,3);
ACsum2 = zeros(nob,3);
for w = 1:length(giantAC)
   ACbin = floor((giantAC(1,w)/binwidth) + 1.0);
      if (ACbin < (nob+1))
         ACsamples(ACbin) = ACsamples(ACbin) + 1;
         ACsum(ACbin,1) = ACsum(ACbin,1) + giantAC(2,w);
         ACsum(ACbin,2) = ACsum(ACbin,2) + giantAC(3,w);
         ACsum(ACbin,3) = ACsum(ACbin,3) + giantAC(4,w);
         ACsum2(ACbin,1) = ACsum2(ACbin,1) + ((giantAC(2,w))^2);
         ACsum2(ACbin,2) = ACsum2(ACbin,2) + ((giantAC(3,w))^2);
         ACsum2(ACbin,3) = ACsum2(ACbin,3) + ((giantAC(4,w))^2);
      end;
end;

ACsamples
figure(10+7)
plot(ACsamples);

% stopper = 10*(nob/15);
stopper = nob;

% Initialize the matrices
AC_mean_by_bin = zeros(nob,3);

for i = 1:nob
   if (ACsamples(i) > 0)
%      AC_mean_by_bin(i,:) = ACsum(i,:)/ACsamples(i);  % uses residual
     AC_mean_by_bin(i,:) = ACsum2(i,:)/ACsamples(i); % uses (residual^2)
   elseif (ACsamples(i) == 0)
      AC_mean_by_bin(i,1) = AC_overall_mean(2);
      AC_mean_by_bin(i,2) = AC_overall_mean(3);
      AC_mean_by_bin(i,3) = AC_overall_mean(4);
      % AC_mean_by_bin(i,:) = NaN;
      % AC_mean_by_bin(i,:) = 0.0;
   end; % if ACsamples(i) > 1
end; % for i


% Look for "NaN" values, and don't use them in calculating a mean value for
% each bin
```

```
% rowtemp = 0;
% tempNan = isnan(AC_mean_by_bin)
% for i = 1:nob
%     if (tempNan(i) == 1)
%         rowtemp = rowtemp + 1
%         AC_mean_by_bin(i,:) = []
%         deleted_timesteps(rowtemp) = i
%     end;
% end;

% Reassign the mean value of each bin to be the observations used for
% Autocorreation

AC_obs = AC_mean_by_bin
AC_obs_mean = mean(AC_obs)

% ------------------------------------------------------------------
% AUTOCORRELATION computations                              %% COEFF
% Using "xcov" MATLAB cross covariance function

xcov_c1_full = xcov(AC_obs(:,1),'coeff');
xcov_c2_full = xcov(AC_obs(:,2),'coeff');
xcov_c3_full = xcov(AC_obs(:,3),'coeff');

% xcov_c1 = xcov_c1_full([stopper:(stopper+(ceil(nob/5)))])
% xcov_c2 = xcov_c2_full([stopper:(stopper+(ceil(nob/5)))])
% xcov_c3 = xcov_c3_full([stopper:(stopper+(ceil(nob/5)))])

xcov_c1 = xcov_c1_full([stopper:length(xcov_c1_full)])
xcov_c2 = xcov_c2_full([stopper:length(xcov_c2_full)])
xcov_c3 = xcov_c3_full([stopper:length(xcov_c3_full)])


% AC_xfile = ['I:\My Documents\Thesis\Output\AutoCorr_sat',catnr,'.xls'];
% xlswrite(AC_xfile, AC_final, 'AutoCorrelation');

% ------------------------------------------------------------------
% AUTOCORRELATION plot

% xsteps_old = [0:binwidth:(stopper-1)/(nob/ndays)]
leend = length(xcov_c1);
xsteps = [0:binwidth:((leend-1)*binwidth)]

figure(fignr*10+8)
clf; figurenr = gcf; hold on;
plot(xsteps,xcov_c1,'ro-','LineWidth',2);
plot(xsteps,xcov_c2,'bd--','LineWidth',2);
plot(xsteps,xcov_c3,'kx:','LineWidth',2);
ylim([-1 1]);
title({'Normalized Autocorrelation of Positional Differences';...
   ['NORAD Catalog Number ',catnr];...
   'All Time Windows Grouped with Bin Averages as Observations'},...
   'Fontsize',12);
legend('Velocity (in-track)','Normal (along radial)','Cross-track','Location','Best');
```

```
%legend('Radial','Transverse (along-track)','Cross-track','Location','Best');
set(gca,'XTick',0:1:ndays);
set(gca,'YGrid','on');
xlabel(['Time Shift (days) with Bin Width of: ',num2str(binwidth),' days)']);
ylabel('Correlation');
hold off;

saveas(figurenr,['I:\My Documents\Thesis\Output\AC_sat',...
   catnr,'_Coeff_not_squared.jpg']);

%saveas(figurenr,['I:\My Documents\Thesis\Output\AC_sat',...
%    catnr,'_Coeff_VNC_thin_extraTime.jpg']);

% ---------------------------------------------------------------------
% ---------------------------------------------------------------------
% AUTOCORRELATION computations                          %% UNBIASED
% Using "xcov" MATLAB cross covariance function

% xcov_c4 = xcov(AC_obs((1:stopper),1),'unbiased');
% xcov_c5 = xcov(AC_obs((1:stopper),2),'unbiased');
% xcov_c6 = xcov(AC_obs((1:stopper),3),'unbiased');
%
% xcov_c4 = xcov_c4(stopper:length(xcov_c4))
% xcov_c5 = xcov_c5(stopper:length(xcov_c5))
% xcov_c6 = xcov_c6(stopper:length(xcov_c6))
%
%
% % AC_xfile = ['I:\My Documents\Thesis\Output\AutoCorr_sat',catnr,'.xls'];
% % xlswrite(AC_xfile, AC_final, 'AutoCorrelation');
%
% % ---------------------------------------------------------------------
% % AUTOCORRELATION plot
%
% xsteps = [0:binwidth:ndays-binwidth]
%
% figure(fignr*10+9)
% clf; figurenr = gcf; hold on;
% plot(xsteps,xcov_c4,'ro-','LineWidth',2);
% plot(xsteps,xcov_c5,'bd-','LineWidth',2);
% plot(xsteps,xcov_c6,'kx-','LineWidth',2);
% title({'Unbiased Autocorrelation of Positional Differences';...
%     ['NORAD Catalog Number ',catnr];...
%     'All Time Windows Grouped with Bin Averages as Observations'},...
%     'Fontsize',12);
% legend('Velocity (in-track)','Normal (along radial)','Cross-track','Location','Best');
% %legend('Radial','Transverse (along-track)','Cross-track','Location','Best');
% set(gca,'XTick',0:1:ndays);
% set(gca,'YGrid','on');
% xlabel('Time Shift (days)'); ylabel('Correlation');
% hold off;
%
% saveas(figurenr,['I:\My Documents\Thesis\Output\AC_sat',...
%     catnr,'_Unbiased_VNC_thin_extraTime.jpg']);
```

```
% ------------------------------------------------------------
% close all;
diary off;

end;  % if autocorrelate
% ------------------------------------------------------------**
% ************************************************************************
%                   AUTOCORRELATION FUNCTION
% ************************************************************************
% ------------------------------------------------------------**

%%%% Now CLEAR the variables before incrementing to next satellite #
clear TLEperTimeWindow count padamount tempAC1 tempAC2;
clear data_at_epoch AutoCorr tempNan N giantAC AC_overall_mean;
clear ACin1 ACin2 ACin3 ACin4 ACin5 ACin6 ACin7 ACin8;
clear ACsamples deleted_timesteps AC_obs_mean number_of_shifts AC_obs_sq;
clear AC_final

end;  % for satnr 1:6
% close all;
% clc;
% end of file

% ------------------------------------------------------------

function e2p = Epoch2Date(epoch);
  year2 = str2num(epoch(1:2));
  doy = str2num(epoch(3:14));
  if (year2 > 56)
    e2p = datenum(1900 + year2,1,1) + doy - 1;
  else
    e2p = datenum(2000 + year2,1,1) + doy - 1;
  end; % if

% ------------------------------------------------------------

function td = TwoDigit(n);
  if (n < 10)
    td = ['0',int2str(n)];
  else
    td = int2str(n);
  end; % if

% ------------------------------------------------------------

function mag = mag ( vec );

        temp= vec(1)*vec(1) + vec(2)*vec(2) + vec(3)*vec(3);

        if abs( temp ) >= 1.0e-16
            mag= sqrt( temp );
          else
            mag= 0.0;
          end
```

```
% ------------------------------------------------------------
%
%                           function rv2vnc
%
%  This function converts position and velocity vectors into
%  Velocity, Normal, and Cross-track coordinate frame (VNC)
%
%  NOTE: that sometimes the second vector is called along-radial.
%
%  author        : david vallado               719-573-2600    5 jul
2002
%
%  revisions
%                - Capt Victor Osweiler        719-310-1801    4 Feb
2006
%
%  inputs          description                    range / units
%    r           - position vector                km
%    v           - velocity vector                km/s
%
%  outputs       :
%    rvnc        - position vector                km
%    vvnc        - velocity vector                km/s
%
%  locals        :
%    temp        - temporary position vector
%
%  coupling      :
%    mag         - magnitude of a vector
%
%  references    :
%    vallado       2001, xx
%
% [rvnc,vvnc,transmat] = rv2vnc( r,v );
% ------------------------------------------------------------------

function [rvnc,vvnc,transmat] = rv2vnc( r,v );

        % compute satellite position vector magnitude
        rmag = mag(r);

        % compute satellite velocity vector magnitude
        vmag = mag(v);

        % in order to work correctly each of the components must be
        %  unit vectors !
        % in-velocity component
        vvec = v / vmag;

        % cross-track component
        cvec = cross(r,v);
        cvec = unit( cvec );
```

```
        % along-radial component
        nvec = cross(vvec,cvec);
        nvec = unit( nvec );

        % assemble transformation matrix from to vnc frame (individual
        %  components arranged in row vectors)
        transmat(1,1) = vvec(1);
        transmat(1,2) = vvec(2);
        transmat(1,3) = vvec(3);
        transmat(2,1) = nvec(1);
        transmat(2,2) = nvec(2);
        transmat(2,3) = nvec(3);
        transmat(3,1) = cvec(1);
        transmat(3,2) = cvec(2);
        transmat(3,3) = cvec(3);

        rvnc = transmat*r;
        vvnc = transmat*v;

% ------------------------------------------------------------
%
%                           function rv2rtc
%
%  This function converts position and velocity vectors into a
%  Radial, Transverse, and Cross-track coordinate system frame.
%
%  Radial positions are parallel to the position vector (along R axis)
%  Transverse displacements are normal to position vector (along S
axis).
%  Cross-track positions are normal to the plane defined by the current
%  position and velocity vectors (along the W axis)
%
% NOTE: sometimes the second vector (Transverse) is called the along-
track
%
%  Modified file from original file:  rv2ivc by Vallado
%  original author     : david vallado       719-573-2600    5 Jul 2002
%
%  revisions
%                - Capt Victor Osweiler      719-310-1801   24 Jan 2006
%
%  inputs          description                    range / units
%    r           - position vector                km
%    v           - velocity vector                km/s
%
%  outputs       :
%    rrtc        - position vector                km
%    vrtc        - velocity vector                km/s
%
%  locals        :
%
%
%  coupling      :
%    mag         - magnitude of a vector
%    unit        - calculates the unit vector
```

```
%
%  references    :
%    vallado       2001, xx
%
% [rrtc,vrtc,transmat] = rv2rtc( r,v );
% ------------------------------------------------------------------

function [rrtc,vrtc,transmat] = rv2rtc( r,v );

        % compute satellite position vector magnitude
        rmag = mag(r);

        % compute satellite velocity vector magnitude
        vmag = mag(v);

        % in order to work correctly each of the components must be
        % unit vectors !

        % Radial component
        rvec = r / rmag;

        % Normal component
        cvec = cross(r,v);
        cvec = unit( cvec );  % calls function "unit.m" to calculate


        % Transverse component
        tvec = cross(cvec,rvec);
        tvec = unit( tvec );

        % assemble transformation matrix from to ivc frame (individual
        %  components arranged in row vectors)
        transmat(1,1) = rvec(1);
        transmat(1,2) = rvec(2);
        transmat(1,3) = rvec(3);
        transmat(2,1) = tvec(1);
        transmat(2,2) = tvec(2);
        transmat(2,3) = tvec(3);
        transmat(3,1) = cvec(1);
        transmat(3,2) = cvec(2);
        transmat(3,3) = cvec(3);

        rrtc = transmat*r;
        vrtc = transmat*v;


% ------------------------------------------------------------------
```

Appendix D. Complete Covariance Matrix Results

The following tables summarize the covariance results for this study. Full 6x6 covariance matrices for each time window are offered in both the VNC coordinate system elements and classical orbital elements (COE). The two-line element (TLE) sets that correspond to these covariance matrices follow in Appendix E.

LAGEOS COVARIANCE MATRIX IN VNC ELEMENTS

TIME1	R_v (km)	R_n (km)	R_c (km)	V_v (km/sec)	V_n (km/sec)	V_c (km/sec)
R_v (km)	0.378619709	-0.034359821	0.027715274	1.55115E-05	-0.000171498	-1.90966E-05
R_n (km)	-0.034359821	0.004002483	-0.002717183	-1.81855E-06	1.5463E-05	1.89775E-06
R_c (km)	0.027715274	-0.002717183	0.008430228	1.22177E-06	-1.21872E-05	-5.33055E-06
V_v (km/sec)	1.55115E-05	-1.81855E-06	1.22177E-06	8.26397E-10	-6.9792E-09	-8.54481E-10
V_n (km/sec)	-0.000171498	1.5463E-05	-1.21872E-05	-6.9792E-09	7.79043E-08	8.3125E-09
V_c (km/sec)	-1.90966E-05	1.89775E-06	-5.33055E-06	-8.54481E-10	8.3125E-09	3.77679E-09

TIME2	R_v (km)	R_n (km)	R_c (km)	V_v (km/sec)	V_n (km/sec)	V_c (km/sec)
R_v (km)	0.534304775	0.000129375	0.038910851	-7.90485E-07	-0.000244815	3.2897E-05
R_n (km)	0.000129375	0.001010328	0.000203891	-4.70718E-07	-1.93425E-07	-2.39118E-08
R_c (km)	0.038910851	0.000203891	0.010459526	-1.50656E-07	-1.81015E-05	-6.0677E-06
V_v (km/sec)	-7.90485E-07	-4.70718E-07	-1.50656E-07	2.20309E-10	4.25173E-10	-3.05101E-11
V_n (km/sec)	-0.000244815	-1.93425E-07	-1.81015E-05	4.25173E-10	1.13087E-07	-1.35752E-08
V_c (km/sec)	3.2897E-05	-2.39118E-08	-6.0677E-06	-3.05101E-11	-1.35752E-08	1.58056E-08

TIME3	R_v (km)	R_n (km)	R_c (km)	V_v (km/sec)	V_n (km/sec)	V_c (km/sec)
R_v (km)	0.504294604	0.009915559	-0.064747732	-5.58294E-06	-0.000245144	7.94077E-06
R_n (km)	0.009915559	0.002319658	-0.003505881	-1.09451E-06	-4.863E-06	8.03357E-07
R_c (km)	-0.064747732	-0.003505881	0.016918095	1.7535E-06	3.26951E-05	-2.21394E-06
V_v (km/sec)	-5.58294E-06	-1.09451E-06	1.7535E-06	5.18205E-10	2.73415E-09	-3.87451E-10
V_n (km/sec)	-0.000245144	-4.863E-06	3.26951E-05	2.73415E-09	1.19486E-07	-4.22385E-09
V_c (km/sec)	7.94077E-06	8.03357E-07	-2.21394E-06	-3.87451E-10	-4.22385E-09	1.90193E-09

TIME4	R_v (km)	R_n (km)	R_c (km)	V_v (km/sec)	V_n (km/sec)	V_c (km/sec)
R_v (km)	0.247098686	0.015949995	0.046395697	-7.93297E-06	-0.000119778	1.76517E-05
R_n (km)	0.015949995	0.00285397	0.004785827	-1.36049E-06	-7.97061E-06	2.43241E-06
R_c (km)	0.046395697	0.004785827	0.015020711	-2.3223E-06	-2.22845E-05	6.16589E-06
V_v (km/sec)	-7.93297E-06	-1.36049E-06	-2.3223E-06	6.49239E-10	3.95679E-09	-1.16814E-09
V_n (km/sec)	-0.000119778	-7.97061E-06	-2.22845E-05	3.95679E-09	5.81921E-08	-8.60078E-09
V_c (km/sec)	1.76517E-05	2.43241E-06	6.16589E-06	-1.16814E-09	-8.60078E-09	2.93096E-09

TIME5	R_v (km)	R_n (km)	R_c (km)	V_v (km/sec)	V_n (km/sec)	V_c (km/sec)
R_v (km)	0.244902939	-0.01444024	0.012540795	6.22561E-06	-0.000115063	1.19525E-05
R_n (km)	-0.01444024	0.003010741	-0.005762847	-1.37006E-06	5.38064E-06	-3.12251E-06
R_c (km)	0.012540795	-0.005762847	0.032974422	2.66016E-06	-9.86342E-08	1.39066E-05
V_v (km/sec)	6.22561E-06	-1.37006E-06	2.66016E-06	6.24143E-10	-2.2718E-09	1.42998E-09
V_n (km/sec)	-0.000115063	5.38064E-06	-9.86342E-08	-2.2718E-09	5.54955E-08	-2.92786E-09
V_c (km/sec)	1.19525E-05	-3.12251E-06	1.39066E-05	1.42998E-09	-2.92786E-09	6.40896E-09

TIME6	R_v (km)	R_n (km)	R_c (km)	V_v (km/sec)	V_n (km/sec)	V_c (km/sec)
R_v (km)	0.260476403	0.006807341	-0.049497021	-3.62882E-06	-0.000119278	5.17528E-06
R_n (km)	0.006807341	0.000533211	-0.000997833	-2.59627E-07	-3.10255E-06	-1.12845E-07
R_c (km)	-0.049497021	-0.000997833	0.013348064	5.52639E-07	2.28261E-05	-2.08037E-06
V_v (km/sec)	-3.62882E-06	-2.59627E-07	5.52639E-07	1.26985E-10	1.65501E-09	4.29595E-11
V_n (km/sec)	-0.000119278	-3.10255E-06	2.28261E-05	1.65501E-09	5.46418E-08	-2.40754E-09
V_c (km/sec)	5.17528E-06	-1.12845E-07	-2.08037E-06	4.29595E-11	-2.40754E-09	5.7289E-10

TIME7	R_v (km)	R_n (km)	R_c (km)	V_v (km/sec)	V_n (km/sec)	V_c (km/sec)
R_v (km)	0.054871084	-0.000978602	-0.000826974	3.75571E-07	-2.36602E-05	6.5568E-06
R_n (km)	-0.000978602	0.003440623	0.000646066	-1.59277E-06	1.269E-06	-4.96541E-06
R_c (km)	-0.000826974	0.000646066	0.000947342	-2.98109E-07	6.50997E-07	-4.20554E-07
V_v (km/sec)	3.75571E-07	-1.59277E-06	-2.98109E-07	7.37457E-10	-5.54347E-10	2.29152E-09
V_n (km/sec)	-2.36602E-05	1.269E-06	6.50997E-07	-5.54347E-10	1.05474E-08	-3.6684E-09
V_c (km/sec)	6.5568E-06	-4.96541E-06	-4.20554E-07	2.29152E-09	-3.6684E-09	1.02768E-08

TIME8	R_v (km)	R_n (km)	R_c (km)	V_v (km/sec)	V_n (km/sec)	V_c (km/sec)
R_v (km)	0.043812286	0.005469355	-0.000934959	-2.5521E-06	-1.75903E-05	2.58034E-06
R_n (km)	0.005469355	0.002689648	0.000916317	-1.24679E-06	-1.208E-06	5.63758E-09
R_c (km)	-0.000934959	0.000916317	0.008055267	-4.25117E-07	2.71875E-06	-2.94304E-06
V_v (km/sec)	-2.5521E-06	-1.24679E-06	-4.25117E-07	5.77961E-10	5.67204E-10	-3.28579E-12
V_n (km/sec)	-1.75903E-05	-1.208E-06	2.71875E-06	5.67204E-10	8.0979E-09	-1.84275E-09
V_c (km/sec)	2.58034E-06	5.63758E-09	-2.94304E-06	-3.28579E-12	-1.84275E-09	1.579E-09

LAGEOS COVARIANCE MATRIX IN CLASSICAL ORBITAL ELEMENTS

TIME1	*a*	*e*	*i*	*node*	*w*	*M*
a	0.000868469	-3.91742E-09	7.75371E-09	5.99667E-09	-2.4212E-07	2.03335E-07
e	-3.91742E-09	2.8245E-14	-3.19216E-14	-2.17944E-14	8.94369E-13	-6.66835E-13
i	7.75371E-09	-3.19216E-14	1.15755E-13	8.11605E-14	4.70358E-13	-7.11031E-13
node	5.99667E-09	-2.17944E-14	8.11605E-14	6.3738E-14	-1.31752E-15	-1.72884E-13
w	-2.4212E-07	8.94369E-13	4.70358E-13	-1.31752E-15	3.59334E-10	-3.43956E-10
M	2.03335E-07	-6.66835E-13	-7.11031E-13	-1.72884E-13	-3.43956E-10	3.31154E-10

TIME2	*a*	*e*	*i*	*node*	*w*	*M*
a	0.000594661	-2.03644E-10	-3.44967E-09	4.43934E-09	7.68182E-08	-1.19738E-07
e	-2.03644E-10	1.57681E-14	3.07283E-14	1.26806E-15	-2.64202E-12	2.65387E-12
i	-3.44967E-09	3.07283E-14	4.83751E-13	9.25065E-14	-1.04047E-11	1.08306E-11
node	4.43934E-09	1.26806E-15	9.25065E-14	7.90356E-14	3.43316E-13	-5.88712E-13
w	7.68182E-08	-2.64202E-12	-1.04047E-11	3.43316E-13	1.12513E-09	-1.1293E-09
M	-1.19738E-07	2.65387E-12	1.08306E-11	-5.88712E-13	-1.1293E-09	1.13671E-09

TIME3	*a*	*e*	*i*	*node*	*w*	*M*
a	0.000313177	1.42385E-09	-8.93994E-11	3.55579E-09	-1.33523E-07	1.04503E-07
e	1.42385E-09	1.83297E-14	-1.84211E-14	4.36736E-14	8.16695E-13	-9.95351E-13
i	-8.93994E-11	-1.84211E-14	5.87144E-14	-3.40836E-14	-2.13265E-12	2.25609E-12
node	3.55579E-09	4.36736E-14	-3.40836E-14	1.27053E-13	4.4188E-12	-4.9124E-12
w	-1.33523E-07	8.16695E-13	-2.13265E-12	4.4188E-12	9.23348E-10	-9.33309E-10
M	1.04503E-07	-9.95351E-13	2.25609E-12	-4.9124E-12	-9.33309E-10	9.46906E-10

TIME4	*a*	*e*	*i*	*node*	*w*	*M*
a	0.000532921	1.75744E-09	-5.1185E-09	-6.11787E-09	5.52521E-07	-5.78785E-07
e	1.75744E-09	8.91543E-15	-1.57927E-14	-1.45584E-14	2.37755E-12	-2.45299E-12
i	-5.1185E-09	-1.57927E-14	8.95594E-14	9.32886E-14	-8.69882E-12	8.91176E-12
node	-6.11787E-09	-1.45584E-14	9.32886E-14	1.12661E-13	-8.52965E-12	8.81233E-12
w	5.52521E-07	2.37755E-12	-8.69882E-12	-8.52965E-12	1.17101E-09	-1.19323E-09
M	-5.78785E-07	-2.45299E-12	8.91176E-12	8.81233E-12	-1.19323E-09	1.21684E-09

TIME5	*a*	*e*	*i*	*node*	*w*	*M*
a	0.000498839	2.302E-09	1.48507E-09	3.44634E-09	6.68034E-08	-9.32559E-08
e	2.302E-09	2.6374E-14	5.52367E-14	6.26414E-14	5.68688E-12	-5.78436E-12
i	1.48507E-09	5.52367E-14	1.9661E-13	2.10512E-13	1.91253E-11	-1.90857E-11
node	3.44634E-09	6.26414E-14	2.10512E-13	2.46465E-13	1.88775E-11	-1.8932E-11
w	6.68034E-08	5.68688E-12	1.91253E-11	1.88775E-11	2.58202E-09	-2.57646E-09
M	-9.32559E-08	-5.78436E-12	-1.90857E-11	-1.8932E-11	-2.57646E-09	2.57244E-09

TIME6	*a*	*e*	*i*	*node*	*w*	*M*
a	0.000375166	-5.39537E-10	-1.00737E-09	5.04018E-09	1.38556E-07	-1.65628E-07
e	-5.39537E-10	2.19227E-15	-9.78873E-16	-5.0519E-15	-4.07553E-13	4.51459E-13
i	-1.00737E-09	-9.78873E-16	1.79081E-14	-3.19265E-14	3.21093E-13	-2.36061E-13
node	5.04018E-09	-5.0519E-15	-3.19265E-14	9.97139E-14	1.45844E-12	-1.84694E-12
w	1.38556E-07	-4.07553E-13	3.21093E-13	1.45844E-12	1.6129E-10	-1.70523E-10
M	-1.65628E-07	4.51459E-13	-2.36061E-13	-1.84694E-12	-1.70523E-10	1.81806E-10

TIME7	*a*	*e*	*i*	*node*	*w*	*M*
a	7.94727E-05	-7.45293E-10	6.24319E-10	-1.0569E-11	-3.36426E-08	2.90826E-08
e	-7.45293E-10	3.00475E-14	-6.70413E-14	6.07929E-15	-8.44535E-13	8.58875E-13
i	6.24319E-10	-6.70413E-14	3.184E-13	-6.33395E-15	7.9746E-12	-7.92566E-12
node	-1.0569E-11	6.07929E-15	-6.33395E-15	7.05988E-15	4.19126E-14	-5.03962E-14
w	-3.36426E-08	-8.44535E-13	7.9746E-12	4.19126E-14	3.41239E-10	-3.37399E-10
M	2.90826E-08	8.58875E-13	-7.92566E-12	-5.03962E-14	-3.37399E-10	3.33871E-10

TIME8	*a*	*e*	*i*	*node*	*w*	*M*
a	4.82353E-05	-6.51979E-10	1.085889E-10	-6.42123E-10	-2.01251E-07	1.998859E-07
e	-6.51979E-10	2.47424E-14	-3.3142E-15	1.22087E-14	5.09944E-12	-5.10257E-12
i	1.08589E-10	-3.3142E-15	4.91183E-14	-4.47739E-14	-4.80268E-12	4.89435E-12
node	-6.42123E-10	1.22087E-14	-4.47739E-14	5.98996E-14	7.99421E-12	-8.08645E-12
w	-2.01251E-07	5.09944E-12	-4.80268E-12	7.99421E-12	1.76643E-09	-1.77589E-09
M	1.99859E-07	-5.10257E-12	4.89435E-12	-8.08645E-12	-1.77589E-09	1.7857E-09

TOPEX COVARIANCE MATRIX IN VNC COORDINATES

TIME1	R_v (km)	R_n (km)	R_c (km)	V_v (km/sec)	V_n (km/sec)	V_c (km/sec)
R_v (km)	10.80789368	0.172006167	-0.174091692	-0.000168794	-0.010058717	3.31348E-05
R_n (km)	0.172006167	0.023807454	-0.043945423	-2.24849E-05	-0.000164396	6.96262E-06
R_c (km)	-0.174091692	-0.043945423	0.138256066	4.1363E-05	0.000165206	-3.24025E-05
V_v (km/sec)	-0.000168794	-2.24849E-05	4.1363E-05	2.12417E-08	1.61176E-07	-6.52866E-09
V_n (km/sec)	-0.010058717	-0.000164396	0.000165206	1.61176E-07	9.36503E-06	-2.85147E-08
V_c (km/sec)	3.31348E-05	6.96262E-06	-3.24025E-05	-6.52866E-09	-2.85147E-08	1.15397E-08

TIME2	R_v (km)	R_n (km)	R_c (km)	V_v (km/sec)	V_n (km/sec)	V_c (km/sec)
R_v (km)	5.412894564	0.200909618	0.094893723	-0.000190886	-0.005014678	-8.46399E-06
R_n (km)	0.200909618	0.130599436	-0.110691922	-0.000121741	-0.000192953	2.53358E-06
R_c (km)	0.094893723	-0.110691922	0.175687923	0.000102998	-8.11635E-05	-1.07476E-06
V_v (km/sec)	-0.000190886	-0.000121741	0.000102998	1.13487E-07	1.83216E-07	-2.33581E-09
V_n (km/sec)	-0.005014678	-0.000192953	-8.11635E-05	1.83216E-07	4.64986E-06	8.95796E-09
V_c (km/sec)	-8.46399E-06	2.53358E-06	-1.07476E-06	-2.33581E-09	8.95796E-09	4.03845E-09

TIME3	R_v (km)	R_n (km)	R_c (km)	V_v (km/sec)	V_n (km/sec)	V_c (km/sec)
R_v (km)	23.05593235	0.525296572	-0.721977353	-0.000529072	-0.021562464	-0.000306404
R_n (km)	0.525296572	0.032194431	-0.051200489	-3.09708E-05	-0.000486692	-1.17465E-05
R_c (km)	-0.721977353	-0.051200489	0.135260564	4.89986E-05	0.000673395	2.49582E-05
V_v (km/sec)	-0.000529072	-3.09708E-05	4.89986E-05	2.98381E-08	4.90525E-07	1.15423E-08
V_n (km/sec)	-0.021562464	-0.000486692	0.000673395	4.90525E-07	2.01708E-05	2.87397E-07
V_c (km/sec)	-0.000306404	-1.17465E-05	2.49582E-05	1.15423E-08	2.87397E-07	1.37255E-08

TIME4	R_v (km)	R_n (km)	R_c (km)	V_v (km/sec)	V_n (km/sec)	V_c (km/sec)
R_v (km)	3.204532902	0.295859153	-0.270406068	-0.000278374	-0.003104095	-0.00027179
R_n (km)	0.295859153	0.038743397	-0.042053681	-3.63257E-05	-0.000283532	-2.90133E-05
R_c (km)	-0.270406068	-0.042053681	0.114643823	3.94111E-05	0.00025151	9.86117E-06
V_v (km/sec)	-0.000278374	-3.63257E-05	3.94111E-05	3.40599E-08	2.66804E-07	2.72428E-08
V_n (km/sec)	-0.003104095	-0.000283532	0.00025151	2.66804E-07	3.00973E-06	2.64511E-07
V_c (km/sec)	-0.00027179	-2.90133E-05	9.86117E-06	2.72428E-08	2.64511E-07	3.21944E-08

TIME5	R_v (km)	R_n (km)	R_c (km)	V_v (km/sec)	V_n (km/sec)	V_c (km/sec)
R_v (km)	9.425362076	0.51376439	-0.540765472	-0.00048784	-0.008920078	-4.54031E-05
R_n (km)	0.51376439	0.063901545	-0.086109823	-5.99857E-05	-0.000491408	-1.67094E-06
R_c (km)	-0.540765472	-0.086109823	0.155073797	8.0685E-05	0.000514069	-1.90744E-06
V_v (km/sec)	-0.00048784	-5.99857E-05	8.0685E-05	5.63178E-08	4.66542E-07	1.58966E-09
V_n (km/sec)	-0.008920078	-0.000491408	0.000514069	4.66542E-07	8.44605E-06	4.34017E-08
V_c (km/sec)	-4.54031E-05	-1.67094E-06	-1.90744E-06	1.58966E-09	4.34017E-08	4.27668E-09

TIME6	R_v (km)	R_n (km)	R_c (km)	V_v (km/sec)	V_n (km/sec)	V_c (km/sec)
R_v (km)	3.903619626	-0.139219593	0.494736994	0.000127803	-0.003635027	-9.85158E-05
R_n (km)	-0.139219593	0.032620971	-0.073628726	-3.03443E-05	0.000130345	-8.93096E-07
R_c (km)	0.494736994	-0.073628726	0.204740949	6.84121E-05	-0.000461753	-1.73876E-05
V_v (km/sec)	0.000127803	-3.03443E-05	6.84121E-05	2.82282E-08	-1.19662E-07	8.52824E-10
V_n (km/sec)	-0.003635027	0.000130345	-0.000461753	-1.19662E-07	3.38615E-06	9.10717E-08
V_c (km/sec)	-9.85158E-05	-8.93096E-07	-1.73876E-05	8.52824E-10	9.10717E-08	1.70774E-08

TIME7	R_v (km)	R_n (km)	R_c (km)	V_v (km/sec)	V_n (km/sec)	V_c (km/sec)
R_v (km)	14.48711688	0.27589929	-0.787687092	-0.000274957	-0.013641907	1.62798E-05
R_n (km)	0.27589929	0.056727058	-0.144046928	-5.34772E-05	-0.0002704	1.73248E-05
R_c (km)	-0.787687092	-0.144046928	0.376891988	0.000135913	0.000771018	-4.8354E-05
V_v (km/sec)	-0.000274957	-5.34772E-05	0.000135913	5.04321E-08	2.68874E-07	-1.62178E-08
V_n (km/sec)	-0.013641907	-0.0002704	0.000771018	2.68874E-07	1.28498E-05	-1.89186E-08
V_c (km/sec)	1.62798E-05	1.73248E-05	-4.8354E-05	-1.62178E-08	-1.89186E-08	2.01692E-08

TIME8	R_v (km)	R_n (km)	R_c (km)	V_v (km/sec)	V_n (km/sec)	V_c (km/sec)
R_v (km)	3.863648827	-0.009264806	0.224759941	9.11996E-06	-0.003597641	-4.1097E-05
R_n (km)	-0.009264806	0.049947551	-0.061182845	-4.65993E-05	7.35572E-07	-8.10436E-06
R_c (km)	0.224759941	-0.061182845	0.136456669	5.71849E-05	-0.00019463	1.12411E-05
V_v (km/sec)	9.11996E-06	-4.65993E-05	5.71849E-05	4.34759E-08	-1.10677E-09	7.56968E-09
V_n (km/sec)	-0.003597641	7.35572E-07	-0.00019463	-1.10677E-09	3.35358E-06	4.17296E-08
V_c (km/sec)	-4.1097E-05	-8.10436E-06	1.12411E-05	7.56968E-09	4.17296E-08	9.87144E-09

TOPEX COVARIANCE MATRIX IN CLASSICAL ORBITAL ELEMENTS

TIME1	*a*	*e*	*i*	*node*	*w*	*M*
a	0.053357543	9.56379E-08	-1.47138E-08	-1.41907E-07	-7.26927E-05	7.0055E-05
e	9.56379E-08	3.9046E-13	-1.32645E-13	-8.04915E-13	-2.73068E-10	2.69946E-10
i	-1.47138E-08	-1.32645E-13	2.22929E-13	6.38186E-13	-5.12094E-11	5.1498E-11
node	-1.41907E-07	-8.04915E-13	6.38186E-13	2.77862E-12	3.99212E-10	-3.96765E-10
w	-7.26927E-05	-2.73068E-10	-5.12094E-11	3.99212E-10	4.46798E-07	-4.4557E-07
M	7.0055E-05	2.69946E-10	5.1498E-11	-3.96765E-10	-4.4557E-07	4.44522E-07

TIME2	*a*	*e*	*i*	*node*	*w*	*M*
a	0.020571772	4.81802E-08	7.04348E-09	1.94565E-08	-1.14047E-05	1.02161E-05
e	4.81802E-08	2.14332E-12	-4.70754E-14	-1.99624E-12	-6.40551E-10	6.37088E-10
i	7.04348E-09	-4.70754E-14	7.81454E-14	2.13458E-14	-2.65138E-11	2.63227E-11
node	1.94565E-08	-1.99624E-12	2.13458E-14	3.53097E-12	6.89335E-10	-6.91727E-10
w	-1.14047E-05	-6.40551E-10	-2.65138E-11	6.89335E-10	4.3345E-07	-4.33246E-07
M	1.02161E-05	6.37088E-10	2.63227E-11	-6.91727E-10	-4.33246E-07	4.33134E-07

TIME3	*a*	*e*	*i*	*node*	*w*	*M*
a	0.386639845	3.24197E-07	1.90544E-07	-4.28559E-07	-0.00024886	0.000237011
e	3.24197E-07	6.13308E-13	2.21568E-13	-9.66813E-13	-1.54322E-10	1.44858E-10
i	1.90544E-07	2.21568E-13	2.65369E-13	-4.91562E-13	-1.85592E-10	1.80099E-10
node	-4.28559E-07	-9.66813E-13	-4.91562E-13	2.71829E-12	4.83577E-10	-4.70964E-10
w	-0.00024886	-1.54322E-10	-1.85592E-10	4.83577E-10	4.74646E-07	-4.66344E-07
M	0.000237011	1.44858E-10	1.80099E-10	-4.70964E-10	-4.66344E-07	4.58435E-07

TIME4	*a*	*e*	*i*	*node*	*w*	*M*
a	0.015251884	7.26524E-08	7.67811E-08	-8.70162E-08	-0.000106538	0.000105576
e	7.26524E-08	5.95511E-13	4.80623E-13	-7.70138E-13	-4.98292E-10	4.93566E-10
i	7.67811E-08	4.80623E-13	6.22972E-13	-1.94105E-13	-6.69803E-10	6.64361E-10
node	-8.70162E-08	-7.70138E-13	-1.94105E-13	2.30401E-12	3.01812E-10	-2.97499E-10
w	-0.000106538	-4.98292E-10	-6.69803E-10	3.01812E-10	9.67901E-07	-9.60616E-07
M	0.000105576	4.93566E-10	6.64361E-10	-2.97499E-10	-9.60616E-07	9.53394E-07

TIME5	*a*	*e*	*i*	*node*	*w*	*M*
a	0.058703105	1.46341E-07	1.08796E-08	-1.65937E-07	-0.000127914	0.000125066
e	1.46341E-07	1.05496E-12	2.9721E-14	-1.57501E-12	-6.22148E-10	6.13443E-10
i	1.08796E-08	2.9721E-14	8.27374E-14	3.67415E-14	-4.67281E-11	4.58432E-11
node	-1.65937E-07	-1.57501E-12	3.67415E-14	3.11636E-12	6.76286E-10	-6.66908E-10
w	-0.000127914	-6.22148E-10	-4.67281E-11	6.76286E-10	6.28804E-07	-6.21929E-07
M	0.000125066	6.13443E-10	4.58432E-11	-6.66908E-10	-6.21929E-07	6.15219E-07

TIME6	*a*	*e*	*i*	*node*	*w*	*M*
a	0.008526816	-7.81231E-09	7.8103E-09	4.82083E-08	-1.15873E-06	5.82959E-07
e	-7.81231E-09	5.42607E-13	1.81335E-14	-1.34136E-12	-6.99996E-11	7.27218E-11
i	7.8103E-09	1.81335E-14	3.30518E-13	3.4312E-13	2.01354E-11	-2.20277E-11
node	4.82083E-08	-1.34136E-12	3.4312E-13	4.11412E-12	2.00999E-10	-2.1153E-10
w	-1.15873E-06	-6.99996E-11	2.01354E-11	2.00999E-10	9.34414E-08	-9.38048E-08
M	5.82959E-07	7.27218E-11	-2.20277E-11	-2.1153E-10	-9.38048E-08	9.42407E-08

TIME7	*a*	*e*	*i*	*node*	*w*	*M*
a	0.128873735	1.97384E-07	-2.69251E-08	5.6255E-07	-0.000214055	0.000208874
e	1.97384E-07	9.52026E-13	-3.08082E-13	2.6439E-12	-6.69797E-10	6.65178E-10
i	-2.69251E-08	-3.08082E-13	3.90266E-13	-9.53577E-13	2.03074E-10	-2.0297E-10
node	5.6255E-07	2.6439E-12	-9.53577E-13	7.5781E-12	-1.98783E-09	1.9745E-09
w	-0.000214055	-6.69797E-10	2.03074E-10	-1.98783E-09	6.47358E-07	-6.40921E-07
M	0.000208874	6.65178E-10	-2.0297E-10	1.9745E-09	-6.40921E-07	6.34729E-07

TIME8	*a*	*e*	*i*	*node*	*w*	*M*
a	0.002896355	2.72745E-08	8.2437E-09	-6.65038E-08	-3.51616E-05	3.52373E-05
e	2.72745E-08	7.93844E-13	1.36445E-13	-1.0838E-12	-5.45761E-10	5.45891E-10
i	8.2437E-09	1.36445E-13	1.90882E-13	-2.20703E-13	-1.95195E-10	1.94373E-10
node	-6.65038E-08	-1.0838E-12	-2.20703E-13	2.74255E-12	9.88159E-10	-9.92533E-10
w	-3.51616E-05	-5.45761E-10	-1.95195E-10	9.88159E-10	6.27133E-07	-6.26994E-07
M	3.52373E-05	5.45891E-10	1.94373E-10	-9.92533E-10	-6.26994E-07	6.26923E-07

GPS COVARIANCE MATRIX IN VNC COORDINATES

TIME1	R_v (km)	R_n (km)	R_c (km)	V_v (km/sec)	V_n (km/sec)	V_c (km/sec)
R_v (km)	3.139624532	-0.211883741	-0.031315013	3.01986E-05	-0.000538722	8.94711E-06
R_n (km)	-0.211883741	0.044533741	-0.00495294	-6.43662E-06	4.28361E-05	-6.89659E-07
R_c (km)	-0.031315013	-0.00495294	0.009466743	7.25805E-07	4.18859E-06	-1.56973E-07
V_v (km/sec)	3.01986E-05	-6.43662E-06	7.25805E-07	9.30395E-10	-6.12451E-09	9.85073E-11
V_n (km/sec)	-0.000538722	4.28361E-05	4.18859E-06	-6.12451E-09	9.38662E-08	-1.56381E-09
V_c (km/sec)	8.94711E-06	-6.89659E-07	-1.56973E-07	9.85073E-11	-1.56381E-09	6.03607E-11

TIME2	R_v (km)	R_n (km)	R_c (km)	V_v (km/sec)	V_n (km/sec)	V_c (km/sec)
R_v (km)	0.578261738	-0.040887146	0.057303236	5.84644E-06	-8.61412E-05	5.60954E-06
R_n (km)	-0.040887146	0.036868714	-0.016491814	-5.35953E-06	1.24859E-05	-2.11823E-06
R_c (km)	0.057303236	-0.016491814	0.014923258	2.38977E-06	-1.08593E-05	1.62499E-06
V_v (km/sec)	5.84644E-06	-5.35953E-06	2.38977E-06	7.79123E-10	-1.80184E-09	3.0726E-10
V_n (km/sec)	-8.61412E-05	1.24859E-05	-1.08593E-05	-1.80184E-09	1.40415E-08	-1.154E-09
V_c (km/sec)	5.60954E-06	-2.11823E-06	1.62499E-06	3.0726E-10	-1.154E-09	2.41517E-10

TIME3	R_v (km)	R_n (km)	R_c (km)	V_v (km/sec)	V_n (km/sec)	V_c (km/sec)
R_v (km)	1.259665555	0.332239099	-0.2101824	-4.88871E-05	-0.000208321	-2.80725E-05
R_n (km)	0.332239099	0.388682293	-0.090087838	-5.68489E-05	-6.9281E-05	-2.82621E-05
R_c (km)	-0.2101824	-0.090087838	0.097957381	1.32395E-05	3.766E-05	9.08282E-06
V_v (km/sec)	-4.88871E-05	-5.68489E-05	1.32395E-05	8.31485E-09	1.01785E-08	4.13611E-09
V_n (km/sec)	-0.000208321	-6.9281E-05	3.766E-05	1.01785E-08	3.51826E-08	5.72371E-09
V_c (km/sec)	-2.80725E-05	-2.82621E-05	9.08282E-06	4.13611E-09	5.72371E-09	2.45894E-09

TIME4	R_v (km)	R_n (km)	R_c (km)	V_v (km/sec)	V_n (km/sec)	V_c (km/sec)
R_v (km)	10.21325038	-0.57171928	-1.294073987	8.03844E-05	-0.00149586	-9.41498E-05
R_n (km)	-0.57171928	0.290129205	0.15694459	-4.21493E-05	8.54856E-05	9.03529E-06
R_c (km)	-1.294073987	0.15694459	0.30591598	-2.2524E-05	0.000188797	9.52522E-06
V_v (km/sec)	8.03844E-05	-4.21493E-05	-2.2524E-05	6.12414E-09	-1.20283E-08	-1.28919E-09
V_n (km/sec)	-0.00149586	8.54856E-05	0.000188797	-1.20283E-08	2.19122E-07	1.38982E-08
V_c (km/sec)	-9.41498E-05	9.03529E-06	9.52522E-06	-1.28919E-09	1.38982E-08	1.76062E-09

TIME5	R_v (km)	R_n (km)	R_c (km)	V_v (km/sec)	V_n (km/sec)	V_c (km/sec)
R_v (km)	4.744524623	0.542308292	0.096965283	-7.99652E-05	-0.000617425	-6.28756E-07
R_n (km)	0.542308292	0.113818015	-0.01883341	-1.66881E-05	-6.33814E-05	-1.70686E-06
R_c (km)	0.096965283	-0.01883341	0.044328068	2.71496E-06	-1.78738E-05	1.67132E-07
V_v (km/sec)	-7.99652E-05	-1.66881E-05	2.71496E-06	2.44691E-09	9.35984E-09	2.49059E-10
V_n (km/sec)	-0.000617425	-6.33814E-05	-1.78738E-05	9.35984E-09	8.15311E-08	-2.38927E-10
V_c (km/sec)	-6.28756E-07	-1.70686E-06	1.67132E-07	2.49059E-10	-2.38927E-10	8.33342E-10

TIME6	R_v (km)	R_n (km)	R_c (km)	V_v (km/sec)	V_n (km/sec)	V_c (km/sec)
R_v (km)	6.739370858	0.197124829	-0.353543171	-3.07996E-05	-0.000990906	-2.61211E-05
R_n (km)	0.197124829	0.339810693	0.152882186	-4.96755E-05	8.86813E-06	3.65454E-05
R_c (km)	-0.353543171	0.152882186	0.978606608	-2.21816E-05	6.01204E-05	0.000130707
V_v (km/sec)	-3.07996E-05	-4.96755E-05	-2.21816E-05	7.26245E-09	-9.98583E-10	-5.32411E-09
V_n (km/sec)	-0.000990906	8.86813E-06	6.01204E-05	-9.98583E-10	1.50165E-07	6.69753E-09
V_c (km/sec)	-2.61211E-05	3.65454E-05	0.000130707	-5.32411E-09	6.69753E-09	1.91283E-08

TIME7	R_v (km)	R_n (km)	R_c (km)	V_v (km/sec)	V_n (km/sec)	V_c (km/sec)
R_v (km)	3.872429589	-0.000257365	-0.355843962	-9.99942E-07	-0.000577633	9.64363E-05
R_n (km)	-0.000257365	0.10339706	0.211231654	-1.52232E-05	-1.69063E-05	3.01736E-05
R_c (km)	-0.355843962	0.211231654	0.583798705	-3.09544E-05	2.50349E-05	6.44655E-05
V_v (km/sec)	-9.99942E-07	-1.52232E-05	-3.09544E-05	2.24162E-09	2.64619E-09	-4.46554E-09
V_n (km/sec)	-0.000577633	-1.69063E-05	2.50349E-05	2.64619E-09	8.93831E-08	-1.84527E-08
V_c (km/sec)	9.64363E-05	3.01736E-05	6.44655E-05	-4.46554E-09	-1.84527E-08	1.34923E-08

TIME8	R_v (km)	R_n (km)	R_c (km)	V_v (km/sec)	V_n (km/sec)	V_c (km/sec)
R_v (km)	3.719562126	-1.210436692	-0.236771296	0.00017666	-0.000534322	-3.22021E-05
R_n (km)	-1.210436692	0.421038947	0.075569809	-6.1447E-05	0.000174023	9.0078E-06
R_c (km)	-0.236771296	0.075569809	0.022922919	-1.10297E-05	3.41806E-05	1.36796E-06
V_v (km/sec)	0.00017666	-6.1447E-05	-1.10297E-05	8.96765E-09	-2.53983E-08	-1.31449E-09
V_n (km/sec)	-0.000534322	0.000174023	3.41806E-05	-2.53983E-08	7.67831E-08	4.5641E-09
V_c (km/sec)	-3.22021E-05	9.0078E-06	1.36796E-06	-1.31449E-09	4.5641E-09	5.46156E-10

GPS COVARIANCE MATRIX IN CLASSICAL ORBITAL ELEMENTS

TIME1	*a*	*e*	*i*	*node*	*w*	*M*
a	0.02395419	-1.48139E-08	-6.38261E-09	5.38815E-10	-4.50119E-05	4.45614E-05
e	-1.48139E-08	2.27206E-14	2.80888E-15	7.74394E-15	4.33626E-11	-4.30997E-11
i	-6.38261E-09	2.80888E-15	4.01127E-15	-1.93526E-15	1.12935E-11	-1.11726E-11
node	5.38815E-10	7.74394E-15	-1.93526E-15	2.1488E-14	4.06246E-12	-4.09274E-12
w	-4.50119E-05	4.33626E-11	1.12935E-11	4.06246E-12	1.05561E-07	-1.04716E-07
M	4.45614E-05	-4.30997E-11	-1.11726E-11	-4.09274E-12	-1.04716E-07	1.03879E-07

TIME2	*a*	*e*	*i*	*node*	*w*	*M*
a	0.005150566	-1.01644E-08	-6.85772E-09	-1.11268E-08	-8.91375E-06	8.82519E-06
e	-1.01644E-08	3.12378E-14	1.62352E-14	2.35887E-14	3.33002E-11	-3.31265E-11
i	-6.85772E-09	1.62352E-14	1.6028E-14	1.99539E-14	1.55513E-11	-1.54349E-11
node	-1.11268E-08	2.35887E-14	1.99539E-14	3.39144E-14	2.15417E-11	-2.13492E-11
w	-8.91375E-06	3.33002E-11	1.55513E-11	2.15417E-11	3.79593E-08	-3.78086E-08
M	8.82519E-06	-3.31265E-11	-1.54349E-11	-2.13492E-11	-3.78086E-08	3.76594E-08

TIME3	*a*	*e*	*i*	*node*	*w*	*M*
a	0.013922523	1.80038E-08	1.57381E-08	4.16874E-08	-5.08551E-06	4.95048E-06
e	1.80038E-08	6.04578E-13	2.88545E-13	1.75528E-13	-5.45937E-11	5.3968E-11
i	1.57381E-08	2.88545E-13	1.63094E-13	1.11777E-13	-2.91564E-11	2.88325E-11
node	4.16874E-08	1.75528E-13	1.11777E-13	2.2382E-13	-2.73481E-11	2.69943E-11
w	-5.08551E-06	-5.45937E-11	-2.91564E-11	-2.73481E-11	6.13556E-09	-6.05378E-09
M	4.95048E-06	5.3968E-11	2.88325E-11	2.69943E-11	-6.05378E-09	5.97397E-09

TIME4	*a*	*e*	*i*	*node*	*w*	*M*
a	0.13845267	-1.10404E-07	9.49947E-08	2.31525E-07	-1.00025E-05	8.71363E-06
e	-1.10404E-07	3.88296E-13	-8.16517E-14	-2.71372E-13	3.4526E-11	-3.37981E-11
i	9.49947E-08	-8.16517E-14	1.16727E-13	1.17052E-13	-9.69321E-12	8.81245E-12
node	2.31525E-07	-2.71372E-13	1.17052E-13	6.99204E-13	-1.61406E-11	1.41737E-11
w	-1.00025E-05	3.4526E-11	-9.69321E-12	-1.61406E-11	3.40792E-09	-3.33978E-09
M	8.71363E-06	-3.37981E-11	8.81245E-12	1.41737E-11	-3.33978E-09	3.28401E-09

TIME5	*a*	*e*	*i*	*node*	*w*	*M*
a	0.025845125	2.80937E-08	-1.96216E-09	-2.6922E-08	7.68145E-06	-8.03033E-06
e	2.80937E-08	1.74954E-13	1.72777E-14	3.46399E-14	5.54731E-11	-5.59501E-11
i	-1.96216E-09	1.72777E-14	5.52233E-14	2.06798E-15	7.63482E-12	-7.59704E-12
node	-2.6922E-08	3.46399E-14	2.06798E-15	1.01715E-13	1.59347E-11	-1.56091E-11
w	7.68145E-06	5.54731E-11	7.63482E-12	1.59347E-11	1.9095E-08	-1.92328E-08
M	-8.03033E-06	-5.59501E-11	-7.59704E-12	-1.56091E-11	-1.92328E-08	1.93755E-08

TIME6	*a*	*e*	*i*	*node*	*w*	*M*
a	0.137309934	-7.40034E-09	7.69635E-08	1.24547E-07	-1.29911E-05	1.18766E-05
e	-7.40034E-09	5.29734E-13	-3.63454E-13	-2.77685E-13	1.2099E-10	-1.20782E-10
i	7.69635E-08	-3.63454E-13	1.26751E-12	1.61277E-12	-5.6905E-11	5.73138E-11
node	1.24547E-07	-2.77685E-13	1.61277E-12	2.24838E-12	-2.82559E-11	2.88346E-11
w	-1.29911E-05	1.2099E-10	-5.6905E-11	-2.82559E-11	2.99997E-08	-2.98202E-08
M	1.18766E-05	-1.20782E-10	5.73138E-11	2.88346E-11	-2.98202E-08	2.96514E-08

TIME7	*a*	*e*	*i*	*node*	*w*	*M*
a	0.092482673	4.74128E-08	-1.97692E-07	-2.83326E-08	-2.77973E-05	2.70002E-05
e	4.74128E-08	1.20542E-13	-2.72163E-13	-3.50262E-13	-5.36136E-11	5.30695E-11
i	-1.97692E-07	-2.72163E-13	8.94037E-13	7.96021E-13	1.0647E-10	-1.04421E-10
node	-2.83326E-08	-3.50262E-13	7.96021E-13	1.34288E-12	1.24631E-10	-1.23712E-10
w	-2.77973E-05	-5.36136E-11	1.0647E-10	1.24631E-10	2.80674E-08	-2.77885E-08
M	2.70002E-05	5.30695E-11	-1.04421E-10	-1.23712E-10	-2.77885E-08	2.75171E-08

TIME8	*a*	*e*	*i*	*node*	*w*	*M*
a	0.021007693	-1.08819E-07	1.74296E-08	2.51508E-08	4.24349E-06	-4.51656E-06
e	-1.08819E-07	5.80574E-13	-8.56153E-14	-1.34972E-13	-2.17563E-11	2.32111E-11
i	1.74296E-08	-8.56153E-14	3.6154E-14	1.69266E-14	4.81662E-12	-5.08441E-12
node	2.51508E-08	-1.34972E-13	1.69266E-14	5.29593E-14	4.75369E-12	-5.11586E-12
w	4.24349E-06	-2.17563E-11	4.81662E-12	4.75369E-12	9.92122E-10	-1.0488E-09
M	-4.51656E-06	2.32111E-11	-5.08441E-12	-5.11586E-12	-1.0488E-09	1.1094E-09

GRACE COVARIANCE MATRIX IN VNC COORDINATES

TIME1	R_v (km)	R_n (km)	R_c (km)	V_v (km/sec)	V_n (km/sec)	V_c (km/sec)
R_v (km)	4576.391045	78.68374826	7.756933124	0.036047018	-5.121077773	-0.009400608
R_n (km)	78.68374826	1.402009227	0.126999016	0.000619898	-0.088061048	-0.00016047
R_c (km)	7.756933124	0.126999016	0.057329072	-2.6441E-05	-0.008690695	-3.7398E-05
V_v (km/sec)	0.036047018	0.000619898	-2.6441E-05	4.76564E-07	-4.0309E-05	-2.92033E-08
V_n (km/sec)	-5.121077773	-0.088061048	-0.008690695	-4.0309E-05	0.005730602	1.05256E-05
V_c (km/sec)	-0.009400608	-0.00016047	-3.7398E-05	-2.92033E-08	1.05256E-05	3.01548E-08

TIME2	R_v (km)	R_n (km)	R_c (km)	V_v (km/sec)	V_n (km/sec)	V_c (km/sec)
R_v (km)	1568.320998	-14.51976085	-1.965026465	0.005713019	-1.733679018	0.001290524
R_n (km)	-14.51976085	0.329552067	-0.002913227	-0.000185667	0.015966685	-2.6661E-06
R_c (km)	-1.965026465	-0.002913227	0.011989646	1.68414E-05	0.0021812	-6.26275E-06
V_v (km/sec)	0.005713019	-0.000185667	1.68414E-05	1.90048E-07	-6.23848E-06	-9.19079E-09
V_n (km/sec)	-1.733679018	0.015966685	0.0021812	-6.23848E-06	0.001916516	-1.43133E-06
V_c (km/sec)	0.001290524	-2.6661E-06	-6.26275E-06	-9.19079E-09	-1.43133E-06	4.08815E-09

TIME3	R_v (km)	R_n (km)	R_c (km)	V_v (km/sec)	V_n (km/sec)	V_c (km/sec)
R_v (km)	130.6549379	3.67684032	-1.959217027	-0.003870484	-0.149041027	0.000471805
R_n (km)	3.67684032	0.294946406	-0.137579391	-0.000321055	-0.0043592	2.67841E-05
R_c (km)	-1.959217027	-0.137579391	0.069309465	0.00014999	0.002311974	-1.58957E-05
V_v (km/sec)	-0.003870484	-0.000321055	0.00014999	3.50181E-07	4.5995E-06	-2.94602E-08
V_n (km/sec)	-0.149041027	-0.0043592	0.002311974	4.5995E-06	0.00017017	-5.54258E-07
V_c (km/sec)	0.000471805	2.67841E-05	-1.58957E-05	-2.94602E-08	-5.54258E-07	5.07797E-09

TIME4	R_v (km)	R_n (km)	R_c (km)	V_v (km/sec)	V_n (km/sec)	V_c (km/sec)
R_v (km)	2009.19487	46.55840212	-1.383639981	0.003451045	-2.247791792	0.000268336
R_n (km)	46.55840212	1.105910038	-0.036144117	5.58648E-05	-0.052109052	5.63351E-06
R_c (km)	-1.383639981	-0.036144117	0.006617955	-1.37157E-05	0.001551536	-3.7673E-07
V_v (km/sec)	0.003451045	5.58648E-05	-1.37157E-05	1.97663E-07	-3.81673E-06	-7.95853E-10
V_n (km/sec)	-2.247791792	-0.052109052	0.001551536	-3.81673E-06	0.00251475	-3.00345E-07
V_c (km/sec)	0.000268336	5.63351E-06	-3.7673E-07	-7.95853E-10	-3.00345E-07	1.2693E-09

TIME5	R_v (km)	R_n (km)	R_c (km)	V_v (km/sec)	V_n (km/sec)	V_c (km/sec)
R_v (km)	814.2441332	-14.60585289	1.472013898	0.007284495	-0.900082144	0.002413325
R_n (km)	-14.60585289	0.283537967	-0.027645094	-0.000161301	0.016120457	-5.21507E-05
R_c (km)	1.472013898	-0.027645094	0.011984732	1.41788E-05	-0.00162641	-4.37632E-07
V_v (km/sec)	0.007284495	-0.000161301	1.41788E-05	1.22781E-07	-8.01188E-06	4.10029E-08
V_n (km/sec)	-0.900082144	0.016120457	-0.00162641	-8.01188E-06	0.000995004	-2.65277E-06
V_c (km/sec)	0.002413325	-5.21507E-05	-4.37632E-07	4.10029E-08	-2.65277E-06	2.04543E-08

TIME6	R_v (km)	R_n (km)	R_c (km)	V_v (km/sec)	V_n (km/sec)	V_c (km/sec)
R_v (km)	832.5447188	11.38248356	-5.208341145	-0.003022429	-0.935121081	0.002117007
R_n (km)	11.38248356	0.237314476	-0.111942388	-0.000140002	-0.012841474	4.13187E-05
R_c (km)	-5.208341145	-0.111942388	0.063962156	7.29903E-05	0.005881701	-2.39015E-05
V_v (km/sec)	-0.003022429	-0.000140002	7.29903E-05	1.38799E-07	3.46816E-06	-2.56298E-08
V_n (km/sec)	-0.935121081	-0.012841474	0.005881701	3.46816E-06	0.001050381	-2.38832E-06
V_c (km/sec)	0.002117007	4.13187E-05	-2.39015E-05	-2.56298E-08	-2.38832E-06	1.00164E-08

TIME7	R_v (km)	R_n (km)	R_c (km)	V_v (km/sec)	V_n (km/sec)	V_c (km/sec)
R_v (km)	343.3926612	-0.553568458	-0.212854071	0.000587415	-0.38393375	-0.000168523
R_n (km)	-0.553568458	0.25499683	-0.062986941	-0.000249426	0.000420674	-1.30342E-05
R_c (km)	-0.212854071	-0.062986941	0.028433338	5.49065E-05	0.000281374	-6.0264E-06
V_v (km/sec)	0.000587415	-0.000249426	5.49065E-05	2.49645E-07	-4.60951E-07	1.90028E-08
V_n (km/sec)	-0.38393375	0.000420674	0.000281374	-4.60951E-07	0.000429426	1.99573E-07
V_c (km/sec)	-0.000168523	-1.30342E-05	-6.0264E-06	1.90028E-08	1.99573E-07	1.14015E-08

TIME8	R_v (km)	R_n (km)	R_c (km)	V_v (km/sec)	V_n (km/sec)	V_c (km/sec)
R_v (km)	146.9807826	-2.809897528	1.403905003	0.002249954	-0.161664454	-0.000463434
R_n (km)	-2.809897528	0.295313437	-0.159675047	-0.000307227	0.002913145	5.82713E-05
R_c (km)	1.403905003	-0.159675047	0.098690694	0.000165548	-0.001442963	-3.61506E-05
V_v (km/sec)	0.002249954	-0.000307227	0.000165548	3.23895E-07	-2.28109E-06	-6.07103E-08
V_n (km/sec)	-0.161664454	0.002913145	-0.001442963	-2.28109E-06	0.000177953	4.74342E-07
V_c (km/sec)	-0.000463434	5.82713E-05	-3.61506E-05	-6.07103E-08	4.74342E-07	1.44301E-08

GRACE COVARIANCE MATRIX IN CLASSICAL ORBITAL ELEMENTS

TIME1	*a*	*e*	*i*	*node*	*w*	*M*
a	11496.44515	0.001119741	-4.85396E-05	2.97041E-05	0.039288911	-0.007017611
e	0.001119741	1.10536E-10	-4.11458E-12	1.75583E-12	3.31723E-09	-2.48816E-10
i	-4.85396E-05	-4.11458E-12	5.17393E-13	-7.14795E-13	-4.01593E-10	2.21005E-10
node	2.97041E-05	1.75583E-12	-7.14795E-13	1.2207E-12	5.36417E-10	-3.6975E-10
w	0.039288911	3.31723E-09	-4.01593E-10	5.36417E-10	3.26269E-07	-1.83537E-07
M	-0.007017611	-2.48816E-10	2.21005E-10	-3.6975E-10	-1.83537E-07	1.38613E-07

TIME2	*a*	*e*	*i*	*node*	*w*	*M*
a	566.1541684	-1.65996E-05	-2.73173E-06	3.32893E-06	0.083304872	-0.085846341
e	-1.65996E-05	1.09738E-12	4.1445E-14	-3.26183E-14	8.84266E-10	-7.56957E-10
i	-2.73173E-06	4.1445E-14	7.05512E-14	-1.19848E-13	-8.05989E-10	8.30742E-10
node	3.32893E-06	-3.26183E-14	-1.19848E-13	2.5432E-13	1.27717E-09	-1.31895E-09
w	0.083304872	8.84266E-10	-8.05989E-10	1.27717E-09	3.21444E-05	-3.22627E-05
M	-0.085846341	-7.56957E-10	8.30742E-10	-1.31895E-09	-3.22627E-05	3.24143E-05

TIME3	*a*	*e*	*i*	*node*	*w*	*M*
a	2.742160395	1.22022E-06	6.40173E-08	-7.12328E-07	-0.002071867	0.002130095
e	1.22022E-06	5.54545E-12	4.88074E-13	-2.74001E-12	-8.37393E-09	8.45199E-09
i	6.40173E-08	4.88074E-13	8.75721E-14	-3.04024E-13	-8.79051E-10	8.89165E-10
node	-7.12328E-07	-2.74001E-12	-3.04024E-13	1.47E-12	4.39107E-09	-4.43807E-09
w	-0.002071867	-8.37393E-09	-8.79051E-10	4.39107E-09	1.34614E-05	-1.36066E-05
M	0.002130095	8.45199E-09	8.89165E-10	-4.43807E-09	-1.36066E-05	1.3755E-05

TIME4	*a*	*e*	*i*	*node*	*w*	*M*
a	4616.687209	-8.36775E-05	1.1066E-06	-1.32098E-05	-0.149197176	0.162740386
e	-8.36775E-05	4.52314E-12	1.32974E-14	2.8394E-13	3.41648E-09	-3.55766E-09
i	1.1066E-06	1.32974E-14	2.18765E-14	-6.90363E-15	-2.81851E-11	3.33341E-11
node	-1.32098E-05	2.8394E-13	-6.90363E-15	1.40222E-13	4.67587E-10	-4.98108E-10
w	-0.149197176	3.41648E-09	-2.81851E-11	4.67587E-10	5.01183E-06	-5.42105E-06
M	0.162740386	-3.55766E-09	3.33341E-11	-4.98108E-10	-5.42105E-06	5.875E-06

TIME5	*a*	*e*	*i*	*node*	*w*	*M*
a	582.2822909	3.1192E-05	-5.82395E-06	-5.58105E-06	-0.005792041	0.002750149
e	3.1192E-05	1.75937E-12	-4.10539E-13	-3.06656E-13	-2.20601E-10	5.45094E-11
i	-5.82395E-06	-4.10539E-13	3.50839E-13	-7.65453E-15	-1.27814E-10	1.73475E-10
node	-5.58105E-06	-3.06656E-13	-7.65453E-15	2.55564E-13	2.40081E-11	7.35308E-12
w	-0.005792041	-2.20601E-10	-1.27814E-10	2.40081E-11	2.49365E-07	-2.32249E-07
M	0.002750149	5.45094E-11	1.73475E-10	7.35308E-12	-2.32249E-07	2.32486E-07

TIME6	*a*	*e*	*i*	*node*	*w*	*M*
a	351.247476	2.49126E-05	4.44787E-06	-1.26386E-05	0.005223427	-0.002824137
e	2.49126E-05	3.18116E-12	1.73231E-14	7.46716E-14	-3.77525E-10	5.19838E-10
i	4.44787E-06	1.73231E-14	1.71012E-13	-4.56201E-13	2.45392E-10	-2.04117E-10
node	-1.26386E-05	7.46716E-14	-4.56201E-13	1.36542E-12	-7.43895E-10	6.30046E-10
w	0.005223427	-3.77525E-10	2.45392E-10	-7.43895E-10	5.04777E-07	-4.50035E-07
M	-0.002824137	5.19838E-10	-2.04117E-10	6.30046E-10	-4.50035E-07	4.13363E-07

TIME7	*a*	*e*	*i*	*node*	*w*	*M*
a	37.76975051	-8.63399E-08	1.12343E-06	-3.92042E-06	0.00233939	-0.002500162
e	-8.63399E-08	4.87258E-13	2.18142E-13	1.35472E-13	-4.39679E-10	4.42566E-10
i	1.12343E-06	2.18142E-13	1.94886E-13	-1.14208E-13	-1.45681E-10	1.418E-10
node	-3.92042E-06	1.35472E-13	-1.14208E-13	6.07371E-13	-4.06556E-10	4.00193E-10
w	0.00233939	-4.39679E-10	-1.45681E-10	-4.06556E-10	7.57647E-07	-7.43665E-07
M	-0.002500162	4.42566E-10	1.418E-10	4.00193E-10	-7.43665E-07	7.3706E-07

TIME8	*a*	*e*	*i*	*node*	*w*	*M*
a	19.54295471	3.32976E-06	9.67039E-07	-3.16569E-06	-0.003386125	0.003155798
e	3.32976E-06	6.37842E-12	1.09463E-12	-3.32686E-12	-3.67383E-09	3.64787E-09
i	9.67039E-07	1.09463E-12	2.47936E-13	-6.906E-13	-6.43905E-10	6.35975E-10
node	-3.16569E-06	-3.32686E-12	-6.906E-13	2.09665E-12	2.11354E-09	-2.08674E-09
w	-0.003386125	-3.67383E-09	-6.43905E-10	2.11354E-09	2.43125E-06	-2.40114E-06
M	0.003155798	3.64787E-09	6.35975E-10	-2.08674E-09	-2.40114E-06	2.37407E-06

ICESAT COVARIANCE MATRIX IN VNC COORDINATES

TIME1	R_v (km)	R_n (km)	R_c (km)	V_v (km/sec)	V_n (km/sec)	V_c (km/sec)
R_v (km)	2667.377375	27.248658	-8.222212216	0.025486679	-2.903515364	-0.000959534
R_n (km)	27.248658	0.343232694	-0.123143789	0.000276012	-0.02971902	6.92977E-06
R_c (km)	-8.222212216	-0.123143789	0.073164435	-5.78792E-05	0.009013345	-9.2944E-06
V_v (km/sec)	0.025486679	0.000276012	-5.78792E-05	2.93293E-07	-2.77166E-05	-5.1922E-09
V_n (km/sec)	-2.903515364	-0.02971902	0.009013345	-2.77166E-05	0.003160652	1.02937E-06
V_c (km/sec)	-0.000959534	6.92977E-06	-9.2944E-06	-5.1922E-09	1.02937E-06	9.72002E-09

TIME2	R_v (km)	R_n (km)	R_c (km)	V_v (km/sec)	V_n (km/sec)	V_c (km/sec)
R_v (km)	1811.890652	-2.188383048	6.159397958	0.016639944	-1.960051174	-0.003575802
R_n (km)	-2.188383048	0.278617886	-0.096730678	-0.000181455	0.002175071	4.37372E-05
R_c (km)	6.159397958	-0.096730678	0.06971132	0.000116889	-0.00658008	-3.65365E-05
V_v (km/sec)	0.016639944	-0.000181455	0.000116889	2.95182E-07	-1.78636E-05	-5.86479E-08
V_n (km/sec)	-1.960051174	0.002175071	-0.00658008	-1.78636E-05	0.002120503	3.82993E-06
V_c (km/sec)	-0.003575802	4.37372E-05	-3.65365E-05	-5.86479E-08	3.82993E-06	1.98572E-08

TIME3	R_v (km)	R_n (km)	R_c (km)	V_v (km/sec)	V_n (km/sec)	V_c (km/sec)
R_v (km)	326399.3075	27334.7265	5.304094301	30.2285861	-354.0117641	0.012197704
R_n (km)	27334.7265	2347.784474	-1.287519625	2.594582918	-29.64734114	0.00139736
R_c (km)	5.304094301	-1.287519625	0.061715504	-0.001366828	-0.005742342	-1.73698E-05
V_v (km/sec)	30.2285861	2.594582918	-0.001366828	0.002867405	-0.032786024	1.53789E-06
V_n (km/sec)	-354.0117641	-29.64734114	-0.005742342	-0.032786024	0.383960161	-1.32346E-05
V_c (km/sec)	0.012197704	0.00139736	-1.73698E-05	1.53789E-06	-1.32346E-05	9.11448E-09

TIME4	R_v (km)	R_n (km)	R_c (km)	V_v (km/sec)	V_n (km/sec)	V_c (km/sec)
R_v (km)	10713.10129	-66.28964327	0.599842759	-0.005060832	-11.61266365	0.002545232
R_n (km)	-66.28964327	2.011581892	0.231793501	0.001040958	0.071606577	-0.000236337
R_c (km)	0.599842759	0.231793501	0.093487752	6.80978E-05	-0.000730012	-6.93133E-05
V_v (km/sec)	-0.005060832	0.001040958	6.80978E-05	7.93325E-07	5.41437E-06	-8.6949E-08
V_n (km/sec)	-11.61266365	0.071606577	-0.000730012	5.41437E-06	0.01258787	-2.69444E-06
V_c (km/sec)	0.002545232	-0.000236337	-6.93133E-05	-8.6949E-08	-2.69444E-06	5.69596E-08

TIME5	R_v (km)	R_n (km)	R_c (km)	V_v (km/sec)	V_n (km/sec)	V_c (km/sec)
R_v (km)	7681.249484	125.8222111	17.34549546	0.122462384	-8.370291915	-0.005912067
R_n (km)	125.8222111	2.130025404	0.272198739	0.002076823	-0.137100454	-9.27568E-05
R_c (km)	17.34549546	0.272198739	0.044290481	0.00024806	-0.018913744	-1.57504E-05
V_v (km/sec)	0.122462384	0.002076823	0.00024806	2.14132E-06	-0.000133363	-8.04067E-08
V_n (km/sec)	-8.370291915	-0.137100454	-0.018913744	-0.000133363	0.0091212	6.44962E-06
V_c (km/sec)	-0.005912067	-9.27568E-05	-1.57504E-05	-8.04067E-08	6.44962E-06	5.79865E-09

TIME6	R_v (km)	R_n (km)	R_c (km)	V_v (km/sec)	V_n (km/sec)	V_c (km/sec)
R_v (km)	2189.869023	1.613345356	5.507059425	0.017600768	-2.376008741	-0.00261799
R_n (km)	1.613345356	0.310134944	-0.066750327	-0.000102086	-0.001920908	4.18285E-05
R_c (km)	5.507059425	-0.066750327	0.077123	8.71104E-05	-0.005918993	-3.25554E-05
V_v (km/sec)	0.017600768	-0.000102086	8.71104E-05	2.4096E-07	-1.9014E-05	-4.995E-08
V_n (km/sec)	-2.376008741	-0.001920908	-0.005918993	-1.9014E-05	0.002578084	2.80985E-06
V_c (km/sec)	-0.00261799	4.18285E-05	-3.25554E-05	-4.995E-08	2.80985E-06	1.61786E-08

TIME7	R_v (km)	R_n (km)	R_c (km)	V_v (km/sec)	V_n (km/sec)	V_c (km/sec)
R_v (km)	2128.144791	-10.87068861	-1.594192226	-0.008846831	-2.313966281	-3.49493E-05
R_n (km)	-10.87068861	0.273391171	-0.093485471	6.24994E-05	0.011690791	5.02351E-05
R_c (km)	-1.594192226	-0.093485471	0.071772513	2.06113E-05	0.001800299	-3.24833E-05
V_v (km/sec)	-0.008846831	6.24994E-05	2.06113E-05	1.06446E-07	9.63099E-06	-1.46163E-09
V_n (km/sec)	-2.313966281	0.011690791	0.001800299	9.63099E-06	0.002516102	6.49779E-09
V_c (km/sec)	-3.49493E-05	5.02351E-05	-3.24833E-05	-1.46163E-09	6.49779E-09	1.5827E-08

TIME8	R_v (km)	R_n (km)	R_c (km)	V_v (km/sec)	V_n (km/sec)	V_c (km/sec)
R_v (km)	1395.829495	-18.74468615	6.850035205	0.004752091	-1.505285584	-0.003595272
R_n (km)	-18.74468615	0.257958261	-0.087861355	-6.12216E-05	0.020211735	4.45025E-05
R_c (km)	6.850035205	-0.087861355	0.042313908	2.27685E-05	-0.00738626	-2.34901E-05
V_v (km/sec)	0.004752091	-6.12216E-05	2.27685E-05	2.77665E-08	-5.1263E-06	-1.19218E-08
V_n (km/sec)	-1.505285584	0.020211735	-0.00738626	-5.1263E-06	0.00162333	3.87719E-06
V_c (km/sec)	-0.003595272	4.45025E-05	-2.34901E-05	-1.19218E-08	3.87719E-06	1.35888E-08

ICESAT COVARIANCE MATRIX IN CLASSICAL ORBITAL ELEMENTS

TIME1	*a*	*e*	*i*	*node*	*w*	*M*
a	3925.455505	0.000234978	8.20841E-07	-4.78174E-05	-0.240931178	0.254254303
e	0.000234978	1.48341E-11	1.5017E-13	-3.64317E-12	-1.377E-08	1.45757E-08
i	8.20841E-07	1.5017E-13	1.69561E-13	-1.74583E-13	5.72163E-11	-7.55393E-11
node	-4.78174E-05	-3.64317E-12	-1.74583E-13	1.51038E-12	2.23171E-09	-2.39842E-09
w	-0.240931178	-1.377E-08	5.72163E-11	2.23171E-09	1.53728E-05	-1.61883E-05
M	0.254254303	1.45757E-08	-7.55393E-11	-2.39842E-09	-1.61883E-05	1.70565E-05

TIME2	*a*	*e*	*i*	*node*	*w*	*M*
a	663.7906933	3.93075E-05	-1.59329E-06	1.04487E-06	-0.036931591	0.040027112
e	3.93075E-05	3.0562E-12	2.16514E-13	-6.28238E-13	-1.16344E-09	1.33626E-09
i	-1.59329E-06	2.16514E-13	3.45358E-13	-6.92313E-13	9.35469E-10	-1.00184E-09
node	1.04487E-06	-6.28238E-13	-6.92313E-13	1.43944E-12	-1.96688E-09	2.09117E-09
w	-0.036931591	-1.16344E-09	9.35469E-10	-1.96688E-09	5.4195E-06	-5.75411E-06
M	0.040027112	1.33626E-09	-1.00184E-09	2.09117E-09	-5.75411E-06	6.12504E-06

TIME3	*a*	*e*	*i*	*node*	*w*	*M*
a	37793887.47	1.249782904	0.000740663	-0.00073514	-2699.396526	2712.765506
e	1.249782904	4.13286E-08	2.44793E-11	-2.39105E-11	-8.92647E-05	8.9707E-05
i	0.000740663	2.44793E-11	1.58727E-13	-3.28654E-13	-5.29021E-08	5.30875E-08
node	-0.00073514	-2.39105E-11	-3.28654E-13	1.27396E-12	5.24148E-08	-5.22603E-08
w	-2699.396526	-8.92647E-05	-5.29021E-08	5.24148E-08	0.192802186	-0.193757068
M	2712.765506	8.9707E-05	5.30875E-08	-5.22603E-08	-0.193757068	0.194716844

TIME4	*a*	*e*	*i*	*node*	*w*	*M*
a	19332.7946	0.000758825	-8.46607E-05	8.45164E-05	-1.181027593	1.155216195
e	0.000758825	3.09316E-11	-3.83246E-12	4.11063E-12	-4.588E-08	4.51613E-08
i	-8.46607E-05	-3.83246E-12	9.93431E-13	-1.31492E-12	4.5747E-09	-4.52146E-09
node	8.45164E-05	4.11063E-12	-1.31492E-12	1.92977E-12	-4.26548E-09	4.27311E-09
w	-1.181027593	-4.588E-08	4.5747E-09	-4.26548E-09	7.30562E-05	-7.15786E-05
M	1.155216195	4.51613E-08	-4.52146E-09	4.27311E-09	-7.15786E-05	7.03238E-05

TIME5	*a*	*e*	*i*	*node*	*w*	*M*
a	28944.23531	0.001690783	-4.21933E-05	-0.000138135	-1.857736949	1.921239892
e	0.001690783	9.95685E-11	-2.63223E-12	-8.47411E-12	-1.07737E-07	1.11516E-07
i	-4.21933E-05	-2.63223E-12	1.00898E-13	2.98521E-13	2.54353E-09	-2.65201E-09
node	-0.000138135	-8.47411E-12	2.98521E-13	9.14545E-13	8.49086E-09	-8.83721E-09
w	-1.857736949	-1.07737E-07	2.54353E-09	8.49086E-09	0.000120118	-0.000124133
M	1.921239892	1.11516E-07	-2.65201E-09	-8.83721E-09	-0.000124133	0.000128296

TIME6	*a*	*e*	*i*	*node*	*w*	*M*
a	1150.627204	6.75261E-05	-2.96575E-07	-2.02118E-06	-0.065266753	0.069568615
e	6.75261E-05	4.35101E-12	1.17574E-13	2.11544E-13	-3.43579E-09	3.71719E-09
i	-2.96575E-07	1.17574E-13	2.81919E-13	6.17212E-13	7.27696E-10	-7.7645E-10
node	-2.02118E-06	2.11544E-13	6.17212E-13	1.59201E-12	1.44462E-09	-1.55644E-09
w	-0.065266753	-3.43579E-09	7.27696E-10	1.44462E-09	6.03611E-06	-6.43477E-06
M	0.069568615	3.71719E-09	-7.7645E-10	-1.55644E-09	-6.43477E-06	6.87757E-06

TIME7	*a*	*e*	*i*	*node*	*w*	*M*
a	2126.079881	9.5654E-05	1.29343E-05	2.08527E-05	-0.131960245	0.12558686
e	9.5654E-05	5.25037E-12	8.79655E-13	1.70977E-12	-5.06738E-09	4.92022E-09
i	1.29343E-05	8.79655E-13	2.75466E-13	6.15713E-13	-4.20845E-10	4.19695E-10
node	2.08527E-05	1.70977E-12	6.15713E-13	1.48214E-12	-2.62293E-10	2.94895E-10
w	-0.131960245	-5.06738E-09	-4.20845E-10	-2.62293E-10	9.32985E-06	-8.83202E-06
M	0.12558686	4.92022E-09	4.19695E-10	2.94895E-10	-8.83202E-06	8.379E-06

TIME8	*a*	*e*	*i*	*node*	*w*	*M*
a	823.4588082	3.87435E-05	9.9903E-06	2.16214E-05	-0.033041285	0.028411464
e	3.87435E-05	1.88838E-12	4.86088E-13	1.04723E-12	-1.55527E-09	1.34016E-09
i	9.9903E-06	4.86088E-13	2.36326E-13	4.4515E-13	-3.46433E-10	2.78275E-10
node	2.16214E-05	1.04723E-12	4.4515E-13	8.73971E-13	-7.59324E-10	6.17721E-10
w	-0.033041285	-1.55527E-09	-3.46433E-10	-7.59324E-10	1.50644E-06	-1.34056E-06
M	0.028411464	1.34016E-09	2.78275E-10	6.17721E-10	-1.34056E-06	1.20358E-06

FAST COVARIANCE MATRIX IN VNC COORDINATES

TIME1	R_v (km)	R_n (km)	R_c (km)	V_v (km/sec)	V_n (km/sec)	V_c (km/sec)
R_v (km)	474.1433363	-0.26668047	2.288628072	0.023425177	-0.326596614	-0.000948973
R_n (km)	-0.26668047	0.049507581	0.012363564	-4.4237E-05	0.000175723	1.86891E-06
R_c (km)	2.288628072	0.012363564	0.050819536	0.00010774	-0.001582592	-1.18607E-05
V_v (km/sec)	0.023425177	-4.4237E-05	0.00010774	1.17985E-06	-1.61293E-05	-4.86099E-08
V_n (km/sec)	-0.326596614	0.000175723	-0.001582592	-1.61293E-05	0.000224969	6.53306E-07
V_c (km/sec)	-0.000948973	1.86891E-06	-1.18607E-05	-4.86099E-08	6.53306E-07	1.07827E-08

TIME2	R_v (km)	R_n (km)	R_c (km)	V_v (km/sec)	V_n (km/sec)	V_c (km/sec)
R_v (km)	3556.66808	-14.71327365	-7.036902749	0.458468937	-2.572544238	0.00727172
R_n (km)	-14.71327365	0.091034243	0.029709638	-0.001896275	0.010641036	-1.85579E-05
R_c (km)	-7.036902749	0.029709638	0.032572693	-0.000913658	0.005085855	-2.33832E-05
V_v (km/sec)	0.458468937	-0.001896275	-0.000913658	5.91358E-05	-0.000331586	8.62198E-07
V_n (km/sec)	-2.572544238	0.010641036	0.005085855	-0.000331586	0.001860746	-5.31775E-06
V_c (km/sec)	0.00727172	-1.85579E-05	-2.33832E-05	8.62198E-07	-5.31775E-06	2.24457E-07

TIME3	R_v (km)	R_n (km)	R_c (km)	V_v (km/sec)	V_n (km/sec)	V_c (km/sec)
R_v (km)	3106.587492	-38.41483454	5.406967659	0.3993847	-2.249831314	0.000537029
R_n (km)	-38.41483454	0.657029427	-0.149785917	-0.004991396	0.027843805	3.11858E-05
R_c (km)	5.406967659	-0.149785917	0.085633332	0.000724653	-0.00393878	-4.04931E-05
V_v (km/sec)	0.3993847	-0.004991396	0.000724653	5.13842E-05	-0.000289239	5.39687E-08
V_n (km/sec)	-2.249831314	0.027843805	-0.00393878	-0.000289239	0.001629375	-3.79364E-07
V_c (km/sec)	0.000537029	3.11858E-05	-4.04931E-05	5.39687E-08	-3.79364E-07	2.69075E-08

TIME4	R_v (km)	R_n (km)	R_c (km)	V_v (km/sec)	V_n (km/sec)	V_c (km/sec)
R_v (km)	132.9351656	0.324685894	-1.928062661	0.022829062	-0.107737489	-2.09552E-05
R_n (km)	0.324685894	0.044923352	-0.063128284	1.80834E-05	-0.000255999	1.76738E-05
R_c (km)	-1.928062661	-0.063128284	0.135144289	-0.000281306	0.0015461	-3.07906E-05
V_v (km/sec)	0.022829062	1.80834E-05	-0.000281306	3.95278E-06	-1.8508E-05	-1.86092E-08
V_n (km/sec)	-0.107737489	-0.000255999	0.0015461	-1.8508E-05	8.73229E-05	2.02781E-08
V_c (km/sec)	-2.09552E-05	1.76738E-05	-3.07906E-05	-1.86092E-08	2.02781E-08	1.41025E-08

TIME5	R_v (km)	R_n (km)	R_c (km)	V_v (km/sec)	V_n (km/sec)	V_c (km/sec)
R_v (km)	2453.537751	-45.2451122	-32.88318789	-0.310685034	-1.786178564	0.00709546
R_n (km)	-45.2451122	1.065274316	0.655287563	0.005536442	0.032957162	-0.000125476
R_c (km)	-32.88318789	0.655287563	0.493773286	0.004122854	0.023947022	-0.000106713
V_v (km/sec)	-0.310685034	0.005536442	0.004122854	3.95138E-05	0.000226163	-9.03117E-07
V_n (km/sec)	-1.786178564	0.032957162	0.023947022	0.000226163	0.001300343	-5.1667E-06
V_c (km/sec)	0.00709546	-0.000125476	-0.000106713	-9.03117E-07	-5.1667E-06	2.76531E-08

TIME6	R_v (km)	R_n (km)	R_c (km)	V_v (km/sec)	V_n (km/sec)	V_c (km/sec)
R_v (km)	1147.728674	8.074180665	14.01528528	-0.0422397	-0.802354779	-0.000988356
R_n (km)	8.074180665	0.173306919	0.187077627	-0.000383117	-0.005688293	6.51534E-05
R_c (km)	14.01528528	0.187077627	0.288314835	-0.000582194	-0.009833417	1.46676E-05
V_v (km/sec)	-0.0422397	-0.000383117	-0.000582194	1.62582E-06	2.95652E-05	-3.60249E-08
V_n (km/sec)	-0.802354779	-0.005688293	-0.009833417	2.95652E-05	0.000560934	6.51418E-07
V_c (km/sec)	-0.000988356	6.51534E-05	1.46676E-05	-3.60249E-08	6.51418E-07	1.54189E-07

TIME7	R_v (km)	R_n (km)	R_c (km)	V_v (km/sec)	V_n (km/sec)	V_c (km/sec)
R_v (km)	828.5321965	0.503485212	6.558350283	0.071844994	-0.838565442	-0.003691262
R_n (km)	0.503485212	0.031849382	0.039072877	1.487E-05	-0.000532536	-1.23962E-05
R_c (km)	6.558350283	0.039072877	0.120268103	0.000522561	-0.006677148	-5.62107E-05
V_v (km/sec)	0.071844994	1.487E-05	0.000522561	6.26813E-06	-7.26852E-05	-3.06432E-07
V_n (km/sec)	-0.838565442	-0.000532536	-0.006677148	-7.26852E-05	0.000848747	3.74826E-06
V_c (km/sec)	-0.003691262	-1.23962E-05	-5.62107E-05	-3.06432E-07	3.74826E-06	3.30846E-08

TIME8	R_v (km)	R_n (km)	R_c (km)	V_v (km/sec)	V_n (km/sec)	V_c (km/sec)
R_v (km)	290.2592746	-1.270391977	0.019053046	0.027533909	-0.204719158	-0.000665993
R_n (km)	-1.270391977	0.036398201	0.004560506	-0.000139812	0.000901713	-3.42572E-06
R_c (km)	0.019053046	0.004560506	0.018317991	9.20649E-08	-1.17572E-05	-3.74393E-07
V_v (km/sec)	0.027533909	-0.000139812	9.20649E-08	2.62454E-06	-1.94231E-05	-5.89445E-08
V_n (km/sec)	-0.204719158	0.000901713	-1.17572E-05	-1.94231E-05	0.000144393	4.68227E-07
V_c (km/sec)	-0.000665993	-3.42572E-06	-3.74393E-07	-5.89445E-08	4.68227E-07	3.37191E-09

FAST COVARIANCE MATRIX IN CLASSICAL ORBITAL ELEMENTS

TIME1	*a*	*e*	*i*	*node*	*w*	*M*
a	30.05704599	-3.73699E-06	-1.15864E-06	-2.19207E-06	-2.9142E-06	0.000414064
e	-3.73699E-06	1.16491E-12	2.12145E-13	1.33834E-13	8.75318E-13	-6.29876E-11
i	-1.15864E-06	2.12145E-13	3.15811E-13	1.7674E-13	1.78394E-13	-2.24013E-11
node	-2.19207E-06	1.33834E-13	1.7674E-13	5.03798E-13	4.34824E-13	-3.35107E-11
w	-2.9142E-06	8.75318E-13	1.78394E-13	4.34824E-13	1.76067E-12	-6.25036E-11
M	0.000414064	-6.29876E-11	-2.24013E-11	-3.35107E-11	-6.25036E-11	9.99765E-09

TIME2	*a*	*e*	*i*	*node*	*w*	*M*
a	454.7990103	-3.03038E-05	-3.25309E-05	-4.09483E-06	-0.000147805	-0.003253421
e	-3.03038E-05	2.60871E-12	3.35087E-12	5.8662E-14	1.14573E-11	1.19591E-10
i	-3.25309E-05	3.35087E-12	5.98741E-12	3.48324E-13	1.36302E-11	1.23299E-10
node	-4.09483E-06	5.8662E-14	3.48324E-13	3.75045E-13	6.19718E-13	9.85384E-11
w	-0.000147805	1.14573E-11	1.36302E-11	6.19718E-13	5.36017E-11	7.69333E-10
M	-0.003253421	1.19591E-10	1.23299E-10	9.85384E-11	7.69333E-10	5.95521E-08

TIME3	*a*	*e*	*i*	*node*	*w*	*M*
a	1150.201465	-4.83708E-05	6.1487E-08	1.69004E-05	-0.000176968	-0.006627229
e	-4.83708E-05	2.52428E-12	-4.46289E-14	-7.7179E-13	9.0022E-12	2.3879E-10
i	6.1487E-08	-4.46289E-14	5.15667E-13	5.4641E-13	1.43422E-12	2.32396E-11
node	1.69004E-05	-7.7179E-13	5.4641E-13	9.84002E-13	-6.85233E-14	-7.63424E-11
w	-0.000176968	9.0022E-12	1.43422E-12	-6.85233E-14	4.77283E-11	9.41826E-10
M	-0.006627229	2.3879E-10	2.32396E-11	-7.63424E-11	9.41826E-10	5.16348E-08

TIME4	*a*	*e*	*i*	*node*	*w*	*M*
a	17.2775179	-4.3363E-07	-6.31138E-07	1.88253E-06	-1.12452E-05	0.000177993
e	-4.3363E-07	3.08453E-13	-2.41238E-14	-6.71321E-13	-8.63385E-13	-7.00966E-12
i	-6.31138E-07	-2.41238E-14	1.58056E-13	1.30949E-13	8.8656E-13	-6.80478E-12
node	1.88253E-06	-6.71321E-13	1.30949E-13	2.01344E-12	2.18354E-12	2.49914E-11
w	-1.12452E-05	-8.63385E-13	8.8656E-13	2.18354E-12	1.76231E-11	-1.05725E-10
M	0.000177993	-7.00966E-12	-6.80478E-12	2.49914E-11	-1.05725E-10	1.95613E-09

TIME5	*a*	*e*	*i*	*node*	*w*	*M*
a	1400.195017	-6.0066E-05	-4.17471E-05	8.14658E-05	0.000221162	-0.00778707
e	-6.0066E-05	3.44018E-12	1.59585E-12	-2.83763E-12	-1.83165E-11	3.18465E-10
i	-4.17471E-05	1.59585E-12	1.59171E-12	-2.90994E-12	-4.99159E-12	2.41707E-10
node	8.14658E-05	-2.83763E-12	-2.90994E-12	5.7675E-12	6.41271E-12	-4.75332E-10
w	0.000221162	-1.83165E-11	-4.99159E-12	6.41271E-12	1.30586E-10	-1.03765E-09
M	-0.00778707	3.18465E-10	2.41707E-10	-4.75332E-10	-1.03765E-09	4.48044E-08

TIME6	*a*	*e*	*i*	*node*	*w*	*M*
a	104.7272502	-1.04993E-05	-9.96921E-06	1.00215E-05	-2.29357E-05	0.001346631
e	-1.04993E-05	2.29438E-12	2.33924E-12	1.64898E-13	-3.89213E-12	-9.14215E-11
i	-9.96921E-06	2.33924E-12	4.85888E-12	1.13032E-13	-7.04812E-12	-2.55495E-11
node	1.00215E-05	1.64898E-13	1.13032E-13	2.86573E-12	-9.8818E-12	2.16637E-10
w	-2.29357E-05	-3.89213E-12	-7.04812E-12	-9.8818E-12	4.82368E-11	-7.75906E-10
M	0.001346631	-9.14215E-11	-2.55495E-11	2.16637E-10	-7.75906E-10	2.6165E-08

TIME7	*a*	*e*	*i*	*node*	*w*	*M*
a	430.1022027	3.12941E-05	7.91591E-06	-2.35613E-05	-0.000166216	-0.001500223
e	3.12941E-05	2.43369E-12	6.33027E-13	-2.0714E-12	-1.35859E-11	-1.11356E-10
i	7.91591E-06	6.33027E-13	3.26326E-13	-7.59628E-13	-3.8894E-12	-3.28774E-11
node	-2.35613E-05	-2.0714E-12	-7.59628E-13	2.55818E-12	1.36532E-11	8.51197E-11
w	-0.000166216	-1.35859E-11	-3.8894E-12	1.36532E-11	8.34216E-11	5.99437E-10
M	-0.001500223	-1.11356E-10	-3.28774E-11	8.51197E-11	5.99437E-10	7.19135E-09

TIME8	*a*	*e*	*i*	*node*	*w*	*M*
a	5.549395403	9.43676E-08	2.56788E-07	3.33502E-07	1.34309E-06	-0.000108057
e	9.43676E-08	1.43183E-13	-2.99515E-14	-1.52806E-14	5.29465E-13	-9.00913E-12
i	2.56788E-07	-2.99515E-14	1.01273E-13	1.88886E-14	-5.07259E-13	-1.51663E-11
node	3.33502E-07	-1.52806E-14	1.88886E-14	1.95025E-13	1.62045E-13	9.96876E-14
w	1.34309E-06	5.29465E-13	-5.07259E-13	1.62045E-13	7.12914E-12	-1.44771E-11
M	-0.000108057	-9.00913E-12	-1.51663E-11	9.96876E-14	-1.44771E-11	5.60952E-09

Appendix E. Two-line Element Sets for Covariance Matrices

This appendix contains the prime TLEs (N^{th} TLEs) corresponding to the covariance matrices listed in Appendix D. They correspond to the 48 scenarios in this study. They are grouped by the study satellite number (1-6) and listed in chronological order (increasing time). All of these TLEs were gathered from CelesTrak (13).

LAGEOS Study Satellite #1 Satellite Catalog #08820

```
Time Window 1
1 08820U 76039A   03074.62772535  .00000007  00000-0  10000-3 0  9074
2 08820 109.8227 149.5733 0044466 321.3666  38.3911  6.38664664371085

Time Window 2
1 08820U 76039A   03092.94890240  .00000006  00000-0  10000-3 0  9184
2 08820 109.8150 155.8477 0044416 317.4818  42.2518  6.38664538372252

Time Window 3
1 08820U 76039A   03284.77326730 -.00000008  00000-0  10000-3 0  9684
2 08820 109.8207 221.5003 0044330 276.4589  83.0908  6.38664544384509

Time Window 4
1 08820U 76039A   03304.81695835 -.00000010  00000-0  10000-3 0  9770
2 08820 109.8237 228.3645 0044417 272.2648  87.2859  6.38664509385788

Time Window 5
1 08820U 76039A   04059.76589517  .00000028  00000-0  10000-3 0   264
2 08820 109.8402 269.4700 0044228 246.5937 113.0167  6.38664662393447

Time Window 6
1 08820U 76039A   04079.49639730  .00000031  00000-0  10000-3 0   476
2 08820 109.8431 276.2286 0044154 242.3598 117.2646  6.38664540394702

Time Window 7
1 08820U 76039A   04164.83863788 -.00000001  00000-0  10000-3 0   558
2 08820 109.8558 305.4597 0044196 224.1572 135.5360  6.38664651400154

Time Window 8
1 08820U 76039A   04294.65281357 -.00000002  00000-0  10000-3 0   751
2 08820 109.8594 349.9486 0044244 196.5047 163.4332  6.38664775408443
```

TOPEX Study Satellite #2 Satellite Catalog #22076

Time Window 1
1 22076U 92052A 03074.89509844 -.00000038 00000-0 10000-3 0 5763
2 22076 66.0432 137.4291 0008101 268.6254 91.3867 12.80930375495549

Time Window 2
1 22076U 92052A 03092.46217450 -.00000038 00000-0 10000-3 0 5811
2 22076 66.0409 100.9386 0008179 275.0917 84.9076 12.80930657497798

Time Window 3
1 22076U 92052A 03284.91928311 -.00000038 00000-0 10000-3 0 6292
2 22076 66.0443 61.1890 0007801 269.1075 90.8937 12.80929856522446

Time Window 4
1 22076U 92052A 03304.82865002 -.00000038 00000-0 10000-3 0 6371
2 22076 66.0469 19.8380 0007959 268.2237 91.7851 12.80929256524993

Time Window 5
1 22076U 92052A 04059.90944078 -.00000038 00000-0 10000-3 0 6683
2 22076 66.0416 130.4227 0008358 272.6341 87.3729 12.80929693540374

Time Window 6
1 22076U 92052A 04079.42842756 -.00000038 00000-0 10000-3 0 6716
2 22076 66.0406 89.8767 0008351 272.4184 87.5824 12.80929925542878

Time Window 7
1 22076U 92052A 04164.92155367 -.00000038 00000-0 10000-3 0 6889
2 22076 66.0424 272.3042 0008437 269.6846 90.3190 12.80930709553828

Time Window 8
1 22076U 92052A 04294.83990057 -.00000038 00000-0 10000-3 0 7236
2 22076 66.0462 2.4556 0008295 266.0902 93.9161 12.80930761570462

GPS IIR-03 Study Satellite #3 Satellite Catalog #25933

Time Window 1
1 25933U 99055A 03074.52892487 -.00000001 00000-0 00000-0 0 9395
2 25933 52.3374 305.2747 0016071 339.8061 20.1894 2.00566189 25201

Time Window 2
1 25933U 99055A 03092.97588966 -.00000048 00000-0 00000-0 0 9579
2 25933 52.3222 304.4805 0016341 342.1329 17.8365 2.00566412 25578

Time Window 3
1 25933U 99055A 03284.93036114 -.00000044 00000-0 00000-0 0 1614
2 25933 52.1599 296.2097 0021007 344.3029 15.6516 2.00559714 29429

Time Window 4
1 25933U 99055A 03304.37508863 -.00000025 00000-0 00000-0 0 1833
2 25933 52.1415 295.3686 0021967 345.5152 14.4239 2.00559962 29812

Time Window 5
1 25933U 99055A 04059.53347544 -.00000008 00000-0 00000-0 0 3143
2 25933 52.0369 290.1768 0027413 357.4737   2.5627 2.00560746 32226

Time Window 6
1 25933U 99055A 04079.47667982 -.00000024 00000-0 00000+0 0 3359
2 25933 52.0204 289.3140 0028214 359.4066   0.6192 2.00560779 32621

Time Window 7
1 25933U 99055A 04164.73371438 -.00000085 00000-0 00000-0 0 4271
2 25933 51.9450 285.6244 0029046   1.1191 358.8830 2.00561296 34332

Time Window 8
1 25933U 99055A 04294.86245840 -.00000003 00000-0 00000+0 0 5625
2 25933 51.8434 279.9857 0033524   0.7092 359.2948 2.00562226 36948

GRACE-1 Study Satellite #4 Satellite Catalog #27391

Time Window 1
1 27391U 02012A 03074.66017680 .00005045 00000-0 18429-3 0 3080
2 27391 89.0105 306.6230 0017723 331.1406 28.8820 15.27763419 55389

Time Window 2
1 27391U 02012A 03092.67228130 .00004978 00000-0 18131-3 0 3214
2 27391 89.0083 304.2240 0015990 251.4400 108.5153 15.27887956 58135

Time Window 3
1 27391U 02012A 03284.76139796 .00002928 00000-0 10259-3 0 4785
2 27391 89.0039 278.5891 0015517 225.5866 134.4110 15.29010968 87477

Time Window 4
1 27391U 02012A 03304.72201347 .00014579 00000-0 51008-3 0 4957
2 27391 89.0065 275.9136 0020089 147.1292 213.1188 15.29226248 90521

Time Window 5
1 27391U 02012A 04059.70126067 .00001663 00000-0 55859-4 0 6016
2 27391 89.0068 259.9197 0020888 55.6834 304.6353 15.29985848108860

Time Window 6
1 27391U 02012A 04079.71489477 .00002491 00000-0 84212-4 0 6314
2 27391 89.0075 257.2439 0017304 344.8631 15.2066 15.30072607111924

Time Window 7
1 27391U 02012A 04164.65926590 .00001708 00000-0 56583-4 0 7034
2 27391 89.0167 245.9578 0018805 16.7422 343.4437 15.30490298124915

Time Window 8
1 27391U 02012A 04294.69203977 .00001382 00000-0 45036-4 0 8095
2 27391 89.0237 228.7489 0015252 217.9913 142.0274 15.30934220144806

ICESAT Study Satellite #5 Satellite Catalog #27642

Time Window 1
1 27642U 03002A 03074.87916703 .00001240 00000-0 12856-3 0 646
2 27642 94.0004 212.4670 0002191 60.5901 299.5460 14.90474309 9214

Time Window 2
1 27642U 03002A 03092.87211105 .00001210 00000-0 12543-3 0 819
2 27642 94.0050 221.6118 0002048 50.3498 309.7903 14.90473799 11898

Time Window 3
1 27642U 03002A 03284.95127266 .00001297 00000-0 13297-3 0 2673
2 27642 94.0060 319.1602 0002952 95.0060 265.1497 14.90881770 40500

Time Window 4
1 27642U 03002A 03304.61717355 .00006228 00000-0 63304-3 0 2823
2 27642 93.9992 329.1517 0003036 74.7407 285.4162 14.90897678 43434

Time Window 5
1 27642U 03002A 04059.96250407 .00000896 00000-0 92322-4 0 4100
2 27642 93.9976 30.2319 0002159 42.8133 317.3257 14.90891095 61362

Time Window 6
1 27642U 03002A 04079.96401939 -.00000303 00000-0 -29509-4 0 4258
2 27642 93.9976 40.3799 0001359 84.2290 275.9099 14.90870298 64347

Time Window 7
1 27642U 03002A 04164.80275903 -.00000649 00000-0 -64611-4 0 5095
2 27642 94.0058 83.4997 0002202 53.4411 306.6975 14.90868606 76987

Time Window 8
1 27642U 03002A 04294.62456753 -.00000140 00000-0 -12963-4 0 6486
2 27642 94.0002 149.4295 0001434 93.4496 266.6895 14.90868983 96327

FAST Study Satellite #6 Satellite Catalog #24285

Time Window 1
1 24285U 96049A 03074.62241878 .00008525 00000-0 76994-3 0 13
2 24285 82.9729 119.7402 2054349 165.1652 202.0390 11.14572223262113

Time Window 2
1 24285U 96049A 03092.57625824 .00008359 00000-0 75492-3 0 280
2 24285 82.9603 110.8875 2053099 131.7022 247.8933 11.14793477264119

Time Window 3
1 24285U 96049A 03284.78775089 .00008014 00000-0 71914-3 0 1065
2 24285 82.9814 15.9712 2041971 132.5254 246.7408 11.17164302285558

Time Window 4
1 24285U 96049A 03304.66751913 .00010523 00000-0 95264-3 0 1045
2 24285 82.9786 6.1475 2039835 95.2959 288.2527 11.17448079287772

Time Window 5
1 24285U 96049A 04059.81743723 .00002474 00000-0 22877-3 0 1697
2 24285 82.9787 306.6088 2031627 229.8441 110.6522 11.18795240301207

Time Window 6
1 24285U 96049A 04079.94007238 .00004012 00000-0 36428-3 0 1740
2 24285 82.9727 296.6194 2032274 192.0476 162.3941 11.18930873303456

Time Window 7
1 24285U 96049A 04164.93723932 .00002709 00000-0 24296-3 0 2012
2 24285 82.9702 254.3965 2028367 32.3217 338.7240 11.19776027312960

Time Window 8
1 24285U 96049A 04294.90279416 .00001576 00000-0 13730-3 0 2670
2 24285 82.9786 189.7893 2026896 147.7470 226.5595 11.20367918327511

Bibliography

1. Boyce III, William H. "Examination of NORAD TLE Accuracy Using the Iridium Constellation," *Proceedings of the AAS/AIAA Space Flight Mechanics Meeting, Maui, HI; 8-12 Feb. 2004*. 119: 2133-2141. San Diego: Univelt, Inc., 2005. AAS Paper 04-240.

2. Chan, Joseph C. and Daniel Navarro. "Comparisons of NORAD Two-Line Elements with Intelsat Orbital Elements," *Proceedings of the Third European Conference on Space Debris, Darmstadt, Germany; 19-21 Mar 2001*. 473: 771 – 779. Noordwijk, Netherlands: ESA Publications Division, October 2001.

3. Deguine, B. and others. "Covariance Modelling In Satellite Collision Risk Activities." *AIAA/AAS Astrodynamics Specialist Conference, Monterey, California; 5-8 Aug. 2002*. AIAA Paper 2002-4631.

4. Gelb, Arthur. *Applied Optimal Estimation*. Cambridge, MA: MIT Press, 1974.

5. Glover, David M. "*Sequence Analysis I: Uniform Series, Cross- and Auto-Correlation, and Fourier Transforms*," Online Lecture Notes (October 2000). 15 February 2006. http://w3eos.whoi.edu/12.747/notes/lect06/l06s02.html.

6. Hoots, Felix R., P. W. Schumacher and R. A. Glover. "History of Analytical Orbit Modeling in the U. S. Space Surveillance System," *Journal of Guidance, Control, and Dynamics*, 27:174-185 (April 2004).

7. Hoots, Felix R. and Richard G. France. "Satellite Drag Error Growth Estimation," *Proceedings of the AAS/AIAA Astrodynamics Specialist Conference, Girdwood, AK; 16-19 Aug. 1999*. 103:1871-1879. San Diego, Univelt, Inc., 2000. AAS Paper 99-419.

8. Hoots, Felix R., and Ronald L. Roehrich. *Spacetrack Report No. 3: Models for Propagation of NORAD Element Sets*. December 1980 http://celestrak.com/NORAD/documentation/spacetrk.pdf.

9. Kaya, Denise A. and Daniel E. Snow. "Element Set Prediction Accuracy Assessment," *Proceedings of the AAS/AIAA Astrodynamics Specialist Conference, Girdwood, AK; 16-19 Aug. 1999*. 103:1937-1956. San Diego, Univelt, Inc., 2000. AAS Paper 99-425.

10. Kelso, T.S., and S. Alfano. "Satellite Orbital Conjunction Reports Assessing Threatening Encounters in Space (SOCRATES)," *AAS/AIAA Space Flight Mechanics Conference, Copper Mountain, Colorado 23-27 Jan. 2005*. AAS Paper 05-124. http://www.celestrak.com/SOCRATES/SSW6-SOCRATES.pdf

11. Kelso, T.S. *Computers & Satellites* Columns. CelesTrak, 2006. http://www.celestrak.com/columns. January 2006.

12. -----. NORAD Two-Line Element Set Format. CelesTrak, 2004. http://www.celestrak.com/NORAD/documentation/tle-fmt.asp. 22 February 2006.

13. -----. TLE Data. CelesTrak, 2006. http://www.celestrak.com. January 2006.

14. Matney, M.J. and others. "Covariance Correlations in Collision Avoidance Probability Calculations," *Advances in Space Research*, 34:1109-1114 (November 2004).

15. NASA/NORAD 2-Line Elements. http://liftoff.msfc.nasa.gov/academy/rocket_sci/orbmech/state/2line.html.

16. Peterson, Glenn E., Robert G. Gist, and Daniel L. Oltrogge. "Covariance Generation for Space Objects Using Public Data," *Proceedings of the AAS/AIAA Space Flight Mechanics Meeting, Santa Barbara, CA; 11-15 Feb. 2001*. 108: 201-214. San Diego: Univelt, Inc., 2001. AAS Paper 01-113.

17. Space-Track. http://www.space-track.org. 15 February 06.

18. USSTRATCOM Space Control. http://www.stratcom.mil/fact_sheets/fact_spc.html. 15 February 06.

19. Vallado, David A. *Fundamentals of Astrodynamics and Applications* (2nd Edition). El Segundo, CA: Microcosm Press, 2004.

20. -----. "An Analysis of State Vector Propagation using Differing Flight Dynamics Programs," *AAS/AIAA Space Flight Mechanics Conference, Copper Mountain, Colorado 23-27 Jan. 2005*. AAS Paper 05-199.

21. -----. "Covariance Transformations for Satellite Flight Dynamics Operations," *AAS/AIAA Astrodynamics Specialist Conference, Big Sky, Montana; 3-7 Aug. 2003*. AAS Paper 03-526.

22. -----. Personal discussions and email correspondence. (November 2005 – February 2006). Formal technical paper has been submitted for publication in 2006.

23. -----. *Astrodynamics Software*, MATLAB source code: "COVCT2CL.m" http://www.celestrak.com/software/vallado-sw.asp 12 January 2006.

24. Wiesel, William E. *Modern Astrodynamics*. Beavercreek, OH: Aphelion Press, 2003.

25. -----. *Modern Orbit Determination*. Beavercreek, OH: Aphelion Press, 2003.

26. Wilkins, Matthew P. and Kyle T. Alfriend. "Characterizing Orbit Uncertainty Due to Atmospheric Uncertainty," *AIAA/AAS Astrodynamics Specialist Conference, Denver, CO; 14-17 Aug. 2000*. AIAA Paper 2000-3931.

Vita

Captain Victor P. Osweiler graduated from Great Falls High School in Great Falls, Montana. He entered undergraduate studies at Montana State University in Bozeman, Montana, where he graduated in May 1998 with a Bachelor of Science in Applied Mathematics. He earned a Regular Commission through the AFROTC Detachment 450.

His first assignment was at Kirtland Air Force Base as an acquisition officer in the Space Vehicles Directorate of the Air Force Research Laboratory in July 1998. He worked in an experimental satellite payload office, responsible for payload integration with the satellite, on-orbit payload tasking and data collection, and data post-processing and dissemination. In July 2001, he was assigned to the Air Force Space Battlelab at Schriever Air Force Base, Colorado. There he served as a research officer of emerging space-related technologies for demonstration of improving capabilities.

He entered the Graduate School of Engineering and Management, Air Force Institute of Technology, in September 2004. Upon graduation, Captain Osweiler will be assigned to Detachment 12 of the Space and Missile Systems Center at Kirtland Air Force Base.

REPORT DOCUMENTATION PAGE

Form Approved
OMB No. 074-0188

1. REPORT DATE *(DD-MM-YYYY)*	2. REPORT TYPE	3. DATES COVERED *(From – To)*
23-03-2006	Master's Thesis	Jun 2005 - Mar 2006

4. TITLE AND SUBTITLE

Covariance Estimation and Autocorrelation of NORAD Two-Line Element Sets

5a. CONTRACT NUMBER

5b. GRANT NUMBER

5c. PROGRAM ELEMENT NUMBER

6. AUTHOR(S)

Osweiler, Victor P., Captain, USAF

5d. PROJECT NUMBER

5e. TASK NUMBER

5f. WORK UNIT NUMBER

7. PERFORMING ORGANIZATION NAMES(S) AND ADDRESS(S)

Air Force Institute of Technology
Graduate School of Engineering and Management (AFIT/EN)
2950 Hobson Way
WPAFB OH 45433-7765

8. PERFORMING ORGANIZATION REPORT NUMBER

AFIT/GSS/ENY/06-M09

9. SPONSORING/MONITORING AGENCY NAME(S) AND ADDRESS(ES)

N/A

10. SPONSOR/MONITOR'S ACRONYM(S)

11. SPONSOR/MONITOR'S REPORT NUMBER(S)

12. DISTRIBUTION/AVAILABILITY STATEMENT

APPROVED FOR PUBLIC RELEASE; DISTRIBUTION UNLIMITED.

13. SUPPLEMENTARY NOTES

14. ABSTRACT

This thesis investigates NORAD two-line element sets (TLE) containing satellite mean orbital elements for the purpose of estimating a covariance matrix and formulating an autocorrelation relationship. Orbit propagation is performed using Simplified General Perturbations Number 4 (SGP4) analytical model as implemented within Satellite Took Kit. For a given satellite, TLEs from a span of two weeks are used to calculate position and velocity differences of estimated state vectors in order to characterize their variance behavior and compute a covariance matrix for the most recent TLE. Six satellites and eight time spans are investigated, with all state vector differences evaluated in satellite-based coordinate systems. An autocorrelation relationship for each satellite is generated to characterize confidence levels of the orbit predictions. Trends in the deterministic dynamics and errors in the model are observed and discussed. Covariance matrix estimates and associated TLEs are presented.

15. SUBJECT TERMS

Covariance, Autocorrelation, Orbiting Satellites, Error Analysis, Collision Avoidance, Simplified General Perturbations, SGP4, Orbit propagation, TLE, Two-Line Element

16. SECURITY CLASSIFICATION OF:			17. LIMITATION OF ABSTRACT	18. NUMBER OF PAGES	19a. NAME OF RESPONSIBLE PERSON
a. REPORT	b. ABSTRACT	c. THIS PAGE			Nathan A. Titus, Lt Col, USAF (ENY)
U	U	U	UU	130	19b. TELEPHONE NUMBER *(Include area code)* (937) 255-3636, ext 7469; e-mail: Nathan.Titus@afit.edu

Standard Form 298 (Rev. 8-98)
Prescribed by ANSI Std. Z39-18